The role of Zuo1 in mitoprotein-induced stress

Dissertation

der Mathematisch-Naturwissenschaftlichen Fakultät

der Eberhard Karls Universität Tübingen

zur Erlangung des Grades eines

Doktors der Naturwissenschaften

(Dr. rer. nat.)

vorgelegt von

Jiaxin Qian

aus Wuhan,China

Tübingen

2025

Gedruckt mit Genehmigung der Mathematisch-Naturwissenschaftlichen Fakultät der Eberhard Karls Universität Tübingen.

Tag der mündlichen Qualifikation:	03.02.2026
Dekan:	Prof. Dr. Thilo Stehle
1. Berichterstatter/-in:	Prof. Dr. Doron Rapaport
2. Berichterstatter/-in:	Prof. Dr. Ralf Jansen

Erklärung/Declaration: Ich erkläre, dass ich die zur Promotion eingereichte Arbeit mit dem Titel:

The role of Zuo1 in mitoprotein-induced stress

selbständig verfasst, nur die angegebenen Quellen und Hilfsmittel benutzt und wörtlich oder inhaltlich übernommene Stellen als solche gekennzeichnet habe. Ich versichere an Eides statt, dass diese Angaben wahr sind und dass ich nichts verschwiegen habe. Mir ist bekannt, dass die falsche Abgabe einer Versicherung an Eides statt mit Freiheitsstrafe bis zu drei Jahren oder mit Geldstrafe bestraft wird.

Übersetzt mit DeepL.com

I hereby declare that I have produced the work entitled:

The role of Zuo1 in mitoprotein-induced stress

Submitted for the award of a doctorate, on my own (without external help), have used only the sources and aids indicated and have marked passages included from other works, whether verbatim or in content, as such. I swear upon oath that these statements are true and that I have not concealed anything. I am aware that making a false declaration under oath is punishable by a term of imprisonment of up to three years or by a fine.

Tübingen, den ....

Datum / Date Unterschrift / Signature

Contents

1 List of abbreviations

AAC2	ADP/ATP Carrier protein 2
Amp	Ampicillin
ATP	Adenosine Triphosphate
BN-PAGE	Blue Native PolyAcrylamide Gel Electrophoresis
BSA	Bovine Serum Albumin
cryo-EM	Cryo-Electron Microscopy
CTD	C-Terminal Domain
DDM	n-Dodecyl-β-D-maltoside
Δψ	Membrane Potential
Δ	Deletion (gene knockout)
DMSO	Dimethyl Sulfoxide
DNAJC2	DnaJ Heat Shock Protein Family (Hsp40) Member C2
dNTP	Deoxynucleotide Triphosphate
DTT	Dithiothreitol
ECL	Enhanced Chemiluminescence
EDTA	Ethylenediaminetetraacetic acid
EGTA	Ethylene Glycol Tetraacetic Acid
EM	Electron Microscopy
ER	Endoplasmic Reticulum
Fum1	Fumarase 1
4HB	Four-Helix Bundle
GPDpr	Glyceraldehyde-3-phosphate dehydrogenase promoter
HA	Hemagglutinin (tag)
HEPES	4-(2-Hydroxyethyl)-1-piperazineethanesulfonic acid
HPD	Histidine-Proline-Aspartic Acid (motif)
HphMX6	Hygromycin B resistance marker
Hsp	Heat Shock Protein

HygB	Hygromycin B (resistance gene/cassette)
Icp55	Intermediate Cleaving Peptidase of 55 kDa
IgG	Immunoglobulin G
IM	Inner Membrane
IMS	Intermembrane Space
KAN	Kanamycin (resistance gene/cassette)
KanMX4	Kanamycin resistance marker
kDa	Kilodalton
KHM	Potassium HEPES MgCl2 (buffer)
LB	Luria-Bertani (medium)
Leu	Leucine
MAD	Mitochondrial-Associate Degradation
MD	Middle Domain
MIA	Mitochondrial Intermembrane Space Import and Assembly
MIM	Mitochondrial Import (complex)
MOPS	3-(N-Morpholino)propanesulfonic acid
MPP	Mitochondrial Processing Peptidase
MPP11	M-phase Phosphoprotein 11
MTS	Mitochondrial Targeting Sequence
mTORC1	Mechanistic Target of Rapamycin Complex 1
MW	Molecular Weight
NAT	Nourseothricin (resistance gene/cassette)
NatNT2	Nourseothricin resistance marker
NBD	Nucleotide-Binding Domain
Oct1	Octapeptidyl Peptidase
OD600	Optical Density at 600 nm
OE	Overexpression
OM	Outer Membrane
ORF	Open Reading Frame

Oxa1	Oxidase Assembly protein 1
PAGE	PolyAcrylamide Gel Electrophoresis
PAM	Presequence Translocase-Associated Motor
PCR	Polymerase Chain Reaction
PMSF	Phenylmethylsulfonyl fluoride
PVDF	Polyvinylidene Difluoride
RAC	Ribosome-Associate Complex
ROS	Reactive Oxygen Species
RPS6	Ribosomal Protein S6
rRNA	Ribosomal RNA
SAM	Sorting and Assembly Machinery
SBD-β	β-Subdomain of the Substrate-Binding Domain
SD	Synthetic Dextrose (medium)
SDS	Sodium Dodecyl Sulfate
SDS-PAGE	SDS-Polyacrylamide Gel Electrophoresis
SEM	Sucrose-EDTA-MOPS (buffer)
SGal	Synthetic Galactose (medium)
sHSP	Small Heat Shock Protein
SP6	A bacteriophage RNA polymerase promoter
StAR	Steroidogenic Acute Regulatory protein
TAE	Tris-Acetate-EDTA (buffer)
TBS	Tris-Buffered Saline
TBST	Tris-Buffered Saline with Tween 20
TIM	Translocase of the Inner Membrane
TOM	Translocase of the Outer Membrane
Tris	Tris(hydroxymethyl)aminomethane
UPR	Unfolded Protein Response
WT	Wild Type
YPD	Yeast Extract-Peptone-Dextrose (medium)

YPG	Yeast Extract-Peptone-Glycerol (medium)
YPGal	Yeast Extract-Peptone-Galactose (medium)
ZHD	Zuotin Homology Domain
ZRF1	Zuotin-Related Factor 1

2 Summary

Mitochondria are essential organelles in almost all eukaryotic cells. They are the powerhouses of the cell, in charge of the production of ATP. In addition, they are also involved in calcium signaling, immune responses, and programmed cell death (apoptosis), all while producing reactive oxygen species (ROS). Their dysfunction can lead to various diseases and aging effects. There are more than 1000 different proteins in mitochondria, with 99% of them encoded by the nuclear genome. They are translated by cytosolic ribosomes, transported to and finally imported into mitochondria. The ribosome-associated complex (RAC) is required for co-translational folding, chaperone coordination, protein quality control and stress response. It consists of an Hsp40 family protein (Zuo1) and a non-typical Hsp70 family protein (Ssz1) in yeast.

This study mainly focuses on:
(1) How does Zuo1 influence the biogenesis of mitochondrial outer membrane proteins?
(2) What are the potential genetic interactions between Zuo1 and the mitochondrial protein import receptors Tom70/Tom71 under normal and heat stress conditions?

To address these questions, I analyzed yeast cells that harbor single or multiple deletions in the genes of interest, namely *ZUO1*, *TOM70* and/or *TOM71*. The results mainly demonstrated that: First, the absence of Zuo1 affects growth differently under normal and heat-stress conditions when Tom70 and Tom71 are lost. Second, the absence of Zuo1 changes the proteostasis of cells lacking Tom70/71. This study introduces a novel paradigm in which RAC functions as a stress-controlled regulatory component of the cytosolic translation machinery.

Zusammenfassung

Mitochondrien sind essentielle Organellen in fast allen eukaryotischen Zellen. Sie dienen als Kraftwerke der Zelle und sind für die Produktion von ATP zuständig. Außerdem sind sie an der Kalzium-Signalgebung, an Immunreaktionen und am programmierten Zelltod (Apoptose) beteiligt, *wobei sie gleichzeitig reaktive Sauerstoffspezies (ROS) erzeugen*. Mitochndriale Defekte können zu einer Vielzahl von Krankheiten sowie zu Alterungsprozessen führen. Mitochondrien besitzen über 1000 verschiedene Proteine, von denen 99 % im Zellkern kodiert werden. Sie werden von zytosolischen Ribosomen synthetisiert, *anschließend weitertransportiert und schließlich in die Mitochondrien importiert*. Der sogenannte „ribosome-associated complex (RAC)“ wird für kotranslationale Faltung, Chaperon-Koordination, Proteinqualitätskontrolle und zelluläre Stressantworten benötigt. In Hefe besteht er aus einem Protein der Hsp40 Chaperonfamilie (Zuo1) und einem *atypischen* Protein der Hsp70 Familie (Ssz1).

Diese Studie konzentriert sich hauptsächlich auf:
(1) Wie Zuo1 die Biogenese von Proteinen der mitochondrialen Außenmembran beeinflusst?
(2) Welche potenziellen genetischen Interaktionen zwischen Zuo1 und Tom70/Tom71 (mitochondriale Proteinimportrezeptoren) unter normalen Bedingungen und unter Hitzestress bestehen?

Um diese Fragen zu beantworten, analysierte ich Hefezellen, die einzelne oder mehrere Deletionen in den relevanten Genen tragen, nämlich *ZUO1*, *TOM70* und/oder *TOM71*. Die Ergebnisse zeigen hauptsächlich Folgendes: Erstens wirkt sich das Fehlen von Zuo1 unter normalen Bedingungen und unter Hitzestressbedingungen unterschiedlich auf das Wachstum aus, wenn Tom70 und Tom71 verloren gegangen sind. Zweitens verändert das Fehlen von Zuo1 die Proteostase von Zellen, denen Tom70/71 fehlt. Diese Studie stellt ein neues Paradigma vor, in dem RAC als *stressabhängig regulierende Komponente* des zytosolischen Translationsapparats fungiert.

3 Introduction

3.1 The origin, structure and function of mitochondria

Mitochondria can be found in almost all of the eukaryotic cells (Rossmann et al. 2021). Two billion years ago, an ancient archaea host cell and an alpha-proteobacterium, which had been engulfed, started to cooperate together (Frezza 2014). This ancient bacterium could respire aerobically. It was not destroyed by the host cell but instead formed a mutualistic relationship, providing energy in exchange for nutrients. Over time, this engulfed bacterium became the mitochondrion. It lost its independence by transferring many of its genes to the host's nucleus (Atlante and Valenti 2023). This is a process known as endosymbiotic gene transfer.

Mitochondria are the "powerhouses" of the cell (Mills, Kelly, and O'Neill 2017). They generate energy in the form of ATP through a process called cellular respiration, and they have a double membrane system. Mitochondria have four sub-compartments: an outer membrane (OM), an inner membrane (IM), an intermembrane space (IMS), and the matrix (Soubannier and McBride 2009). The OM is a smooth and relatively permeable membrane that encloses the organelle (Duarte, Ciampi, and Duarte 2023). The IM is highly folded into cristae structures that dramatically increase the surface area for ATP production (Ferreira and Rodriguez 2024). The IMS is the region between the OM and IM; it is the place where hydrogen protons are pumped to create a gradient for ATP synthesis (Sun et al. 2022). The matrix of mitochondria is the innermost compartment and contains the enzymes for the Krebs cycle, beta-oxidation of fatty acids and ATP synthesis (Atlante and Valenti 2023). Mitochondria contain their own circular DNA molecules and ribosomes. This allows the organelles to synthesize some of mitochondria’s own proteins (Shokolenko, Wilson, and Alexeyev 2016).

The primary function of mitochondria is cellular respiration. This process converts energy from nutrients into ATP via oxidative phosphorylation (Palma et al. 2024). Mitochondria also regulate cellular metabolism and processes like the breakdown of glucose and lipids, the urea cycle and amino acid metabolism (Hu et al. 2022). Furthermore, mitochondria are involved in calcium homeostasis, programmed cell death (apoptosis), cellular signaling, and regulation of reactive

oxygen species (ROS) (Li et al. 2024; Zhang et al. 2022; Nguyen et al. 2023). For an overview of mitochondrial functions see Figure 3.1 (Pfanner, Warscheid, and Wiedemann 2019).

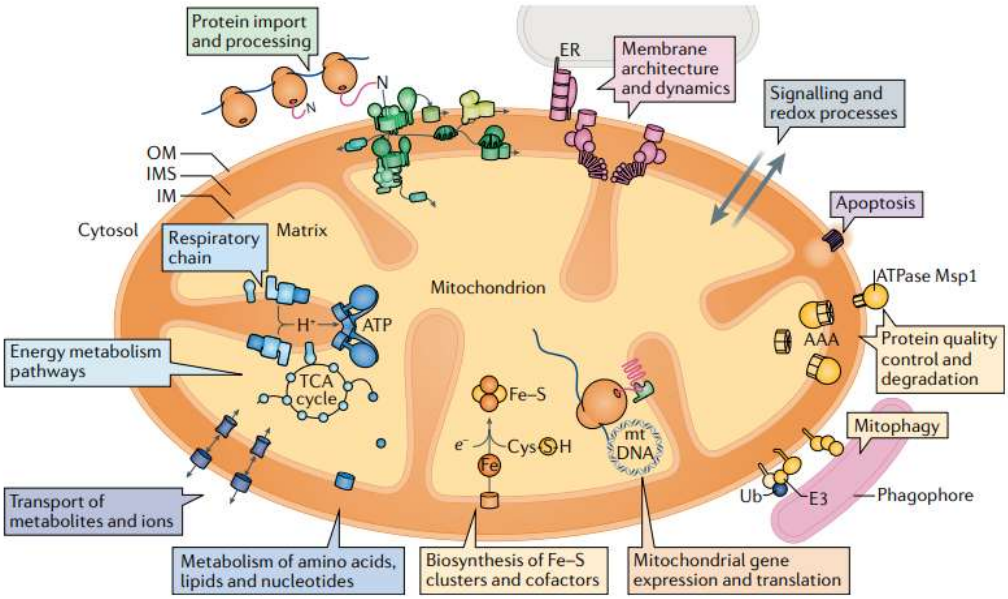

Figure 3.1 Overview of mitochondria and their functions. The outer membrane (OM), matrix, inner membrane (IM), and intermembrane space (IMS) are the four compartments that make up mitochondria. A diverse array of functions has been attributed to mitochondrial proteins and protein complexes, as illustrated in the figure. Taken from (Pfanner, Warscheid, and Wiedemann 2019).

3.2 Protein import into mitochondria

Protein import into mitochondria is a multi-step process. Mitochondrial precursor proteins, which are encoded in the nuclear genome, are translated on cytosolic ribosomes. Next, the proteins are guided to their specific mitochondrial destinations. Finally, the actual import relies on the translocase of the outer membrane (TOM) complex, which serves as the entry gate of mitochondrial and for various translocases of the inner membrane (TIM17/23 and TIM22 complexes). These pathways facilitate sorting into the matrix, the inner membrane or the intermembrane space (den Brave, Engelke, and Becker 2021). Some key factors like the membrane potential (Δψ), ATP hydrolysis, and molecular chaperones provide the necessary driving force to mediate translocation and proper folding.

Newly synthesized mitochondrial proteins, known also as precursor proteins, bear a signal sequence which facilitates their targeting to the organelle. The signal sequences of matrix proteins, and some of those destined to the IM or IMS are often located at the N-terminus of the protein and are known as the mitochondrial targeting sequences (MTS). While the precursor proteins are still in the cytosol, cytosolic chaperones keep them in an unfolded import-competent state. Then the chaperone transports the precursor proteins to the surface of the organelle (Haucke and Lithgow 1997).

The TOM complex acts as the general entry gate in the OM. The signal sequence on the precursor protein binds to receptors on the TOM complex, which then facilitates its translocation through the TOM channel (Hulett et al. 2008).

After crossing the TOM complex, proteins diverge to different pathways depending on their destination. Preproteins with N-terminal presequences destined for the matrix, the IMS or the inner membrane utilize the TIM17/23 complex to cross the inner membrane or to be laterally released into the IM (Neupert and Herrmann 2007). Hydrophobic proteins with internal targeting signals are inserted into the inner membrane via the TIM22 complex, with assistance from small TIM proteins in the IMS (Paschen and Neupert 2001; den Brave, Engelke, and Becker 2021). Cysteine-rich proteins are transported to the intermembrane space (IMS) by the mitochondrial intermembrane space import and assembly (MIA) machinery, which facilitates oxidative folding (den Brave, Engelke, and Becker 2021). The membrane potential across the inner mitochondrial membrane is an essential driving force for protein translocation through both TIM17/23 and TIM22 complexes (Geissler et al. 2000 ; den Brave, Engelke, and Becker 2021). A complex involving the matrix protein mtHsp70 and Tim44 acts as an ATP-dependent motor (presequence translocase-associated motor, PAM) to pull preproteins into the matrix (Paschen and Neupert 2001; Schmidt, Pfanner, and Meisinger 2010; den Brave, Engelke, and Becker 2021) . Chaperones within the mitochondrial matrix play multiple roles in folding and assembling the newly imported proteins into their functional complexes (Paschen and Neupert 2001; den Brave, Engelke, and Becker 2021).

Five major pathways of mitochondrial protein import have been identified. First, the presequence pathway uses the presequence translocase-associated motor (PAM) to move presequence-carrying cleavable preproteins via the outer membrane's translocase (TOM) and the inner membrane's translocase (TIM17/23). The TIM17/23 passage is activated by the membrane potential (Δψ) across the inner membrane (IM), which causes the positively charged sequences to translocate into the matrix. The mitochondrial processing peptidase (MPP) processes the presequences, and octapeptidyl peptidase (Oct1) or intermediate cleaving peptidase of 55 kDa (Icp55) can carry out further proteolytic processing. IM proteins are either carried across the matrix and inserted into the IM by the oxidase assembly protein 1 (Oxa1) insertase, or they are laterally released from the TIM17/23 complex. Oxa1 also inserts IM proteins that are produced on mitochondrial ribosomes. Second, the TOM complex imports cysteine-rich proteins that are intended for the intermembrane space (IMS). The mitochondrial IMS import and assembly protein (Mia40) recognizes these proteins and acts as an oxidoreductase to add disulfide bonds to the imported proteins. In order to transport disulfides from Erv1 to Mia40 to imported proteins, the sulfhydryl oxidase Erv1 and Mia40 create a disulfide relay. Third, the TOM complex imports the precursors of non-cleavable IM proteins, especially the carrier proteins. The TIM22 carrier translocase then receives these precursors from the tiny TIM chaperones in the IMS and inserts them into the IM. Fourth, the sorting and assembly mechanism (SAM) inserts the OM β-barrel protein precursors into the OM after their translocation across the OM by the TOM complex and association at the IMS with tiny TIM chaperones. Fifth, the mitochondrial import (MIM) complex inserts a large number of OM proteins with α-helical transmembrane regions into the membrane (Figure 3.2) (Pfanner, Warscheid, and Wiedemann 2019).

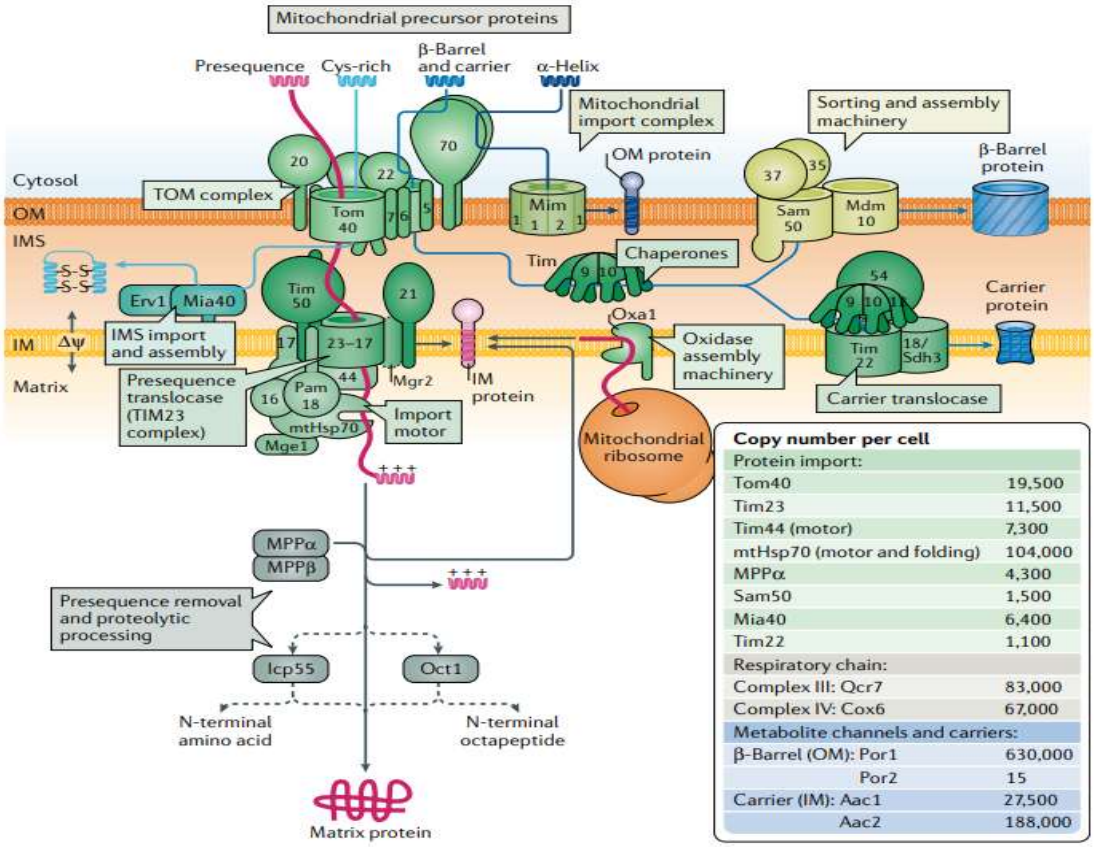

Figure 3.2 Five protein import pathways into mitochondria. Taken from (Pfanner, Warscheid, and Wiedemann 2019). For details see text.

3.3 Structure and function of the TOM complex

The TOM complex is the main protein import channel in the outer mitochondrial membrane (Araiso, Imai, and Endo 2022). This machinery is a multi-subunit membrane complex that includes the central β-barrel pore-forming protein Tom40, the receptors proteins Tom20, Tom22 and Tom70, and three small regulatory subunits Tom5, Tom6 and Tom7.

Tom40 is the core protein-conducting channel of the mitochondrial TOM complex, forming a pore in the OM and mediating the import of most mitochondrial precursor proteins from the cytosol. Its structure consists of an oligomeric assembly, often a dimer, with distinct N- and C-terminal regions that facilitate protein translocation. Tom40 has six major functions. First, it is a protein import pore (Gabriel, Egan, and Lithgow 2003). Second, it is in charge of protein sorting, by directing proteins to their correct mitochondrial locations (Gabriel, Egan, and Lithgow 2003). Third, it can bind presequences. Tom40 forms a specific binding site for the

presequence of precursor proteins, which is crucial for their targeting and translocation into the mitochondrion (Rapaport, Neupert, and Lill 1997). Fourth, it helps protein retrotranslocation. In the mitochondrial-associated degradation (MAD) pathway, Tom40 facilitates the movement of misfolded or damaged protein out of the mitochondria (Liao et al. 2025). Fifth, it has a chaperone-like activity. It helps to prevent non-native proteins from aggregating as they pass through the import channel (Sherman et al. 2006). Lastly, it is involved in cholesterol transport. Tom40 interacts with the StAR protein at the mitochondrial OM to facilitate the transport of cholesterol into mitochondria, a process essential for steroidogenesis (Bose, Bose, and Whittal 2023).

Tom70 is a TOM subunit with a size of 70 kDa, which acts as a receptor of the TOM complex and is anchored to the OM. It has three main functions. First, it contributes to the mitochondrial protein import by recognizing precursor proteins with internal targeting signals (Backes et al. 2021; Liu et al. 2022). Second, it serves as a docking site for heat shock proteins (chaperones) on the mitochondrial surface. This recruitment is important as it can not only prevent proteotoxicity, but also facilitate protein translocation (Backes et al. 2021). By binding to precursor proteins, Tom70 prevents their accumulation in the cytosol and protects against the potential toxic effects of these proteins, especially hydrophobic inner membrane proteins. Chaperones assist in unfolding the precursor proteins and maintaining their import-competent state for entry into the mitochondria. Tom70 was suggested to be part of contact sites with ER (Fenech et al. 2025).

Tom71 is a paralog protein of Tom70 that also functions as a receptor for the TOM complex and has a binding site for chaperones (Li et al. 2009). It binds to molecular chaperones Hsp70 and Hsp90, which deliver preproteins to the surface of the organelle. Tom71 can adopt different conformations, including an "open" state that exposes its binding pocket for preproteins, a change potentially induced by Hsp70/Hsp90 binding (Li et al. 2009).

Tom22 is a crucial component of the TOM complex that can function as a preprotein receptor.

Its N-terminal domain cooperates with Tom20, in binding to MTS. Tom22 also stabilizes the TOM complex and connects the other two receptors, Tom20 and Tom70, to the Tom40 pore.

Tom20 is a receptor for mitochondrial precursor proteins mainly those with MTS. Its cytosolic domain forms a groove where it binds the hydrophobic face of the presequence peptide, which itself assumes a α-helical structure upon binding. The structure is flexible, with the receptor domain capable of adopting multiple positions at the TOM complex interface, acting as a gatekeeper for the translocation pores (Abe et al. 2000; Saitoh et al. 2007; Ornelas et al. 2023). Tom20 has five main functions. First, it can recognize precursor proteins from the cytoplasm. Tom20 identifies and binds to the mitochondrial presequences, short amino acid sequences that act as a "zip code" directing proteins to their mitochondrial destination (Endo and Kohda 2002; Yamano et al. 2008; Yamamoto et al. 2011). Second, it can tether the precursor protein. After recognizing the signal, Tom20 tethers the precursor protein to the TOM40 channel (Yamamoto et al. 2011). Third, it can enhance the import efficiency. By holding the protein close to the Tom40 pore, Tom20 increases the efficiency of protein import into the organelle (Yamamoto et al. 2011). Fourth, it has dynamic association. Tom20 is not permanently fixed to the TOM complex but dynamically associates with it, becoming attached when substrate is available (Bhagawati et al. 2021). Lastly, it can facilitate mitochondrial-associated mRNA localization. Research also suggests that Tom20 is involved in the localization of specific mRNAs to mitochondria (Eliyahu et al. 2010).

Tom5, Tom6, and Tom7 are small accessory proteins of the TOM complex, which serve to modulate complex assembly/stability (Kato and Mihara 2008). Tom5 serves as a core bridging subunit for transferring preprotein from receptor proteins to the Tom40 pore, whereas Tom6 and Tom7 regulate the stability of the TOM complex and its assembly intermediates (Kato and Mihara 2008; Sayyed and Mahalakshmi 2022).

3.4 Biological significance of molecular chaperones

Chaperones play an important role in protein folding, protein quality control and maintenance

of cell homeostasis (Thirunavukarasu and Shi 2016). Chaperones can fold the nascent peptide, and control aggregation and disaggregation of the precursor proteins (Gorenberg and Chandra 2017). Moreover, they can also refold and facilitate degradation of misfolded proteins. In addition, in some case chaperones can help in transporting the client proteins to the proper place (Tebbenkamp and Borchelt 2010).

The chaperones could be classified into several groups: Hsp100 family, Hsp90 family, Hsp70 family, Hsp60 family, Hsp40 family and small heat shock proteins (Li et al. 2019).

Hsp100 proteins' main functions are promoting protein refolding and repairing the denatured proteins. Hsp100 always cooperates with the Hsp70 system or promotes the degradation of proteins. It can function in a manner similar to the unfoldases that transport the misfolded proteins to the ClpP protease.

Hsp90 family proteins are primarily responsible for the folding, maturation, stabilization and activation of client proteins and for multiprotein complexes' assembly. It uses ATP hydrolysis to mediate these functions in a cycle that involves binding to client proteins. Hsp90 can also facilitate conformational changes, and releasing of client proteins in their active state. Hsp90s are crucial for diverse cellular pathways and are involved in signal transduction, protein repair, and maintenance of proteostasis. Thus, Hsp90 proteins are essential for cell survival and are linked to various diseases when overexpressed (Makhnevych and Houry 2012; Chiosis et al. 2023)

The primary functions of Hsp70s are the preservation of cellular protein homeostasis (proteostasis) and the stress response by facilitating protein folding, the refolding of misfolded proteins, the prevention of their aggregation, their transport, and their degradation when irreparable (Ryu et al. 2020). These chaperones perform all these functions via binding to exposed hydrophobic peptide sequences of proteins in an ATP-dependent manner. They can also act in conjunction with co-chaperones like Hsp40, to regulate the binding and release of

the proteins. Apart from these basic functions, Hsp70s also function in cell signaling, immune response, and are implicated in the pathology of cancer and neurodegenerative diseases.

Hsp60's primary function is protein folding. It acts as a molecular chaperone to maintain protein homeostasis, especially within the mitochondria. It often connects with its co-chaperonin partner Hsp10 (Caruso Bavisotto et al. 2020). However, Hsp60 also has some non-canonical functions. For example, it regulates apoptosis and cell cycle, as well as activates the innate immune system. Moreover, Hsp60 also participates in processes like cell proliferation and carcinogenesis. It is also influenced by post-translational modifications and by interactions with various signaling pathways.

Hsp40s are referred to usually as co-chaperones that are expressed constitutively at normal growth temperatures. They play an important role in protein disaggregation, refolding denatured proteins, and protecting cells from various stresses (Stewart and Schisler 2024).

The function of small heat shock proteins (sHSPs) is preventing misfolded or unfolded proteins from aggregating during cellular stress and helping to maintain protein quality control (Miller and Reichow 2025).

3.5 J protein family, structure and classification

The J protein family is commonly known as the Hsp40 family; however, the majority of its members exhibit a molecular weight significantly different from 40 kDa. Historically, J proteins have been categorized into three classes: class I, class II, and class III, which are also referred to as class A, class B, and class C, respectively (Cheetham and Caplan 1998; Hennessy et al. 2000; Ohtsuka and Hata 2000). Class I J proteins have a C-terminal extension that is now known to bind client proteins, four repeats of the CxxCxgxg type zinc finger motif, a Gly and Phe rich region, and an N-terminal J domain (Goffin and Georgopoulos 1998; Lu and Cyr 1998; Li, Oian, and Sha 2003). C-terminal domain I (CTD I) and CTD II are the two barrel topology domains that make up this kind of C-terminal region. Client proteins are believed to bind to CTD I's hydrophobic pocket, and a zinc-finger domain that protrudes from it may also play a

role in substrate binding (Linke et al. 2003; Kota et al. 2009). Because it is a dimerization domain, the extreme C terminus increases the affinity for clients (Wu et al. 2005). If a protein lacked the zinc-finger domain but had an N-terminal J domain with an adjacent Gly–Phe rich sequence, it was categorized as a member of class II. Class III was assigned to any J protein whose structure did not fit into either class I or class II. More details are shown in figure 3.5.

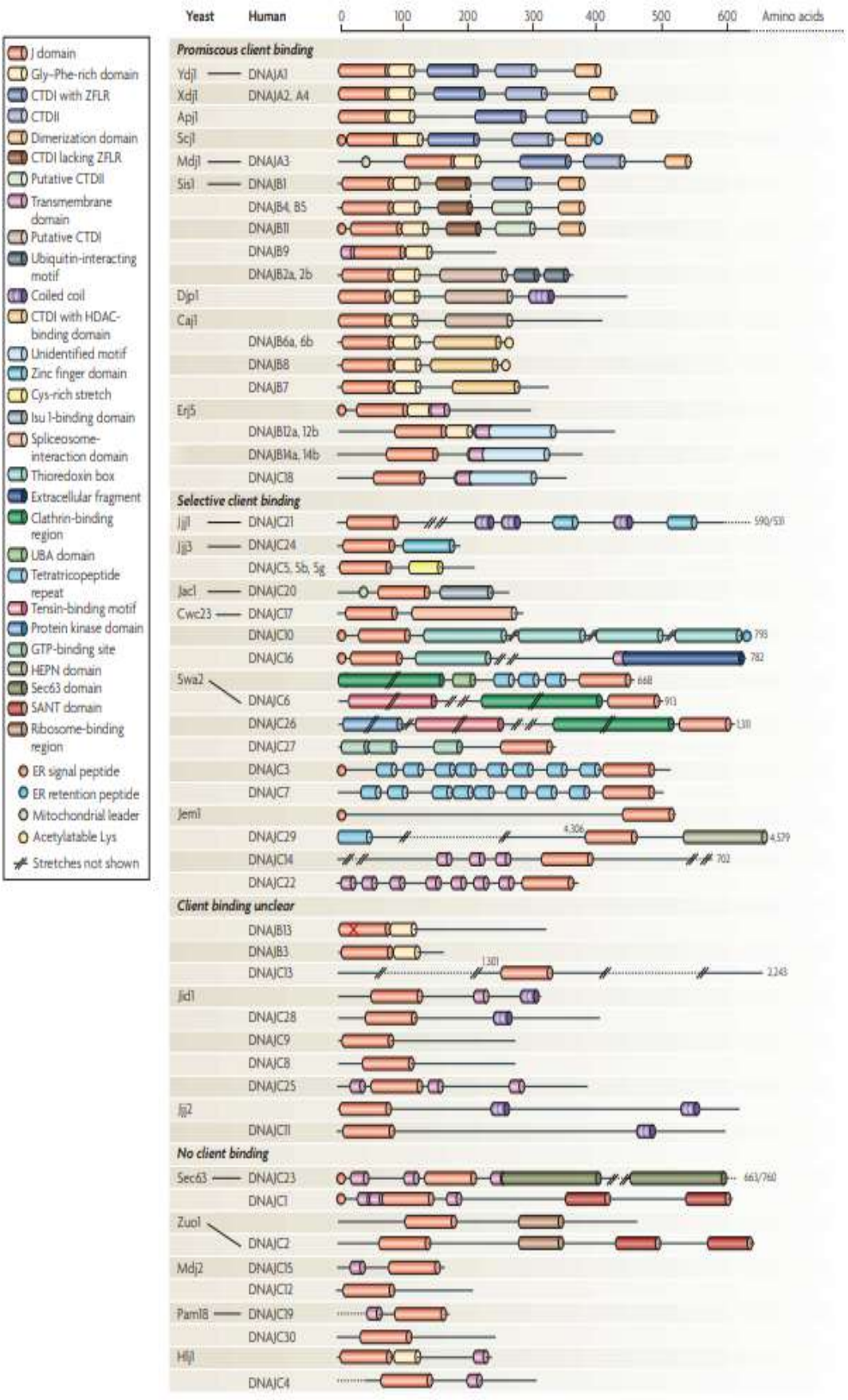
Yeast
Human
0
100
200
300
400
500
600
Amino acids
J domain
Gly–Phe-rich domain
CTDI with ZFLR
CTDII
Dimerization domain
CTDI lacking ZFLR
Putative CTDII
Transmembrane domain
Putative CTDI
Ubiquitin-interacting motif
Coiled coil
CTDI with HDAC-binding domain
Unidentified motif
Zinc finger domain
Cys-rich stretch
Isu 1-binding domain
Spliceosome-interaction domain
Thioredoxin box
Extracellular fragment
Clathrin-binding region
UBA domain
Tetratricopeptide repeat
Tensin-binding motif
Protein kinase domain
GTP-binding site
HEPN domain
Sec63 domain
SANT domain
Ribosome-binding region
ER signal peptide
ER retention peptide
Mitochondrial leader
Acetylatable Lys
Stretches not shown
Promiscous client binding
Ydj1
DNAJA1
Xdj1
DNAJA2, A4
Apj1
Scj1
Mdj1
DNAJA3
Sis1
DNAJB1
DNAJB4, B5
DNAJB11
DNAJB9
DNAJB2a, 2b
Djp1
Caj1
DNAJB6a, 6b
DNAJB8
DNAJB7
Erj5
DNAJB12a, 12b
DNAJB14a, 14b
DNAJC18
Selective client binding
Jjj1
DNAJC21
590/530
Jjj3
DNAJC24
DNAJC5, 5b, 5g
Jac1
DNAJC20
Cwc23
DNAJC17
DNAJC10
793
DNAJC16
782
Swa2
668
DNAJC6
913
DNAJC26
1,311
DNAJC27
DNAJC3
DNAJC7
Jem1
DNAJC29
4,306
4,579
DNAJC14
702
DNAJC22
Client binding unclear
DNAJB13
DNAJB3
DNAJC13
1,301
2,243
Jid1
DNAJC28
DNAJC9
DNAJC8
DNAJC25
Jjj2
DNAJC11
No client binding
Sec63
DNAJC23
663/760
DNAJC1
Zuo1
DNAJC2
Mdj2
DNAJC15
DNAJC12
Pam18
DNAJC19
DNAJC30
Hlj1
DNAJC4

Figure 3.5 Yeast and human J proteins have different domain architectures. Functional orthologues are linked by lines, and members of the *Homo sapiens* J protein family and *Saccharomyces cerevisiae* are grouped based on their known or assumed client-binding capabilities. Some domains and distinctions between yeast and human orthologues are omitted for clarity. Taken from (Kampinga and Craig 2010).

3.6 The structure and the functions of Zuo1

3.6.1 The analysis of Zuo1's structure and functional domain

Zuo1 was initially found in 1992 (Zhang et al. 1992). Later it became clear that Zuo1 and Ssz1 together build the ribosome-associated complex (RAC). It was reported that Zuo1 interacts directly with the ribosome 40s and 60s subunits, while Ssz1 interacts indirectly with the ribosome via its association with Zuo1. The whole RAC complex is located at the nascent polypeptide exit tunnel of the ribosome. The structure of RAC is shown in Figure 3.6.1.

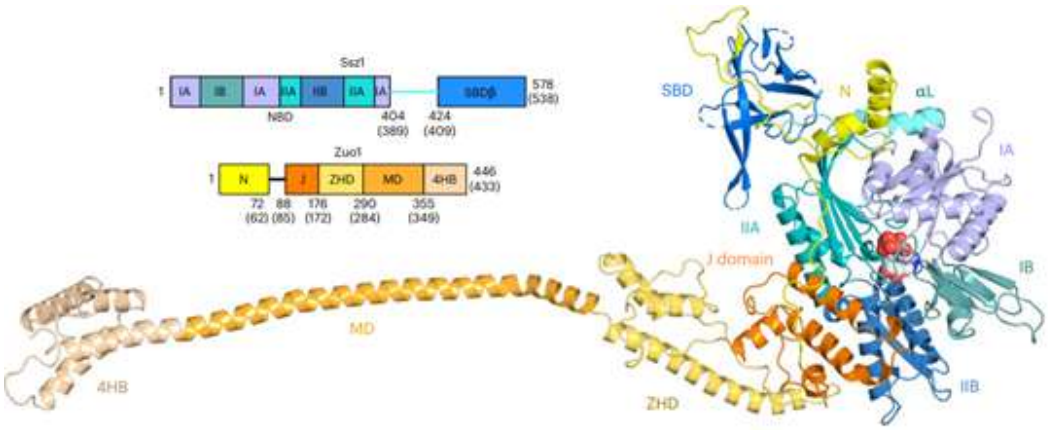

Figure 3.6.1 RAC's architecture shows that Ssz1 and Zuo1 are in contact. The domain architecture and cryo-EM structure of C. thermophilum RAC in ribbon representation. (The corresponding residues in S. cerevisiae are shown in parenthesis after the residue numbers for C. thermophilum). Only the RAC-1 conformation is displayed for representational purposes. Ssz1 comprises an NBD (shades of blue), a linker (αL; cyan) and SBD-β (dark blue). Zuo1 comprises an N-terminal domain (N; yellow), J domain (J; orange), ZHD (pale yellow), MD (pale orange) and four-helix bundle (4HB; tan). ATP is shown in sphere representation. Taken from (Kisonaite et al. 2023).

Zuo1 has a complex domain structure with a long α-helical middle domain (MD), which separates two major functional domains. The N-terminal part has an N-terminal domain (N), the J-domain (J) and the zuotin homology domain (ZHD). Zuo1 contacts the 60 S ribosomal subunit via the ZHD close to Rpl31 (el31) and helix 24 (H24) of the 25 S rRNA at the tunnel

exit. The Zuo1 C-terminal domain has a 4-helix bundle (HD), which contacts the 40S subunit at the tip of helix 44 (h44) and its extension ES12 (Zhang et al. 2020).

The J-domain of Zuo1 has the Histidine-Proline-Aspartic Acid (HPD) motif, which is a critical tripeptide sequence located within the J-domain of J-proteins. The J-domain has several functions. First, it can specifically bind to the ATPase domain of Hsp70, which is the important partner chaperone for J-domain proteins (Greene, Maskos, and Landry 1998; Zhang et al. 2023). Second, it can activate the Hsp70. Once it binds to the J-domain, the Hsp70 chaperone undergoes an allosteric transition that promotes the hydrolysis of ATP (Kelley 1998; Tomiczek et al. 2020). Third, after the J-domain has recruited and activated Hsp70, it effectively directs specific cellular proteins to Hsp70 for folding, refolding, or other quality control functions (Kelley 1998; Ruger-Herreros et al. 2024). Finally, the J-domain acts as a necessary co-chaperone that regulates the activity of Hsp70 (Kelley 1998; Zhang et al. 2023; Ruger-Herreros et al. 2024).

3.6.2 The function of RAC

The ribosome-associated complex (RAC) functions as a chaperone that interacts with ribosomes to guide nascent polypeptide chains, facilitating their initial folding, preventing aggregation, and ensuring translational fidelity by recruiting Hsp70 chaperones (Zhang, Sinning, and Rospert 2017; Deuerling, Gamerdinger, and Kreft 2019). In mammals, RAC also plays a surveillance role in the unfolded protein response (UPR) by modulating the activation of the IRE1α pathway, highlighting its importance in cellular stress responses beyond protein folding (Wu et al. 2021).

3.6.3 Current state of research on Zuo1 and RAC

Huang et al proposed that Ssz1’s role is to facilitate Zuo1’s ability to function as J-protein partner of Ssb on the ribosome (Huang et al. 2005). Another study uncovered a novel function for Zuo1 and Jjj1, and indicated that eukaryotes use two distinct ribosome-anchored J domain proteins to link chaperones to the ribosome assembly process (Albanèse, Reissmann, and

Frydman 2010). Yet another report suggested that human Mpp11 J protein had similar function to that of Zuotin in the yeast cells (Hundley et al. 2005). It was also found that the RAC-Ssb complex is fine-tuning the rate of translation upon TORC1 inhibition, so that the proteostasis is maintained (Black et al. 2023).

DNAJC2, also known as ZRF1 (zuotin-related factor 1) or MPP11 (M-phase phosphoprotein 11), is the mammalian homolog of yeast Zuo1. Previous studies have identified Zrf1 as a novel regulator of the mesodermal lineage that might facilitate spatiotemporal expression of genes (Kaymak and Richly 2016), or as a novel S6 kinase substrate that drives the senescence programme (Barilari et al. 2017). Thus, it is not surprising that DNAJC2 is required for mouse early embryonic development (Helary et al. 2019).

However, despite this progress, the potential involvement of DNAJC2 in diseases, such as cancer and neurodegenerative diseases, is still unknown. In addition, the post-translational modifications of the protein are still unexplored.

It is known that Zuo1 is a ribosome-associated chaperone protein that plays a key role in maintaining cellular proteostasis. But there was no report about the link between Zuo1 and the biogenesis of mitochondrial proteins.

4 Aims of this study

The purpose of this research was to analyze the effect of Zuo1 on mitochondrial protein biogenesis, stability, and correct complex formation at different temperatures as well as under varying growth conditions. This study also attempted to identify which step(s) in the process of biogenesis of mitochondrial proteins is/are affected by *ZUO1* by analyzing yeast strains deleted of *ZUO1* for the level and integrity of mitochondrial proteins. In this work, I also addressed potential genetic and functional interactions of Zuo1 with the mitochondrial import receptors Tom70 and Tom71 by analyzing cellular fitness, growth potential and mitochondrial protein homeostasis at physiological temperature (30°C) and heat stress (37°C). By combining biochemical approaches with growth assays in various media and temperatures, this work will examine whether Zuo1 acts together with or apart from Tom70/Tom71 in preserving mitochondrial protein biogenesis, as well as cell survival under either normal conditions or stress.

5 Materials and methods

5.1 Materials

5.1.1 Media

All media components, including carbon sources and amino acid stock solutions, were individually sterilized by autoclaving prior to use. Carbon sources (glucose, galactose, and glycerol) were supplemented to a final concentration of 2% (v/v). For synthetic media formulations, amino acids (from 100 × stock solutions) were incorporated to select for specific auxotrophic markers. The complete media compositions are detailed in Tables 1 and 2.

Table 1. Composition of media for *Saccharomyces cerevisiae* cultivation

Media	Composition
YP media	2% (w/v) bacto peptone, 1% (w/v) yeast extract, 2% (v/v) carbon source, pH adjusted to 5.5 with NaOH.
Lac media	0.3% (w/v) yeast extract, 0.05% (w/v) glucose, 0.05% (w/v) NaCl, 0.1% (w/v) KH_2PO_4, 0.1% (w/v) NH_4Cl, 0.06% (w/v) $MgCl_2{\cdot}6H_2O$, 0.05% (w/v), $CaCl_2{\cdot}2H_2O$, 2.5% (v/v) lactic acid 80%, 0.8% (w/v) NaOH, pH adjusted to 5.5 with NaOH.
Synthetic (S) media	0.19% (w/v) yeast nitrogen base without ammonium sulfate, 0.5% (w/v) ammonium sulfate, 0.0055% (w/v) adenine sulfate, 0.0055% (w/v) uracil, 2% (v/v) carbon source,1% (v/v) amino acid stock solution, pH adjusted to 5.5 with NaOH.
YP agar	2% (w/v) bacto peptone, 1% (w/v) yeast extract, 2% (w/v) agar, 2% (w/v) glucose or 3% (v/v) glycerol, pH adjusted to 5.5.
S agar	2% (w/v) agar, 0.19% (w/v) yeast nitrogen base without ammonium sulfate, 0.5% (w/v) ammonium sulfate, 0.0055%(w/v) adenine sulfate, 0.0055% (w/v) uracil, 2% (v/v) carbon source,1% (v/v) amino acid stock solution, pH adjusted to 5.5 with NaOH.
D-Glucose stock solution	40% (w/v) D-glucose
Glycerol stock solution	100% glycerol
D-Galactose stock solution	40% (w/v) D-galactose
100X amino acid stock	0.2% (w/v) arginine, 0.4% (w/v) tryptophan, 1% (w/v) leucine, 0.4% (w/v) lysine, 0.2% (w/v) histidine, 0.6% (w/v) phenylalanine, 0.2% (w/v) methionine

Table 2. Composition of media for *Escherichia coli* cultivation

Media	Composition
LB medium	1% (w/v) bacto-tryptone, 0.5% (w/v) yeast extract and 0.5%(w/v) NaCl in sterile H_2O, pH 7.0.
LB agar	LB media + 2 % (w/v) agar
LB medium with ampicillin	Ampicillin stock solution was made of 100 mg/ml in H_2O and sterile filtered. LB medium was supplemented with a final conc. of 100 µg/ml ampicillin. Ampicillin stock solution was added to autoclaved medium or agar solutions only when solutions were below 50°C.

5.1.2 Buffers

Various buffer systems were employed throughout this study, with compositions optimized for specific applications as detailed in Tables 3-8.

Table 3. Electrophoresis buffers

Name	Composition
1×TAE buffer	40 mM Tris-base, 1.14 ml/l acetic acid, 1 mM EDTA, pH 8
10× DNA loading dye	6% (v/v) glycerol, 0.05% (w/v) bromophenol blue, 0.05% (w/v) xylenecyanol

Table 4. Bacterial transformation buffers

Name	Composition
Tfb1 buffer	30 mM potassium acetate, 100 mM RbCl, 100 mM $CaCl_2$, 50 mM $MnCl_2$, 15%(v/v) glycerol, pH adjusted to 5.8 with acetic acid.
Tfb2 buffer	100 mM MOPS, 75 mM $CaCl_2$, 10 mM RbCl, 15% (v/v) glycerol, pH adjusted to 6.5 with NaOH.

Table 5. Mitochondrial isolation buffers

Name	Composition
Resuspension buffer	100 mM Tris, 10 mM DTT
Spheroplasting buffer	1.2 M sorbitol, 20 mM potassium phosphate, pH 7.2
Homogenization buffer	0.6 M sorbitol, 1 mM EDTA, 1 mM PMSF, 0.2% (w/v) fatty acid-free BSA, 10 mM Tris 7.4 pH adjusted with HCl.
SEM buffer	250 mM sucrose, 1 mM EDTA, 10 mM MOPS, pH adjusted to 7.4 with KOH.

Table 6. Buffers for SDS-PAGE, Western blotting and immunodecoration

Name	Composition
SDS-PAGE sample buffer buffer	4% (w/v) SDS, 20% (v/v) glycerol, 0.02% (w/v) bromophenol blue, 5% (v/v) β-mercaptoethanol,160 mM Tris, pH adjusted to 6.8 with HCl.
SDS-running buffer	50 mM Tris, 1.61 M glycine, 1 g/l SDS
Blotting buffer	20 mM Tris, 150 mM glycine, 0.02% (w/v) SDS, 20% (v/v) methanol
Ponceau staining solution	8.5 ml of 72% TCA, 0.4 g Ponceau for 200 ml total volume
TBS buffer	10 mM Tris, 154 mM NaCl, pH adjusted to 7.5 with HCl
TBST buffer	TBS buffer, 0.05% (v/v) Tween20
Blocking buffer	5% (w/v) powdered skim milk in TBS buffer
ECL	0.2 mM p-coumaric acid, 1.25 mM Luminol, 100 mM Tris, pH adjusted to 8.5 with HCl. 30% H_2O_2 was added before use in ratio 1:1000 to the ECL solution.

Table 7. Buffers for blue native PAGE

Name	Composition
3X Gel buffer	200 mM ε-Amino-n-caproic acid, 150 mM Bis-Tris, pH adjusted to 7.0 with HCl
Solubilization buffer	0.1 mM EDTA, 50 mM NaCl, 10% (v/v) glycerol, 1 mM PMSF, 20 mM Tris, pH adjusted to 7.4 with HCl
10× Cathode buffer A	500 mM Tricine, 150 mM Bis-Tris, 0.2% (w/v) Coomassie G, pH 7.0
10× Cathode buffer B	500 mM Tricine, 150 mM Bis-Tris, pH 7.0
10× Anode buffer	500 mM Bis-Tris, pH adjusted to 7.0 with HCl
10× loading buffer	5% (w/v) Coomassie blue G, 500 mM ε-Amino-n caproic acid, 100 mM Bis-Tris, pH 7.0

Table 8. Buffers for pull-down assay

Name	Composition
Pull-down buffer	50 mM sodium phosphate, 10 mM MOPS, 20 % glycerol, pH adjusted to 7.5.
Solubilization buffer	1.2% digitonin, 0.5% Triton X-100 or 0.5% DDM in pull-down buffer

5.1.3 Enzymes and molecular biology reagents

Restriction enzymes and associated buffers were obtained from New England Biolabs. KOD DNA polymerase was bought from Novagen. Yeast cell wall digestion was performed using zymolyase (Seikagaku). All enzymes were used according to manufacturers' protocols.

5.1.4 Antibodies

Immunodetection was performed using the antibodies listed in Table 9, with appropriate HRP-conjugated secondary antibodies (anti-rabbit 1:10,000, anti-rat 1:1,000, anti-mouse 1:3,000). Primary antibodies were diluted in blocking buffer (5% skim milk in TBS).

Table 9. Antibody specifications

Antibody raised against	Species	Dilution	Source
Zuo1	Rabbit	1:15000	Rospert's Lab
Tob55	Rabbit	1:2000	Lab stock
Tom20	Rabbit	1:4000	Lab stock
Tom22	Rabbit	1:1000	Lab stock
Hsp82	Rabbit	1:20000	Buchner's Lab
Fis1	Rabbit	1:1000	Lab stock
Hsp26	Rabbit	1:2000	Buchner's Lab
Sis1	Rabbit	1:25000	Lab stock
Porin	Rabbit	1:5000	Lab stock
Hsp42	Rabbit	1:4000	Buchner's Lab
Bmh1	Rabbit	1:1500	Lab stock
Tom70	Rabbit	1:1000	Lab stock
Hsp104	Rabbit	1:25000	Buchner's Lab
Om45	Rabbit	1:1000	Lab stock
Tom71	Rabbit	1:250	Lab stock
AAC2	Mouse	1:500	Lab stock
Ssa1	Rabbit	1:20000	Lab stock
Om14	Rabbit	1:1000	Lab stock
Fum1	Rabbit	1:10000	Lab stock
Pic2	Rabbit	1:1000	Lab stock
Hxk1	Rabbit	1:2000	Lab stock
Hch1	Rabbit	1:4000	Lab stock
HA	Rat	1:1000	11867423001, Roche

Phospho-RPS6	Rabbit	1:2000	29223-1-AP, Proteintech
Rabbit IgG HRP conjugate	Goat	1:10000	1721019, Bio-Rad
Rat IgG HRP conjugate	Goat	1:1000	Ab6845, Abcam
Mouse IgG HRP conjugate	Goat	1:3000	1721011, Bio-Rad

5.1.5 Yeast and *E. coli* strains

E. coli XL10 Gold was used for cloning and plasmid propagation. The *S. cerevisiae* strains employed in this study are listed in Table 10, with genetic modifications generated using the homologous recombination technique. Plasmids and primers used for strain construction are detailed in Tables 11 and 12.

Table 10. Strains used in this study

Yeast Strains	Genotype	Source
BY4741 Wild Type with Kan cassette	MATa his3Δ1 leu2Δ0 met15Δ0 ura3Δ0 *HO*::KAN	Maya Schuldiner's lab
*zuo*1Δ (BY4741)	MATa his3Δ1 leu2Δ0 met15Δ0 ura3Δ0 *ZUO1*::KAN	Dr. Layla Drwesh
*tom*70Δ (BY4741)	MATa his3Δ1 leu2Δ0 met15Δ0 ura3Δ0 *TOM70*::KAN	Dr. Layla Drwesh
*tom*71Δ (BY4741)	MATa his3Δ1 leu2Δ0 met15Δ0 ura3Δ0 *TOM71*::KAN	Dr. Nitya Aravindan
*tom*70/*tom*71Δ (BY4741)	MATa his3Δ1 leu2Δ0 met15Δ0 ura3Δ0 *TOM70*::KAN *TOM71*::NatNT2	Dr. Nitya Aravindan
*tom*70/*zuo*1Δ (BY4741)	MATa his3Δ1 leu2Δ0 met15Δ0 ura3Δ0 *TOM70*::NatNT2 *ZUO1*::KAN	This study
*tom*70/*tom*71/*zuo*1Δ (BY4741)	MATa his3Δ1 leu2Δ0 met15Δ0 ura3Δ0 *TOM70*::NatNT2 *TOM71*::HygB *ZUO1*::KAN	This study
GPD Tom70 (BY4741)	MATa his3Δ1 leu2Δ0 met15Δ0 ura3Δ0 NAT::GPDpr *TOM70*	Dr. Nitya Aravindan
*tom*71Δ, GPD Tom70 (BY4741)	MATa his3Δ1 leu2Δ0 met15Δ0 ura3Δ0 *TOM71*::KAN NAT::GPDpr *TOM70*	Dr. Nitya Aravindan

Table 11. Primers used in this study

Primers	Sequence (5'-3')	Remarks
Hyg B Cassette (Tom71D) Fwd	TATATATCTCTACATACTTGTATATACCGAACATAAG AAGCTCTTATGGGTACCACTCTTGAC	Amplification of HygB cassette
Hyg B Cassette (Tom71D) Rev	AGTATTAACTAAAAGTATATATTTGACCAATACCTG ACATATCTTTTAGGGGCAGGGCATGC	Amplification of HygB cassette
KAN Cassette (Zuo1D) Fwd	TTATAAAATCTTCGTTTTGTCTCACATATACCAACA AGAGTAACGGACATGGAGGCCCAGAATACCCTC C	Amplification of KAN cassette
KAN Cassette (Zuo1D) Rev	ATATTCGTATACATTCGTATATATTCTATTCCATTTC TTACGGTATCAGTATAGCGACCAGCATTCACATAC	Amplification of KAN cassette
Tom71 Fwd	AGAGAATTCATGGCCGAAAACTCCCTCCTG	Verified the deletion of *tom*71, contains *EcoR*I restriction site
Tom71 Rev	AGAGGATCCCTAAAGCATGCCTTTAGCC	Verified the deletion of *tom*71, contains *BamH*I restriction site
Zuo1 Fwd	CACACGAATTCATGTTTTCTTTACCTACC	Gene clone of *zuo*1, contains *EcoR*I restriction site
Zuo1 Rev	CACACGGATCCTCACACGAAGTAGGAC	Gene clone of *zuo*1, contains *BamH*I restriction site

Table 12. Plasmids used in this study

Plasmids	**Promoter**	**Marker(s)**	**Reference**
pYX142	TPI	Leu, Amp	Lab stock
pYX142-*zuo*1	TPI	Leu, Amp	This study
pGEM4pa-yk-Om14-3HA	SP6	Amp	(Drwesh et al. 2022)

pGEM4pa-yk-Tom20-3HA	SP6	Amp	(Drwesh et al. 2022)
pGEM4pa-yk-Mcr1-3HA	SP6	Amp	(Drwesh et al. 2022)
pGEM4-*zuo*1	SP6	Amp	This study
pFA6a-hphMX6	TEF	Amp, Hyg B	Zacharias Fakih
pFA6a-KanMX4	TEF	Amp, KAN	(Drwesh et al. 2022)

5.2 Methods

5.2.1 Methods in molecular biology

5.2.1.1 PCR (Polymerase chain reaction) amplification

Polymerase chain reaction is a method used to amplify a specific DNA template. As a template for PCR, genomic and plasmid DNA were used in this study. A standard PCR reaction system contains in total 50-100 µl liquid. 1-2 µl template plasmid (0.1-10 ng, in total), 1-2 µl forward primer and reverse primer (0.1–0.5 µM, final). 5-10 µl KOD dNTP, 5-10 µl KOD 10× buffer, 3-6 µl KOD $MgSO_4$, 1-2 µl KOD Polymerase, 1.5-3.0 µl DMSO, 31.5-63 µl nuclease free water. PCR was performed in a thermocycler (Biometra) according to the two-step program mentioned below in Table 13.

Table 13: General PCR program used in this study

Step	Temperature	Time and cycles
1	95 °C	5’
2	95 °C	30’’
3	55 °C	15’’
4	70 °C	1’ Step #2 X 29
5	70° C	10’
6	4 °C	Hold

5.2.1.2 Agarose gel electrophoresis

DNA fragments of different molecular masses were separated by agarose gel electrophoresis. They were separated on 0.5 - 2% (w/v) gels prepared in TAE buffer, containing 1% gel red (Biotium). DNA samples were mixed with 10x loading dye prior to loading onto the gel and electrophoresis was performed in TAE buffer. To estimate the size of the DNA fragments, 1 kb

DNA ladder (Fermentas, Gene RulerTM) was loaded in parallel. The bands were visualized by UV-light.

5.2.1.3 DNA extraction from agarose gel

DNA fragments of interest were extracted from the agarose gel on UV-light table. The purification was performed with Fast geneTM extraction kit (NIPPON Genetics) as mentioned in the user manual.

5.2.1.4 Restriction digestion of DNA

Endonucleases enzymes were used for restriction digestion of DNA. The restriction setup for PCR cloning or sub-cloning was done with 1 µg of DNA and incubation at 37°C for 1h. Inactivation of the enzymes was performed as stated in the user manual.

5.2.1.5 Ligation with T4 DNA ligase

Linearized vector and insert were purified with extraction kit (NIPPON Genetics). Ligation reaction was prepared in 20 µl final reaction volume containing different ratio of vector to insert (1:3 or 1:7), 2 µl 10X T4 ligation buffer and 1 µl of T4 ligase (400 units). Ligation sample were incubated overnight at 4 °C in fridge and transformed into XL10 gold *E. coli* cells.

5.2.1.6 Preparation of chemical competent *E. coli* cells

XL10-gold *E. coli* strain was inoculated for overnight culture at 37 °C in LB chloramphenicol medium. The cells were diluted in 400 ml of fresh LB medium to an OD600=0.1 and grown to OD_{600}=0.5. The cells were harvested by centrifugation (3000g, 5 min, 4 °C) in pre-cooled tubes and the cell pellet was re-suspended in 160 ml of pre-cooled TfbI buffer (Table 4) and incubated on ice for 15 min. The cell suspension was harvested by centrifugation (4000 g, 10 min, 4 °C), the pellet was resuspended in 16 ml pre-cooled TfbII buffer (Table 4) and incubated for 15 min on ice. Aliquots (100 µl) of the competent cells were snap-frozen in liquid nitrogen and stored at -80 °C.

5.2.1.7 Transformation of *E. coli* cells

The plasmid containing gene of interest was transformed into XL10-gold competent cells. The plasmid or ligation mix was added to 100 µl of competent cells and incubated for 30 min on ice. Cells were subjected initially to a heat shock at 42°C for 45 sec and then a cold shock on ice for 2 min. Then, LB medium was added to the cells and incubated at 37°C for 30 min. Next, the cells were harvested by centrifugation (5000g, 5 min, RT) and re-suspended in 100 µl fresh LB medium. The re-suspended cells were plated on LB-Amp agar plates and incubated overnight at 37°C.

5.2.1.8 Large scale plasmid DNA preparation (Midiprep)

E. coli cells were shaken overnight in 50- or 100-ml culture at 37°C. Isolation of plasmid-DNA was done by using PureYield Plasmid Midiprep System (Promega) as mentioned in the user manual. DNA concentration was determined by photometer and the solution was stored at -20°C.

5.2.2 Methods in yeast genetics

5.2.2.1 Strain cultivation

Strains were grown in YP or S media with appropriate carbon sources at 30°C (or specified temperatures) with 120 rpm shaking. For long-term storage, cultures were mixed with 15% glycerol and kept at -80°C.

5.2.2.2 Yeast transformation

Cells were harvested by centrifugation (5000g, 5 min, RT) from freshly growing cells from liquid medium or small number of cells from a plate. The cell pellet was re-suspended in 1 ml of 100 mM lithium-acetate and incubated for 5 min at 30°C with constant shaking at 500 rpm. The cells were collected again by centrifugation (5000g, 5 min, RT) and re-suspended in 240 µl of 50% (w/v) polyethylene glycol 3350, 55 µl H2O, 36 µl 1 M lithium-acetate, 10 µl salmon sperm DNA (5 mg/ml) and 5 µl plasmid DNA or PCR product (100- 600 ng/µl). The cell

suspension was mixed and incubated at 42°C for 30 min with shaking at 800 rpm. The cells were centrifuged (5000g, 5 min, RT) and streaked on a plate with appropriate selective medium. The plates were incubated at 30°C for 2-4 days until single colonies appeared.

5.2.2.3 Gene deletion

Knockout of specific genes was obtained by the homologous recombination technique with the pFA6a-hphMX6 plasmid. For *TOM71* deletion, the ORF was replaced in BY4741 background by the hphMX6 cassette with a PCR product obtained by using the specific primers used in Table 11. The deletion cells were selected on YPD plates with Hygromycin B at 30°C, and the genotype was confirmed by colony PCR with specific primers used in Table 11.

5.2.3 Cell biology methods

5.2.3.1 Drop dilution assay

Yeast cells were cultured overnight in 5 ml of medium. The cultures were diluted to an OD_{600} of 0.2-0.3 and incubated for further 2-4 h until reaching an OD_{600} of 0.8-1.5. Cells equivalent to 2.0 units of OD_{600} were collected, resuspended in 1 ml of sterile water, and the OD_{600} was remeasured. The volume was adjusted to match the lowest OD_{600} among all strains. A 1:10 serial dilutions were prepared, and 4 µl of each dilution were spotted onto agar plates. The plates were incubated at different temperatures for further analysis.

5.2.3.2 Analysis of yeast growth on liquid medium

Yeast cells were grown overnight in 3-5 ml medium at 30°C until reaching an OD_{600} of 1.0. The cells were harvested and resuspended in sterile water to achieve a final OD_{600} of 1.0. A 96-well plate was prepared by adding 180 µl of medium to each well, followed by 20 µl of the cell suspension, resulting in a final OD_{600} of 0.1 per well. The plate was covered with a semi-permeable membrane (Merck, Breathe-easy, Z380059-1PAK) and placed in a plate reader (BMG LABTECH) preheated to the desired temperature. Measurements of the OD_{600} in all wells were initiated immediately.

5.2.3.3 Isolation of mitochondria from yeast cells

Yeast cells were grown in 2–6 L of medium to logarithmic phase and harvested by centrifugation (3000 × g, 5 min, RT). The pellet was resuspended in 100 ml of sterile water, centrifuged again (3000 × g, 5 min, RT), and resuspended in Tris buffer (100 mM Tris, 10 mM 1,4-Dithiothreitol (DTT)). After another centrifugation step (3000 × g, 5 min, RT), the pellet was resuspended in spheroplasting buffer (1.2 M sorbitol, 20 mM potassium phosphate, pH 7.2) containing Zymolyase (6 mg/g wet cells) and incubated for 1 h. The spheroplasts were harvested (2000 × g, 5 min, 4°C) and gently resuspended in homogenization buffer (0.6 M sorbitol, 10 mM Tris, pH 7.4, 1 mM Ethylenediaminetetraacetic acid disodium salt (EDTA), 0.2%(w/v) fatty acid-free Bovine Serum Albumin (BSA), 2 mM phenylmethylsulfonyl fluoride (PMSF)), then the cell were broken using a Douncer homogenizer. Cell debris were removed by two centrifugation steps (2000 × g, 10 min, 4°C). The supernatant was centrifuged twice (18,000 × g, 15 min, 4°C), and the pellet was resuspended in SEM buffer (250 mM sucrose, 10 mM MOPS, 1 mM EDTA, pH 7.2) containing 2 mM PMSF. The mitochondria were pelleted (17,500 × g, 12 min, 4°C), resuspended in 1 ml of SEM buffer with PMSF, aliquoted, flash-frozen in liquid nitrogen, and stored at −80°C.

5.2.3.4 Rapid protein extraction of whole cells

Yeast cells were cultured in liquid medium and harvested at an OD_{600} of 0.5–1.5. Cells equivalent to 10 units of OD_{600} were collected by centrifugation (3000 × g, 5 min, room temperature (RT)). The pellet was resuspended in 800 µl of 0.1 M NaOH and incubated for 5 min at room temperature. After centrifugation (13,000 × g, 1 min, RT), the cells were resuspended in 50 µl of 2× Laemmli buffer containing 5% β-mercaptoethanol. The samples were then incubated at 95°C for 3 min, centrifuged again (13,000 × g, 1 min, RT), and the supernatant was collected for analysis by Sodium dodecyl sulfate polyacrylamide gel electrophoresis (SDS-PAGE) and followed by immunoblotting analysis.

5.2.3.5 In vitro transcription

A transcription mixture was prepared containing 5 µl of 10× transcription buffer, 5 µl of 0.1 M

DTT, 2 µl of RNase inhibitor, 2.5 µl of 10 mM nucleoside triphosphates (NTPs) (final 0.5 mM), 4 µl of 0.5 mM 7-methylguanosine (final conc. 0.04 mM), 5 µg of DNA template, 3.75 µl of SP6 polymerase (75 U), and nuclease-free water to a final volume of 50 µl. The reaction was incubated at 37°C for 1 h, followed by the addition of 5 µl of 10 M LiCl and 150 µl of 96% ethanol (prechilled to −20°C). The RNA was precipitated at −20°C for 30–240 min, pelleted by centrifugation (36,700 × g, 20 min, 2°C), washed with 70% ethanol (prechilled to −20°C), and resuspended in 37 µl of nuclease-free water with 2 µl of RNase inhibitor. Aliquots (12.5 µl) were stored at −80°C.

5.2.3.6 Pull-down assay

A reaction mixture containing energy mix (200 mM HEPES–KOH, pH 7.6; 10 mM ATP; 1 mM GTP; 200 mM Creatine phosphate, 20 mM DTT), 0.06 U/µl creatine phosphokinase, 0.05 M potassium acetate, 0.5 mM magnesium acetate, 0.01 mM complete amino acid mix, 0.2 mM spermidine, 0.2 U/µl RNase inhibitor, mRNA (12.5 µl), and yeast extract (100 µl) was incubated at 26°C for 30 min. Meanwhile, 8 µl of magnetic anti-HA beads were washed with 500 µl of KHM buffer (110 mM potassium acetate, 20 mM HEPES, 2 mM $MgCl_2$, pH 7.4), equilibrated in KHM buffer for 30 min at 4°C on an overhead shaker, and then incubated with the yeast lysate, containing the newly translated protein, for 2 h at 4°C. The beads were washed four times with KHM buffer, with a 10 min incubation during the fourth wash. Bound proteins were eluted in 2× Laemmli buffer containing 0.05% H_2O_2 at 50°C for 10 min, followed by denaturation of the eluate at 95°C for 10 min in the presence of 0.05% β-mercaptoethanol.

5.2.3.7 Preparation of cell-free yeast extract

Yeast cells were grown in 1–2 L of glucose (dextrose)-containing yeast peptone (YPD) medium to an OD600 of 1–2, chilled on ice, and harvested by centrifugation (1500 × g, 5 min, 2°C). The pellet was resuspended in ice-cold Buffer A (30 mM hydroxyeicosapentaenoic acid (HEPES), pH 7.6, 100 mM potassium acetate, 3 mM magnesium acetate, 2 mM DTT) containing 8.5% mannitol. The cells were washed three times through repeated centrifugation (1000 × g, 5 min, 2°C) and resuspension. The final pellet was weighed and resuspended in

Buffer A with 8.5% mannitol and 0.5 mM PMSF (1.5 ml buffer per gram of cells). Glass beads (6 g per gram of cells) were added, and the cells were lysed using a FastPrep-24 homogenizer (6 m/s, 30 s). The lysate was centrifuged (150 × g, 5 min, 2°C) to remove the glass beads and debris, and the supernatant was further clarified by centrifugation (16,000 rpm, 6 min, 2°C). The supernatant was passed through a desalting PD10 column equilibrated with Buffer A containing 0.5 mM PMSF. Fractions (0.5 ml each) were collected, and those with peak absorbance at 260 nm were pooled. The extract was treated with 0.5 M $CaCl_2$ (final conc. 0.001 M) and micrococcal nuclease (1 µl each per 500 µl extract) for 10 min at 26°C, followed by the addition of 0.25 M ethylene glycol bis (β-aminoethylether) tetraacetic acid (EGTA) (5 µl per 500 µl extract). The extract was aliquoted (110 µl), flash-frozen in liquid nitrogen, and stored at −80°C.

5.2.3.8 In vitro transcription

A transcription mixture was prepared containing 5 µl of 10 × transcription buffer, 5 µl of 0.1 M DTT, 2 µl of RNase inhibitor, 2.5 µl of 10 mM nucleoside triphosphates (NTPs) (final 0.5 mM), 4 µl of 0.5 mM 7-methylguanosine (final conc. 0.04 mM), 5 µg of DNA template, 3.75 µl of SP6 polymerase (75 U), and nuclease-free water to a final volume of 50 µl. The reaction was incubated at 37°C for 1 h, followed by the addition of 5 µl of 10 M LiCl and 150 µl of 96%(v/v) ethanol (prechilled to −20°C). The RNA was precipitated at −20°C for 30–240 min, pelleted by centrifugation (36,700 × g, 20 min, 2°C), washed with 70% ethanol (prechilled to −20°C), and resuspended in 37 µl of nuclease-free water with 2 µl of RNase inhibitor. Aliquots (12.5 µl) were stored at −80°C.

5.2.3.9 Phospho-RPS6 detection by Western blot

The strains were inoculated overnight in YPD, diluted in the morning to OD_{600} 0.1, and grown until mid-exponential phase (OD_{600}=0.8) in YPD at 30 C. Treated them with or without 200ng/ml rapamycin for 30min. Cells were collected for 10 units. Then did rapid protein extract which had been shown 5.2.3.4.

5.2.4 Biochemical methods

5.2.4.1 Determination of protein concentration

To determine protein concentration, the Bradford method was applied (Bradford 1976). The protein solution (10 µl) was diluted in 1 ml of Roti-Quant Bradford solution (1:5 dilution in double distilled water) and incubated at room temperature for 5 min in darkness. To determine standard curve, 2-10 µg of BSA from 1 mg/ml stock were used. The absorbance of the samples was measured at 595 nm, and protein concentration was estimated according to the calibration plot.

5.2.4.2 Protein precipitation by chloroform-methanol

To precipitate higher amounts of protein, chloroform-methanol precipitation was performed (Wessel and Flugge 1984). Four volumes of methanol, three volumes of chloroform, and three volumes of water were added to the samples and vortexed thoroughly. The samples were separated by centrifugation (16000g, 1 min, RT) into two phases. The upper phase was carefully removed and three volumes of methanol were added to the lower phase. After vortexing, the samples were centrifuged (16000g, 1 min, RT) and the pellet was air dried at 50°C. Then, the pellet was resuspended with SDS-PAGE sample buffer and incubated at 95°C for 5 min.

5.2.4.3 SDS-PAGE

Protein samples were analyzed under denaturizing condition in 10-15 % SDS-PAGE gels. The SDS gel was casted between two glass plates with 1 mm spacing in between, and to avoid leakage, the bottom gel was separately prepared. The composition of bottom, running, and stacking gel are described in Table 6, and buffer composition in Table 9 above. The protein samples were prepared in SDS-PAGE sample buffer with concentration of 2 µg/µl (15 µg- 100 µg) and denatured at 95°C for 5 min before being subjected to SDS-PAGE. Electrophoresis was performed at 20 mA per gel, for approximately 3 h until the dye front reached the bottom gel. A protein ladder (PAGE RulerTM, Fermentas) was used as a molecular weight marker.

5.2.4.4 Western blotting

Proteins from SDS-PAGE were transferred onto the nitrocellulose membrane (Whatman) by semi-dry blotting technique as described previously(Kyhse-Andersen 1984; Towbin, Staehelin, and Gordon 1979. Three filter papers (3 mm) were soaked in blotting buffer (Table 9) and placed on the blotting apparatus followed by the nitrocellulose membrane. The SDS gel was placed on the membrane, and additional three filter papers were placed on top of the gel. Air bubbles were removed by rolling a glass pipette over the assembled blot. The proteins were transferred for 1.5 h at 220 mA. The efficiency of the protein transfer was monitored by incubating the membrane in Ponceau staining solution for 1-2 min, followed by several washes.

5.2.4.5 Immunodetection of proteins

To avoid unspecific binding of antibodies, membranes with blotted proteins were incubated at room temperature with 5%(w/v) skim-milk in TBS buffer for 1 h. Membranes were briefly washed with TBS before incubating them with primary antibodies at 4°C overnight or at room temperature for 1 h. The membranes were then washed twice with TBS and once with TBST before their incubation at room temperature with secondary antibodies (1:10000) in 5% skim-milk for 1 h. To detect the specific proteins, the secondary antibody was conjugated to HRP. A chemiluminescence signal was obtained upon adding ECL and H_2O_2. This signal was detected by X-ray films (Super RX, Fuji) and these were developed by an X-ray film developing machine (SRX-101A, Konica Minolta). Part of the results also visualized using a ChemiDoc imaging system (Bio-Rad).

5.2.4.6 Blue native PAGE

Mitochondria (100 µg) were solubilized in 45 µl of Buffer N (0.1 mM EDTA, 50 mM NaCl, 10% glycerol, 1 mM PMSF, 20 mM Tris, pH 7.4) containing 1.2% digitonin (digitonin: protein ratio of 5.5:1) for 30 min on ice. After clarifying spin (30,000 × g, 30 min, 4°C), the supernatant was mixed with 10 × loading dye (5 % Coomassie blue G, 500 mM aminocaproic acid, 100 mM Bis-Tris, pH 7.0) (5 µl per lane) and analyzed by BN- PAGE (6%-14% Acrylamide). The gel was run at 250 V for 2.5 h in cathode buffer A (50 mM Tricine, 15 mM Bis-Tris, 0.02% Coomassie

blue G250, pH 7.0), and anode buffer (50 mM Bis-Tris, pH 7.0) followed by a switch to cathode buffer B (50 mM Tricine, 15 mM Bis-Tris, pH 7.0) at 550 V for another 2.5 hr. The gel was equilibrated in SDS running buffer for 5 min, transferred to a PVDF membrane, and processed for immunoblotting. Immunoblotting Protein samples were resolved on either 10% or 12.5% SDS-PAGE and transferred to nitrocellulose membranes using semi-dry blotting. Membranes were blocked in milk (5% milk powder in TBS) for ≥30 min, incubated with primary and secondary antibodies (1 h each), and visualized using a ChemiDoc imaging system.

6 Results

6.1 The absence of Zuo1 decreases growth at normal temperature but enhances growth upon heat stress

To investigate potential genetic interactions between *ZUO1* and *TOM70*/*TOM71*, I monitored the growth of the relevant strains by drop dilution assay on solid medium and growth of liquid cultures. Both assays were performed at different temperatures, either normal (30°C) or enhanced (37°C).

The results of the drop dilution assays and monitoring growth in liquid cultures suggest that, under normal temperature, the combined loss of Tom70 and Tom71 decreased growth at 30°C on glucose rich medium (Figs. 6.1.1 & 6.1.2). Of note, the absence of Zuo1 also decreased the growth of the resulting cells (Figs. 6.1.1 & 6.1.2).

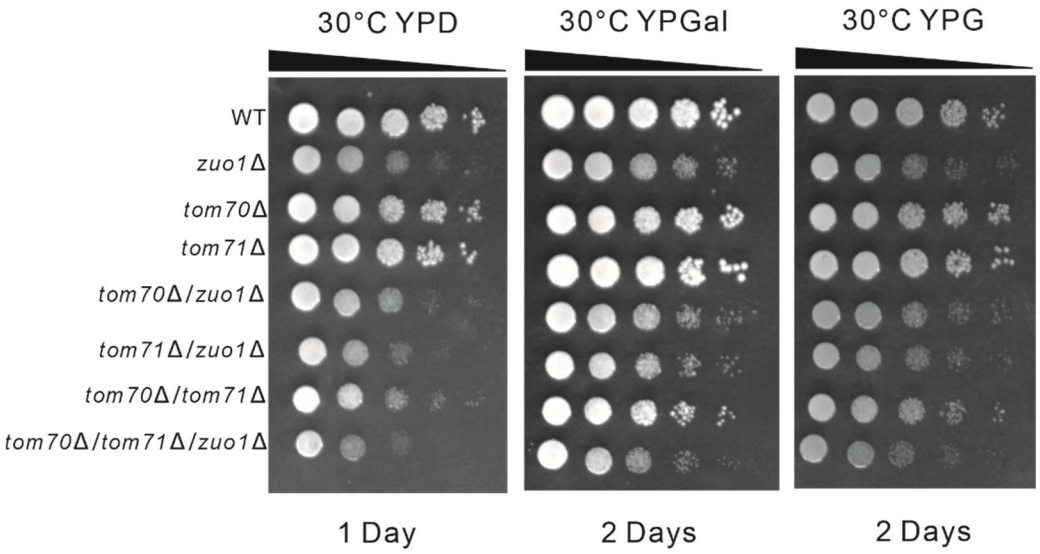

Figure 6.1.1 Deletion of *ZUO1* reduces yeast growth on solid medium at 30°C. The indicated strains' growth was tracked at 30 °C using a drop dilution assay on solid rich medium containing either glucose (YPD), galactose (YPGal) or glycerol (YPG). Images were obtained after the plates had been incubated for a day or two.

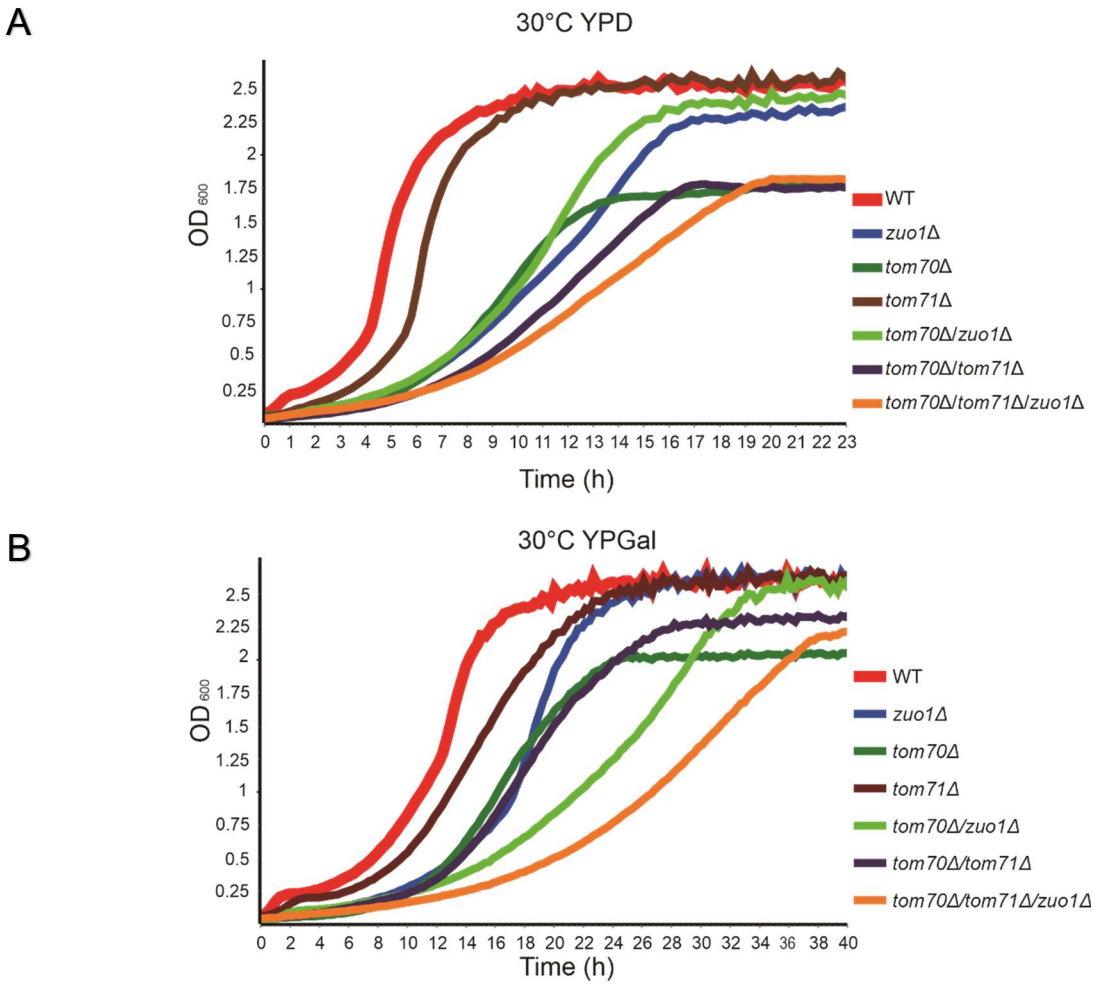

Figure 6.1.2 Deletion of *ZUO1* reduces yeast growth in liquid cultures at 30°C. (A and B) Growth at 30°C of the indicated cells were monitored for 24-40 hours by measurement of OD_{600} in a rich liquid medium containing either glucose (A, YPD) or galactose (B, YPGal) as a carbon source. The cells were diluted to an OD_{600} of 0.1 at the start of the measurements (time 0).

Upon heat stress (37°C), the absence of Tom70 alone or in combination with deletion of Tom71 dramatically decreased cells growth (Figs. 6.1.3 & 6.1.4). In contrast, the single deletion of TOM71 did not cause any growth defect. Interestingly, combining the absence of Zuo1 with deletion of *TOM70* or both *TOM70/71*, resulting in the strains *tom*70Δ/zuo1Δ and *tom*70Δ/*tom*71Δ/ zuo1Δ, respectively, resulted surprisingly in enhanced growth of the cells (Figs. 6.1.3 & 6.1.4).

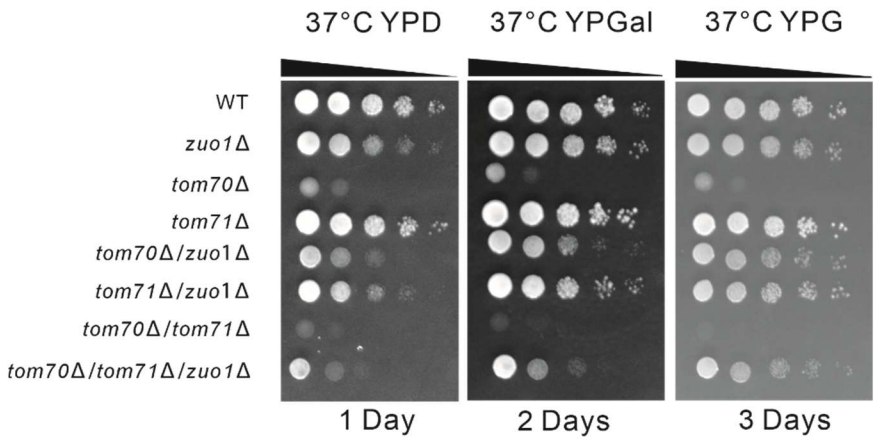

Figure 6.1.3 Loss of Zuo1 enhances the growth of *tom70Δ* and *tom70Δ/tom71Δ* strains under heat stress. The growth of the specified cells was monitored at 37°C using the drop dilution assay. Further analysis was as described in Figure 6.1.2.

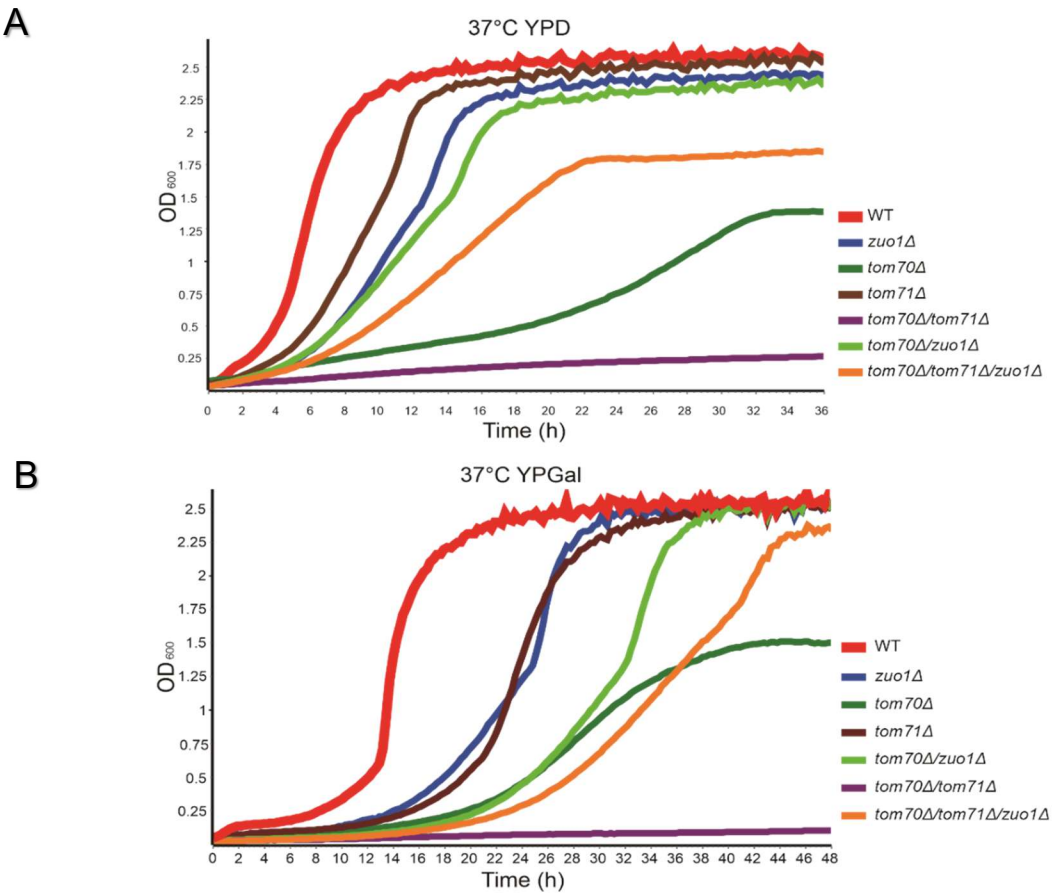

Figure 6.1.4 Loss of Zuo1 enhances the growth of *tom70Δ* and *tom70Δ/tom71Δ* cells under heat stress. (A and B) The growth of the indicated cells at 37°C was observed using the methods outlined in Fig. 6.1.1.

6.2 The absence of Zuo1 changes the proteostasis of cells lacking Tom70/71 both at 30°C and 37°C

The clear phenotype difference between cells grown on either 30°C or 37°C that was observed in the drop dilution and growth curves assays, encouraged me to investigate the protein levels of some cytosolic and mitochondrial outer membrane proteins in these strains.

The absence of Tom70 or both Tom70/71 results in increased amounts of the MOM proteins Om45, Om14, and Mcr1 and the cytosolic chaperones Hsp104, Hsp42 and Hsp26. Of note, these elevated levels reduced back to normal levels, or even lower than normal, upon the additional deletion of ZUO1 on this background. (Figs. 6.2.1 & 6.2.2 & 6.2.3 & 6.2.4). Interestingly, the amounts of some proteins are not affected by the absence of Zuo1. In contrast, the deletion of *TOM70* alone or both *TOM70/TOM71*, the amounts of the MOM proteins Porin, Tom22 and Tob55 are highly compromised (Figs. 6.2.1 & 6.2.2). Of note, upon growth at 30°C, the levels of Tom22 and Porin are reduced only slightly whereas those of Tob55 in the double deletion strain are still reduced (Figs. 6.2.8 & 6.2.9). In addition, the levels of the cytosolic protein Hsp90 increased slightly upon the absence of Zuo1 at 37°C whereas those of Ssa1 increased a little with the absence of Tom70 and Tom70/Tom71 under these conditions (Figs. 6.2.3 & 6.2.4).

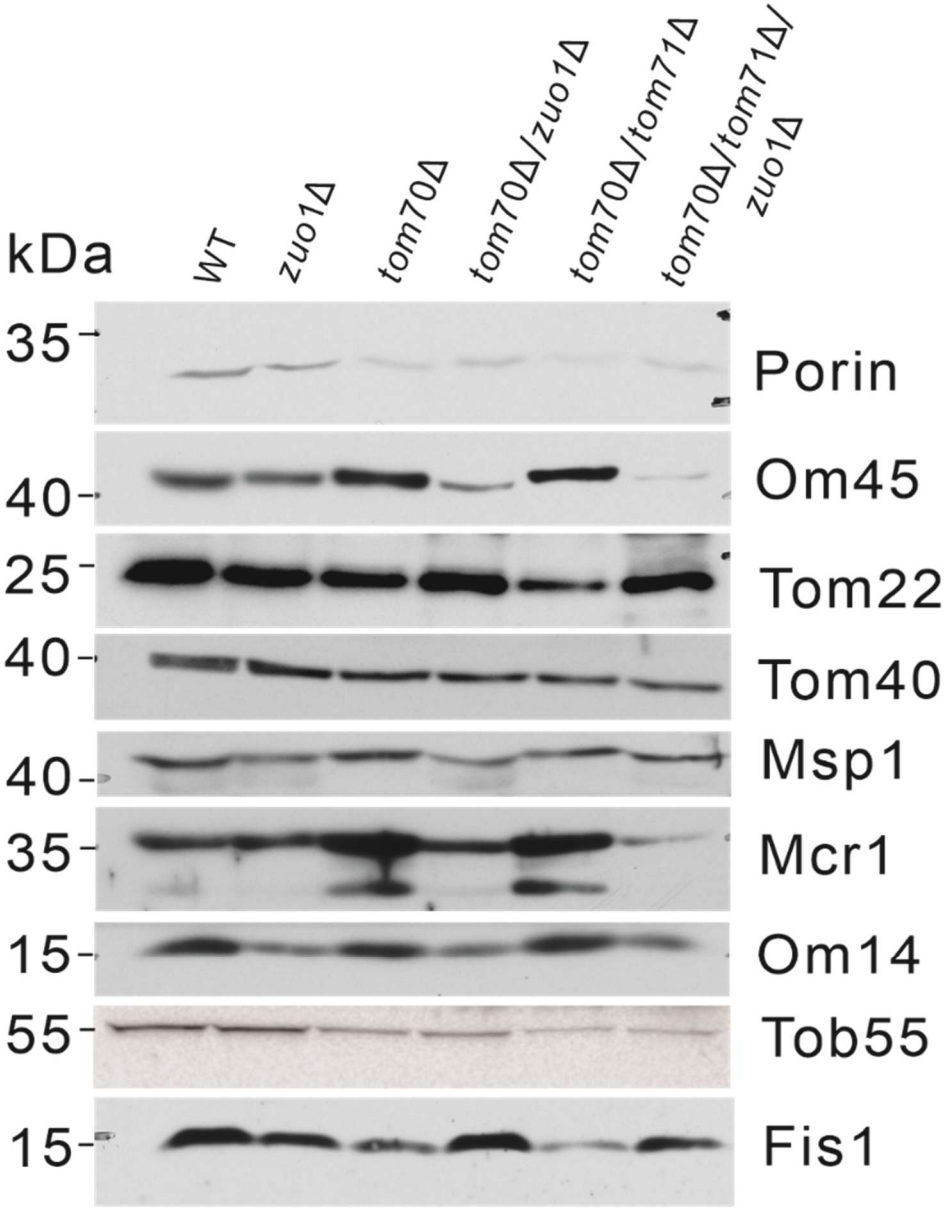

Figure 6.2.1 Steady-state levels of MOM proteins in cells grown under heat stress (37°C) in YPD medium. Proteins were extracted from the specified cells and analyzed by SDS-PAGE and immunodecoration with the indicated antibodies.

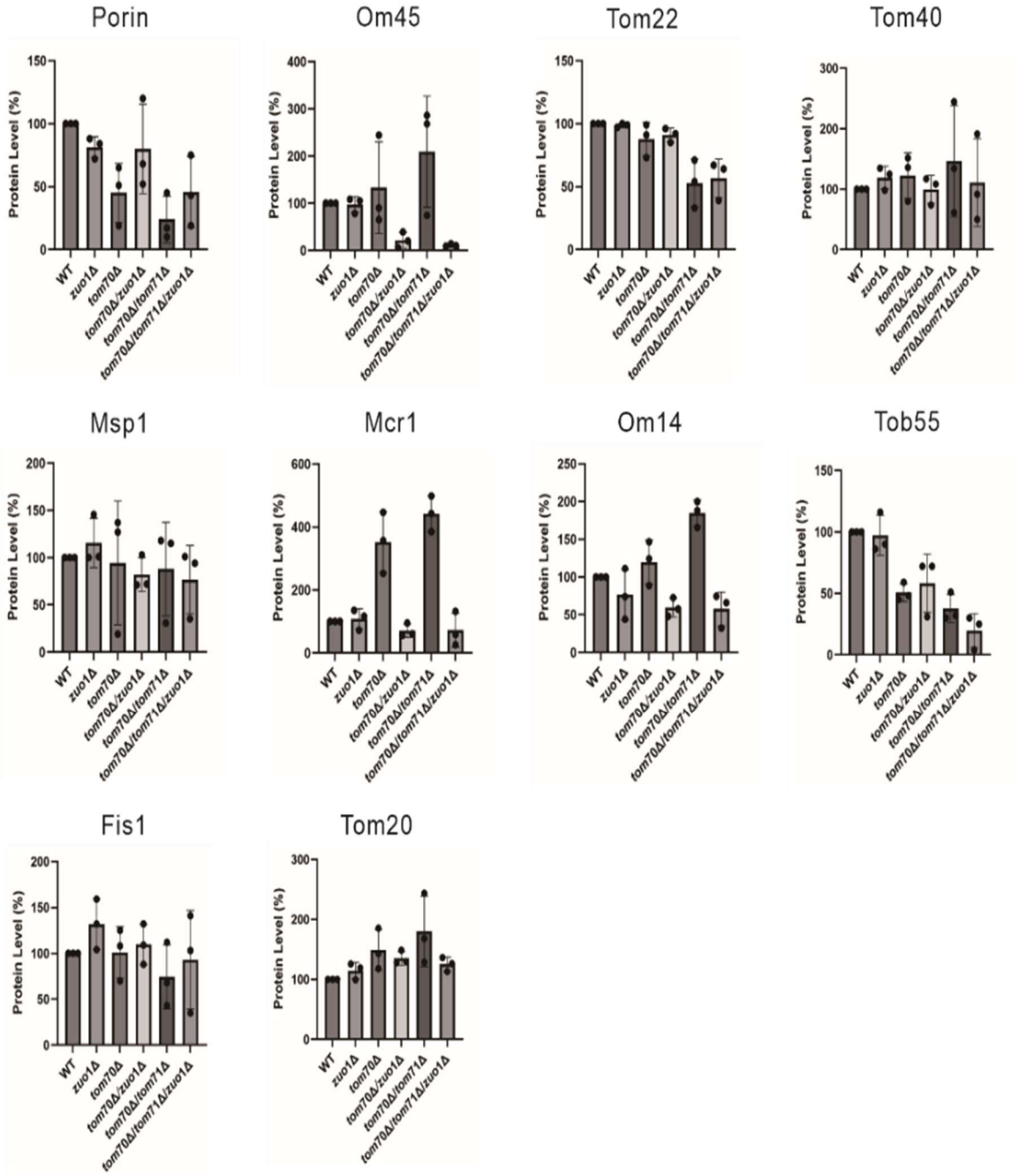

Figure 6.2.2 Quantification of the steady-state levels of MOM proteins in cells grown under heat stress (37°C) in YPD medium. The bands corresponding to the indicated proteins from three independent experiments as the one shown in Fig. 6.2.1 were quantified and normalized to the intensities of the Ponceau S staining. The value of the WT cells was set as 100%. The bar diagram shows the average ± SD of three independent experiments.

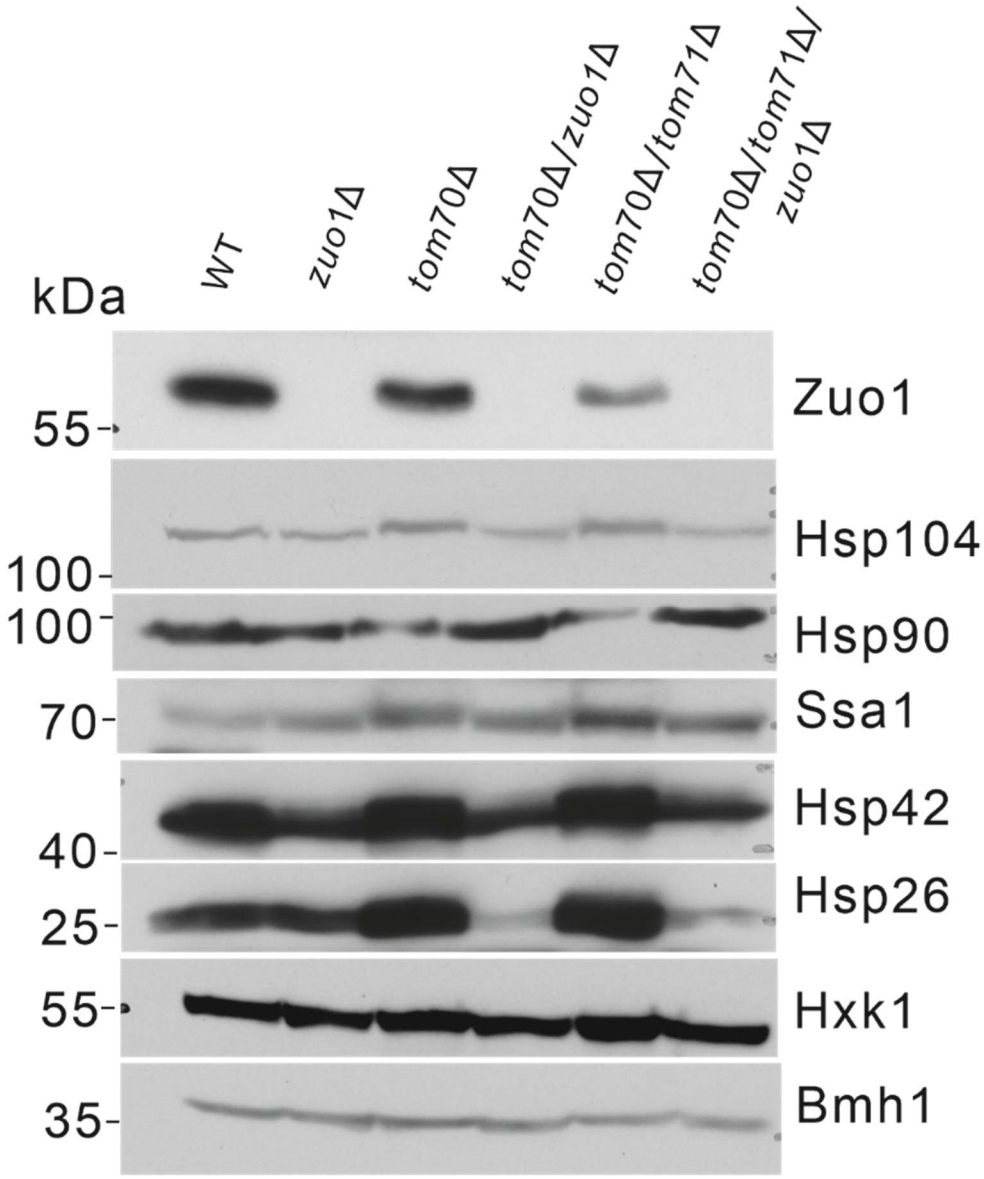

Figure 6.2.3 Steady-state levels of cytosolic proteins in cells grown under heat stress (37°C) in YPD medium. Proteins were extracted from the designated strains and analyzed by SDS-PAGE and immunodecoration with the indicated antibodies.

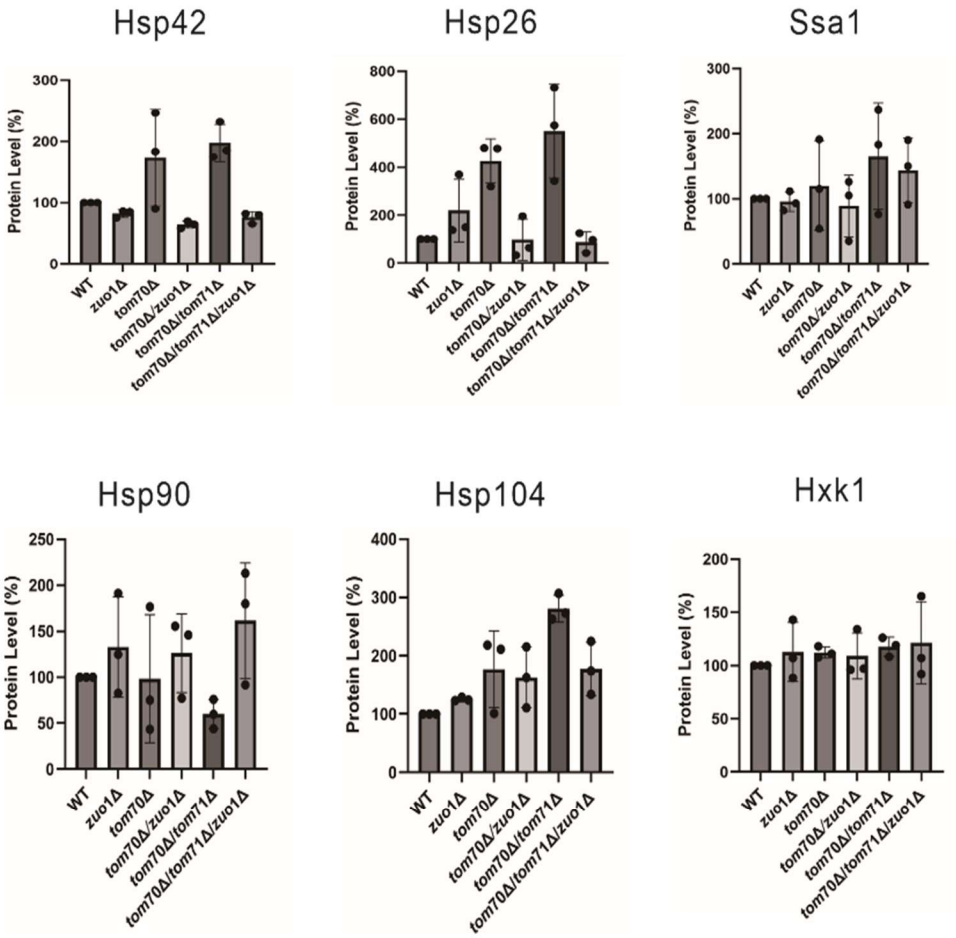

Figure 6.2.4 Quantification of the steady-state levels of cytosolic proteins in cells grown under heat stress (37°C) in YPD medium. The bands corresponding to the indicated proteins from three independent experiments as the one shown in Fig. 6.2.3 were quantified and normalized to the intensities of the Ponceau S staining. The value of the WT cells was set as 100%. The bar diagram shows the average ± SD of three independent experiments.

To better investigate the effect of the double deletion of *TOM70/71* on the levels of mitochondrial proteins, we isolated mitochondria from either control or *tom70/71* cells grown on YPD at 37°C and analysed them by western blotting. As expected, we found reduced levels of the canonical Tom70 clients like the carrier proteins Pic2 (Figs. 6.2.6 & 6.2.7) and the MOM protein Sam50/Tob55 (Figs. 6.2.5 & 6.2.6 & 6.2.7). In addition, the amounts of the MOM proteins Fis1, Tom20, Tom22, as well as the carrier protein Aac2 and the matrix protein fumarase (Fum1) were slightly reduced (Fig. 6.2.6 & 6.2.7).

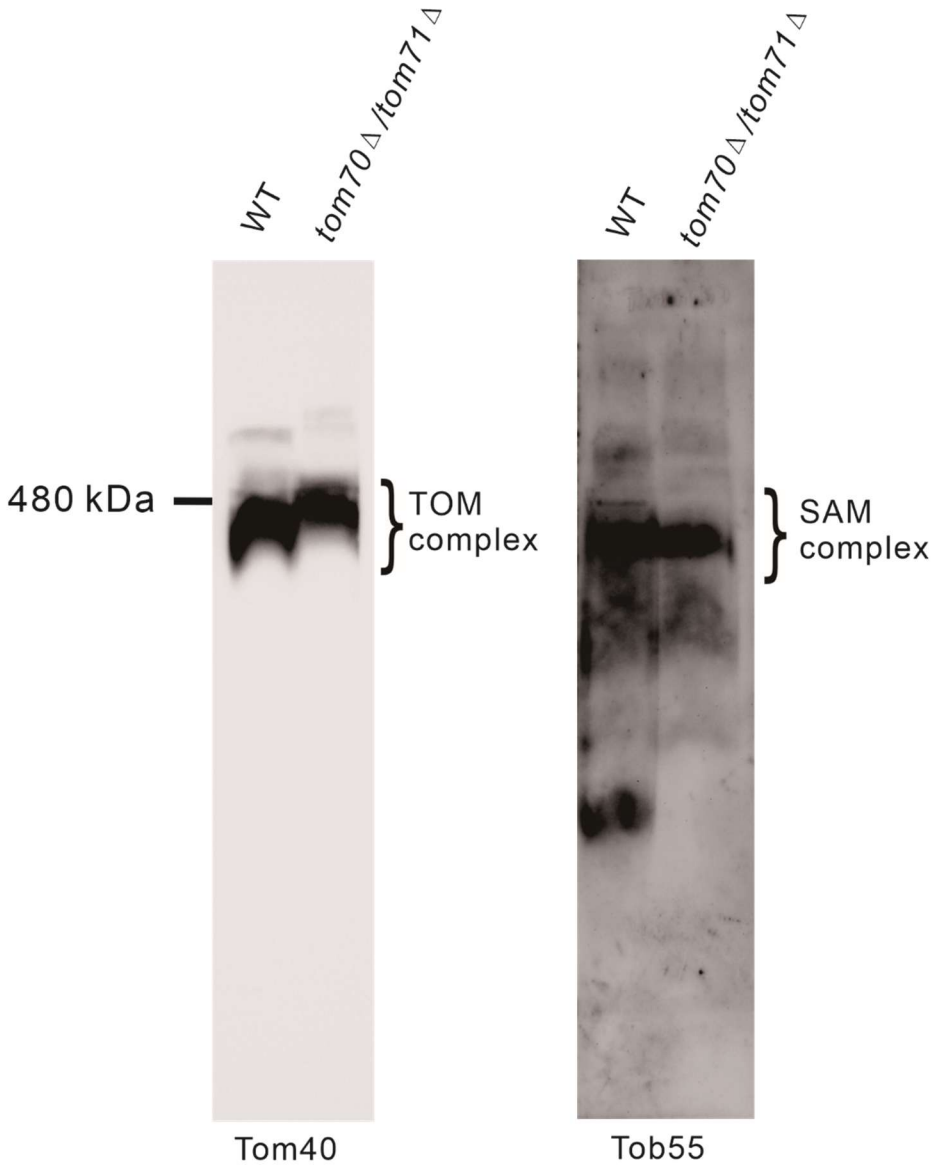

Figure 6.2.5 The loss of *TOM70* and *TOM71* affect the assembly of the SAM/TOB complex. The indicated strains were inoculated in the medium of YPD. Cells were collected in the logarithmic phase. Performed the mitochondrial isolation assay. Mitochondria from the indicated strains were solubilized with 1.2% digitonin (digitonin to protein ratio of 6:1) and analyzed by blue native PAGE. Samples were immunodecorated with the specified antibodies.

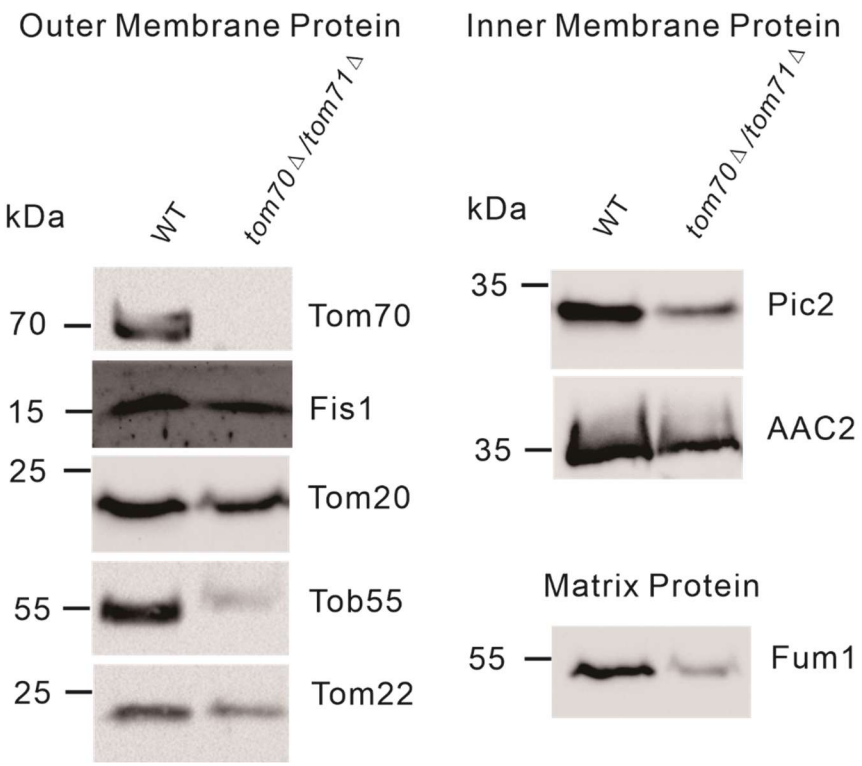

Figure 6.2.6 Under heat stress (37°C), the loss of *TOM70* and *Tom71* causes reduced levels of mitochondrial proteins. The indicated strains were inoculated in the medium of YPD. Cells were collected in the logarithmic phase. Performed the mitochondrial isolation assay. We investigated five OMM proteins' amount. The protein level of Tob55 and Tom22 strongly decreased. Fis1 and Tom20 decreased a little. Two IM protein, Pic2 decreased obviously and AAC2 decreased slightly. In addition, Fum1, a Matrix protein, with also dramatically reduced.

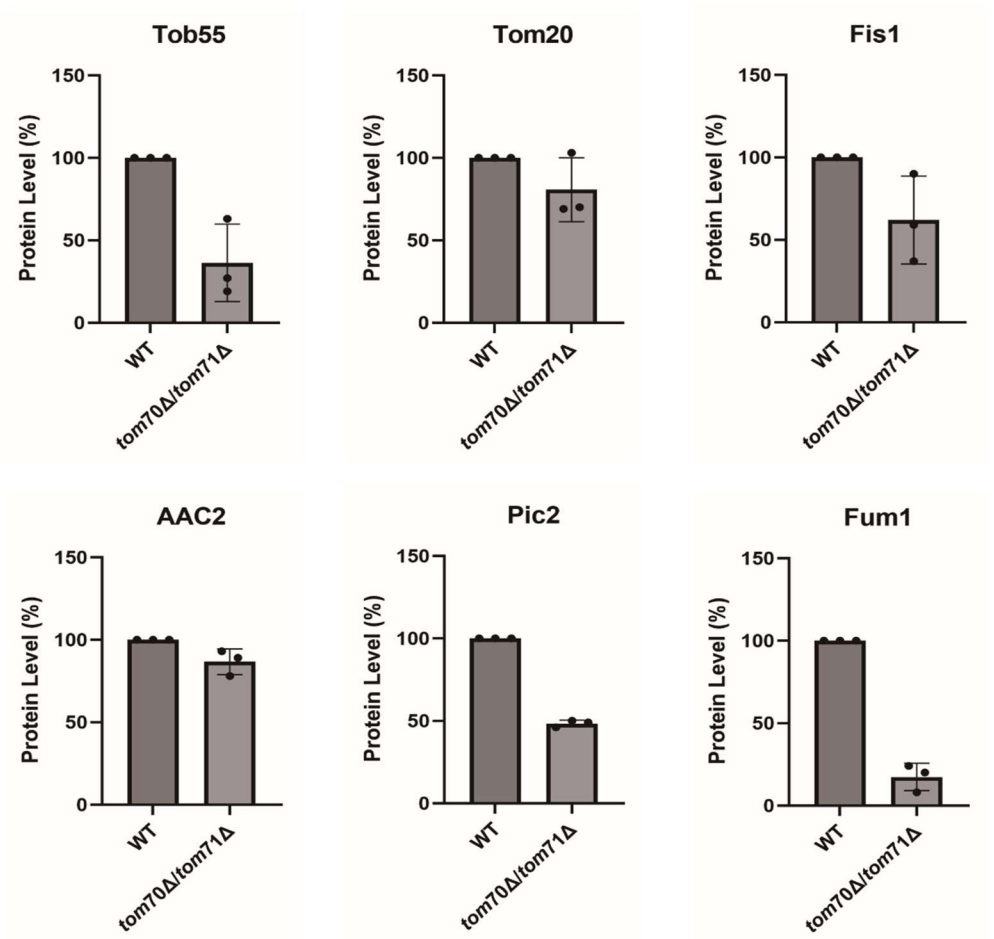

Figure 6.2.7 Quantification of the steady-state levels of cytosolic proteins in cells grown under heat stress (37°C) in YPD medium. The bands corresponding to the indicated proteins from three independent experiments as the one shown in Fig. 6.2.6 were quantified and normalized to the intensities of the Ponceau S staining. The value of the WT cells was set as 100%. The bar diagram shows the average ± SD of three independent experiments.

In previous experiments (Figs. 6.2.1 & 6.2.2 & 6.2.4 & 6.2.8 & 6.2.9), we found that the absence of Tom70/71 resulted in reduced amounts of Sam50(Tob55) at both 30°C and 37°C. To investigate how this change affects the assembly of the SAM/TOB complex, I analysed this complex by blue native PAGE. The results suggest that the double deletion of *TOM70/TOM71* resulted in disappearance of a low Mw band containing Tob55 in the double deletion strain. However, the main specie of the SAM complex appears unaltered in the mutated organelles. As a control, the migration of the TOM complex, as detected by anti-Tom40 antibody, was hardly affected in the organelles from the double deletion cells (Figs. 6.2.8 & 6.2.9).

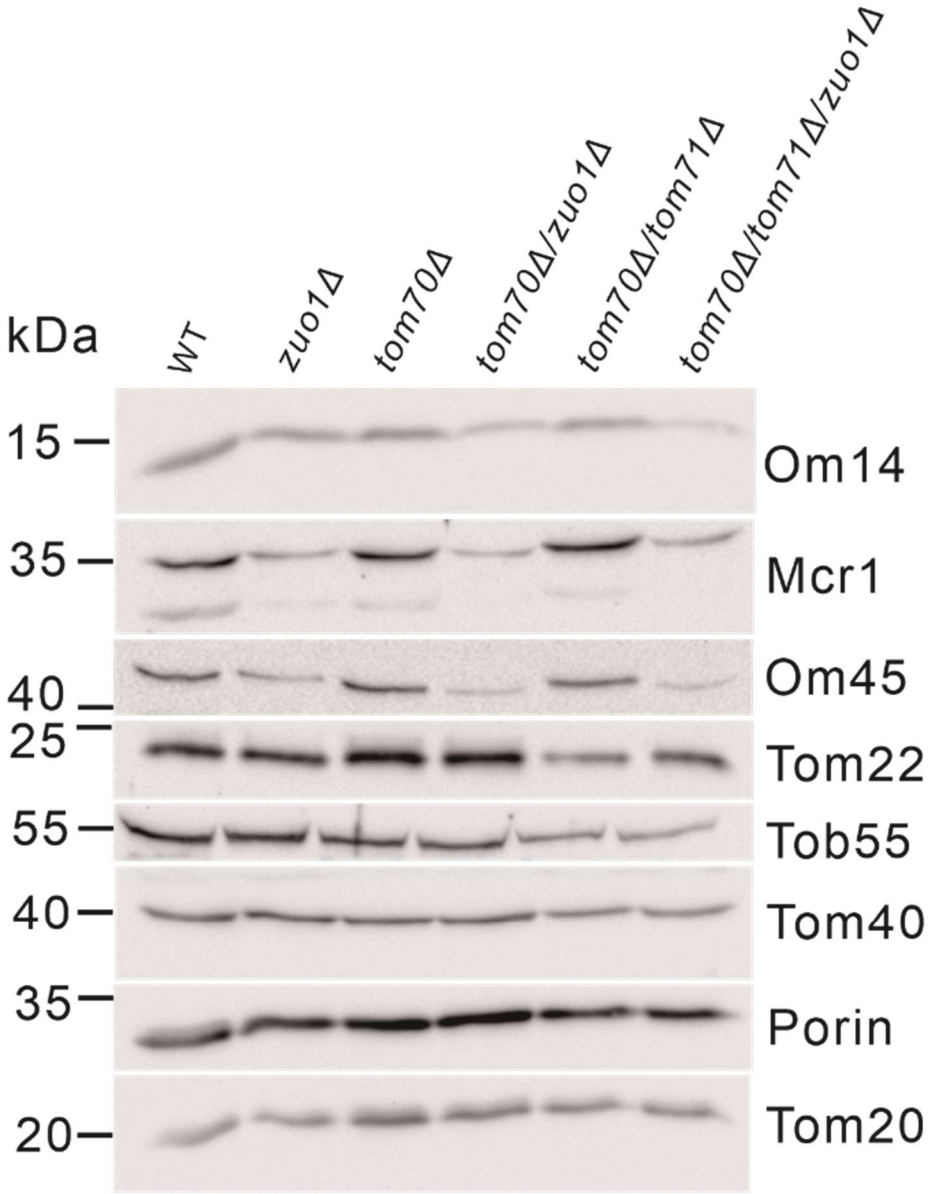

Figure 6.2.8 Yeast mitochondrial outer membrane protein steady-state levels at 30°C in YPD medium. Proteins were extracted from the specified cells and analyzed by SDS-PAGE and immunodecorated with the indicated antibodies.

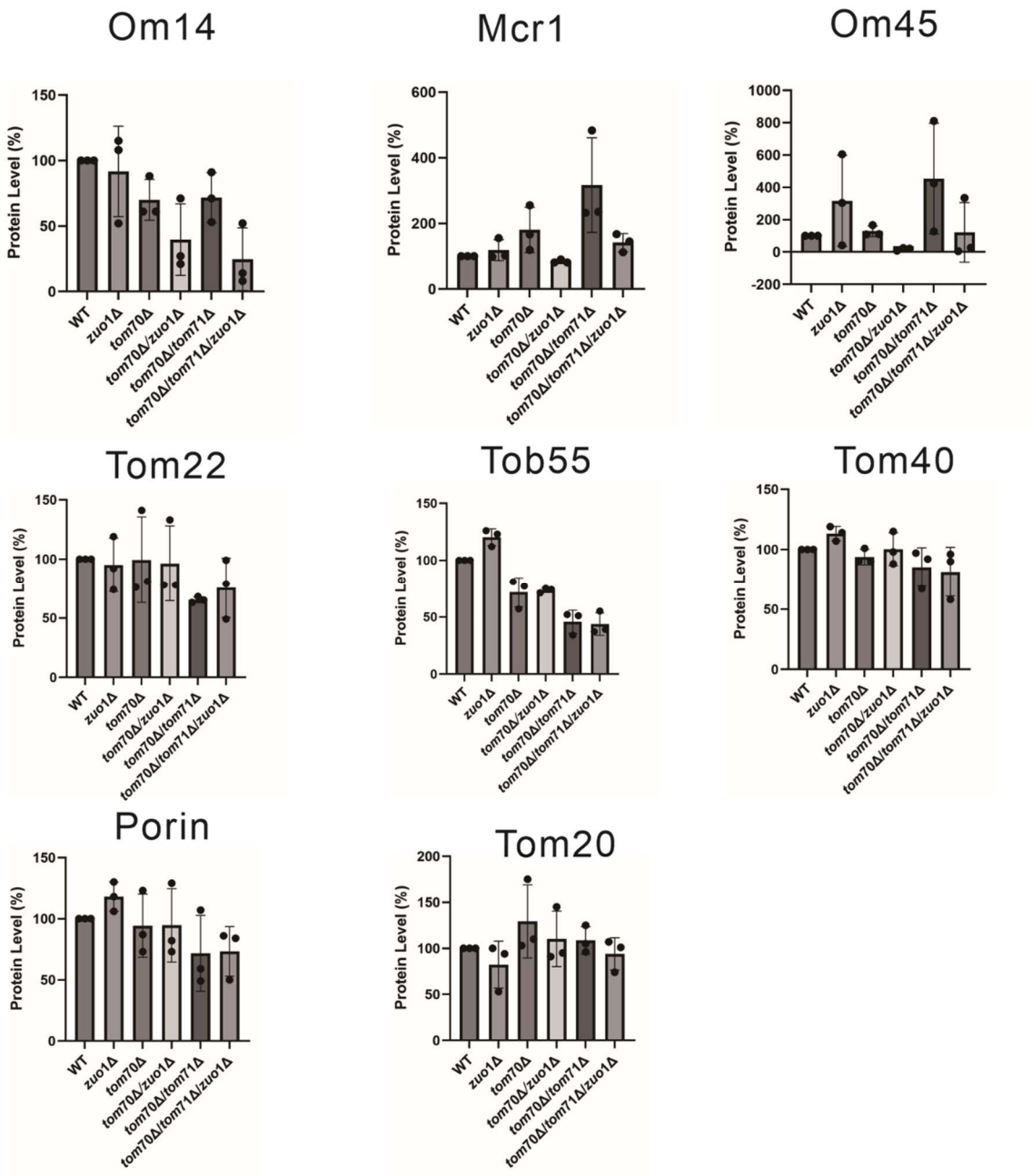

Figure 6.2.9 Quantification of yeast mitochondrial outer membrane protein steady-state levels at 30°C in YPD medium. The bands corresponding to the indicated proteins from three independent experiments as the one shown in Fig. 6.2.8 were quantified and normalized to the intensities of the Ponceau S staining. The value of the WT cells was set as 100%. The bar diagram shows the average ± SD of three independent experiments.

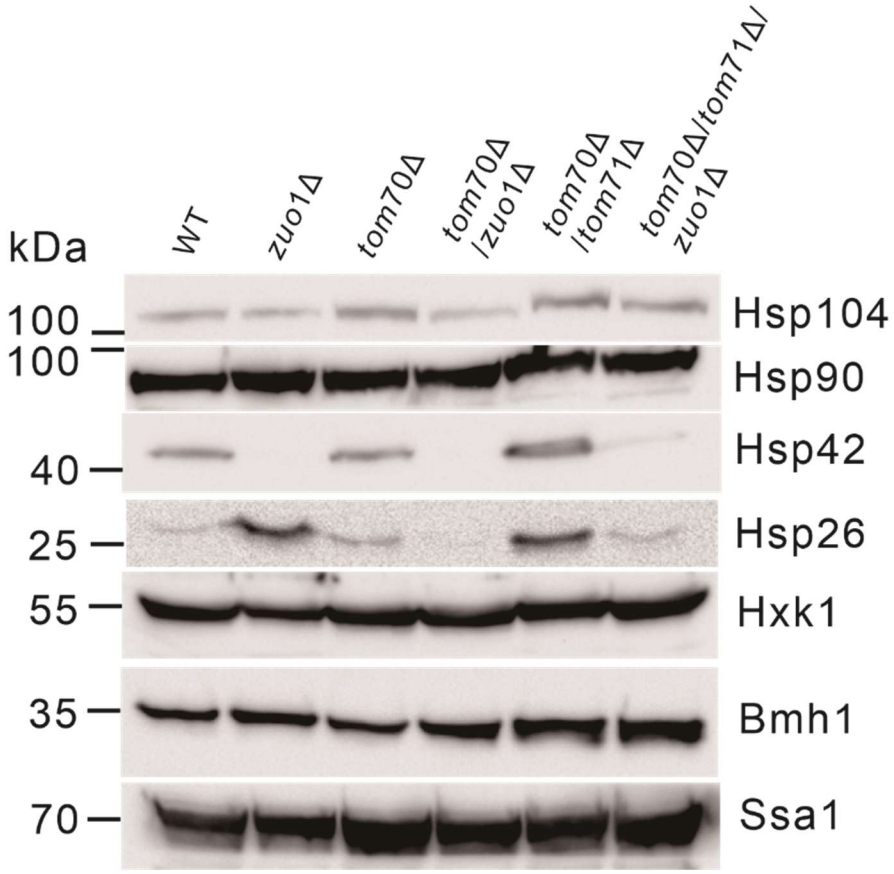

Figure 6.2.10 Yeast cytosolic protein steady-state levels at 30°C in YPD medium. Proteins were extracted from the indicated cells and analyzed by SDS-PAGE and immunodecorated with the specified antibodies.

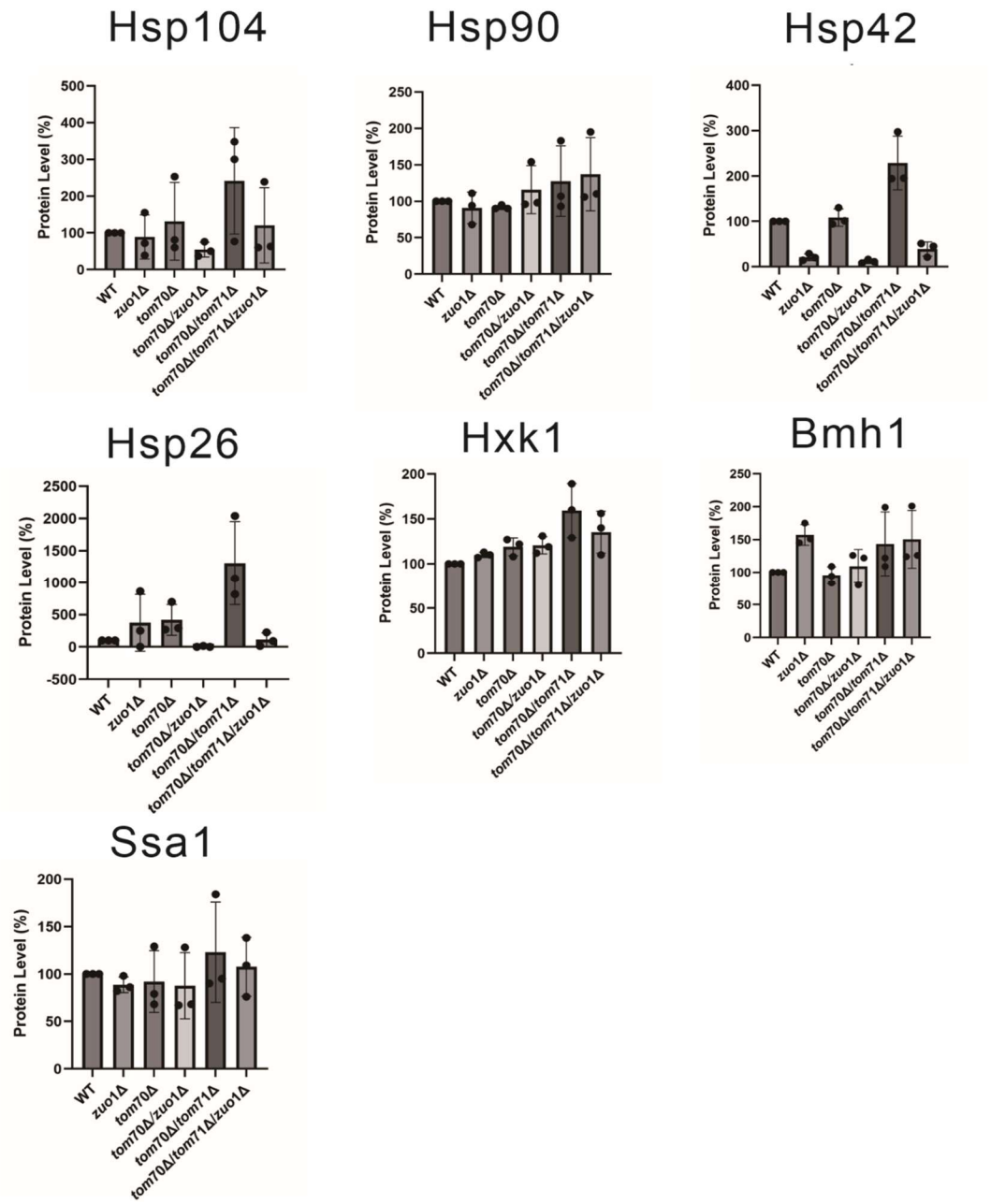

Figure 6.2.11 Quantification of the levels of yeast cytosolic proteins at 30°C in YPD medium. The bands corresponding to the indicated proteins from three independent experiments as the one shown in Fig. 6.2.7 were quantified and normalized to the intensities of the Ponceau S staining. The value of the WT cells was set as 100%. The bar diagram shows the average ± SD of three independent experiments.

The absence of Zuo1 at 30°C causes major reduction in the levels of Hsp42 (Figs. 6.2.10 & 6.2.11). It maybe because the absence of Zuo1 increased the overall translation and promoted the import of the transportation of the precursor proteins. It causes less precursor protein aggregates in the cytosol.

6.3 Mass spectrometry of the proteome of the mutant and control cells

To better understand the biological mechanisms that resulted in the unanticipated advantage of cells deleted for *ZUO1*, we compared in an unbiased manner using mass spectrometry the proteome of the mutant cells to those of control cells. In collaboration with the proteome center Tübingen, we examined proteins from control, double deletion (*tom70Δ/tom71Δ*), and triple deletion (*tom70Δ/tom71Δ/zuo1Δ*) cells cultured at 37°C in galactose-containing media (Fig. 6.3.1A). The analysis of the data, which was done in collaboration with the group of Prof. Johannes Herrmann (Kaiserslautern), indicated a unique protein composition of the different cell types and a similar coverage of the yeast proteome among the investigated cells (Fig. 6.3.1B-C).

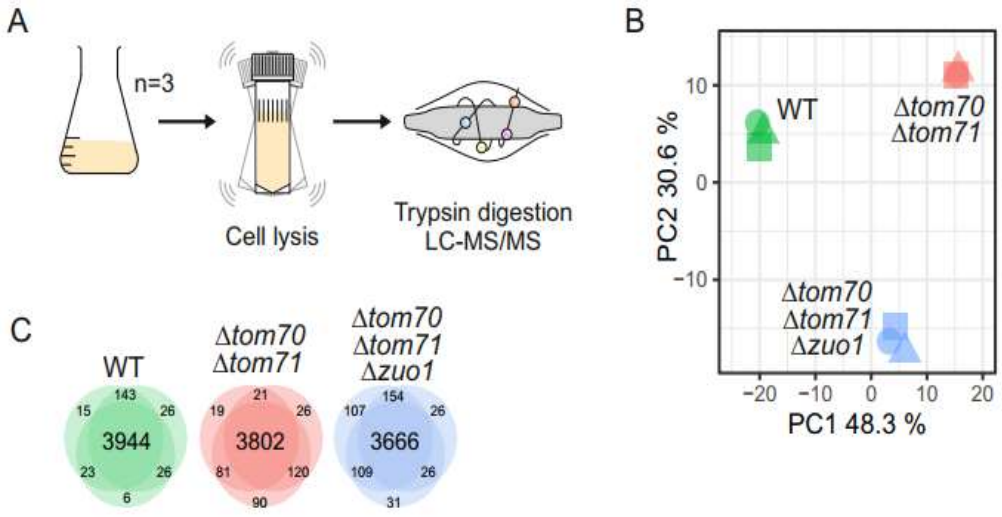

Figure 6.3.1 The depletion of mitochondrial proteins in tom70Δ/tom71Δ cells is not restored when Zuo1 is absent. (A) Diagram for measuring cellular proteins using mass spectrometry. (B) Principal Component Analysis. (C) Venn diagrams illustrating the quantity of proteins identified across the various replicates. This figure was created by the group of Professor Herrmann at Kaiserslautern University.

First, we compared the double deletion cells' proteome with that of the control cells. As observed before for *tom70Δ/tom71Δ* cells (Backes et al. 2021), they harbour reduced amounts of many mitochondrial proteins, among the most affected ones are Coq2 and Mdm36 (Fig. 6.3.2 A-C). Along the same line, the triple deletion cells had less mitochondrial proteins than control cells, with particular decreases in the amounts of respiratory chain complex subunits,

mitochondrial ribosomes, and inner membrane proteins (Fig. 6.3.2 C).

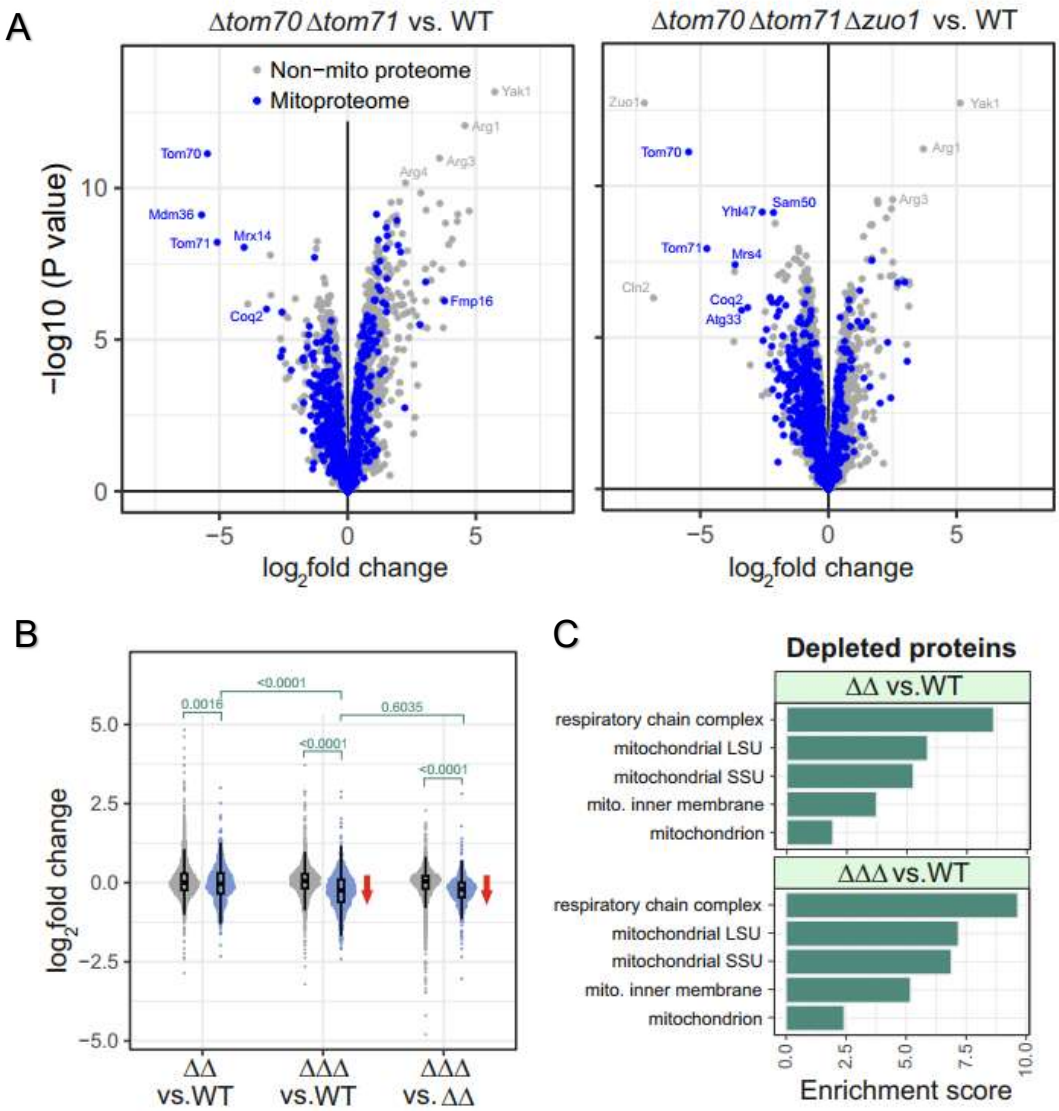

Figure 6.3.2 In *tom70Δ*/*tom71Δ* cells, the lack of Zuo1 does not reverse the decrease of mitochondrial proteins. (A) Volcano plots that compare the indicated strains' proteomes. Blue represents mitochondrial proteins. (B) The abundance of mitochondrial (shown in blue) and non-mitochondrial proteins in the various strains is compared using violin plots. P-values for indicated comparisons were determined using a two-sided Wilcoxon rank sum test with continuity correction. (C) The most severely depleted proteins underwent enrichment of gene ontology terms. (log2 fold change > -0.8 in the limma analysis) using the Gorilla website (http://cbl-gorilla.cs.technion.ac.il). WT, wildtype, ΔΔ, *tom70Δ*/*tom71Δ*, ΔΔΔ, *tom70Δ*/*tom71Δ*/*zuo1Δ*. This figure was created by the group of Professor Herrmann at Kaiserslautern University.

A specialized heat response program regulates the expression of a particular set of yeast

genes (Fig. 6.3.3A, figure was made by the group of Professor Herrmann at Kaiserslautern University) (Yamamoto, Mizukami, and Sakurai 2005). The protein products of these genes are often involved in counteracting cytosolic proteins aggregation and misfolding. Thus, we were particularly interested in the expression of such proteins in the different examined strains. We detected increased levels of the small chaperones Hsp12 and Hsp26 in cells lacking Tom70/71 (Figs. 6.3.3 B & 6.3.4 A-B). Interestingly, the comparison of the triple deletion strain with the control cells indicated that the elevated expression levels were primarily reduced for Hsp26, while the levels of Hsp12 were even lower than those in the control cells (Figs. 6.3.3B & 6.3.4 A-B).

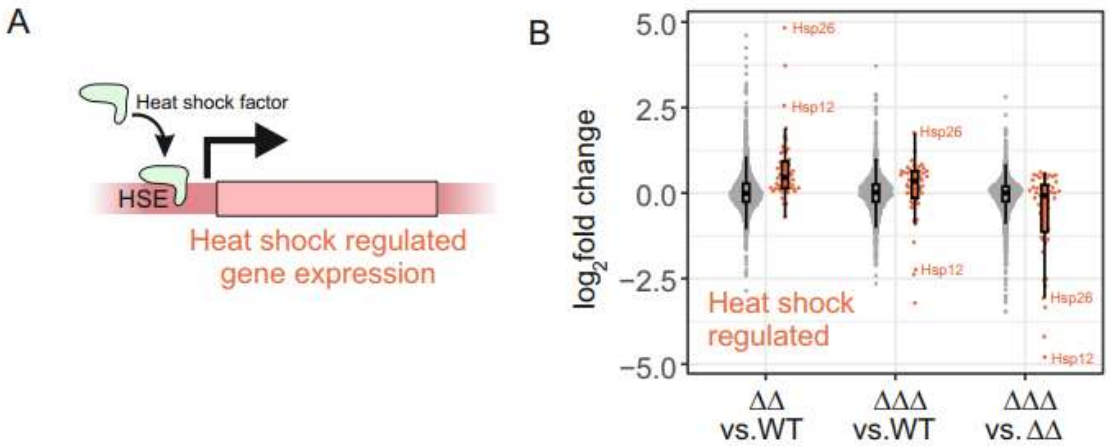

Figure 6.3.3 (A) The heat response program's scheme. (B) The abundance of heat shock-regulated and non-heat shock-regulated proteins in the various strains is compared using violin plots. This figure was created by the group of Professor Herrmann at Kaiserslautern University.

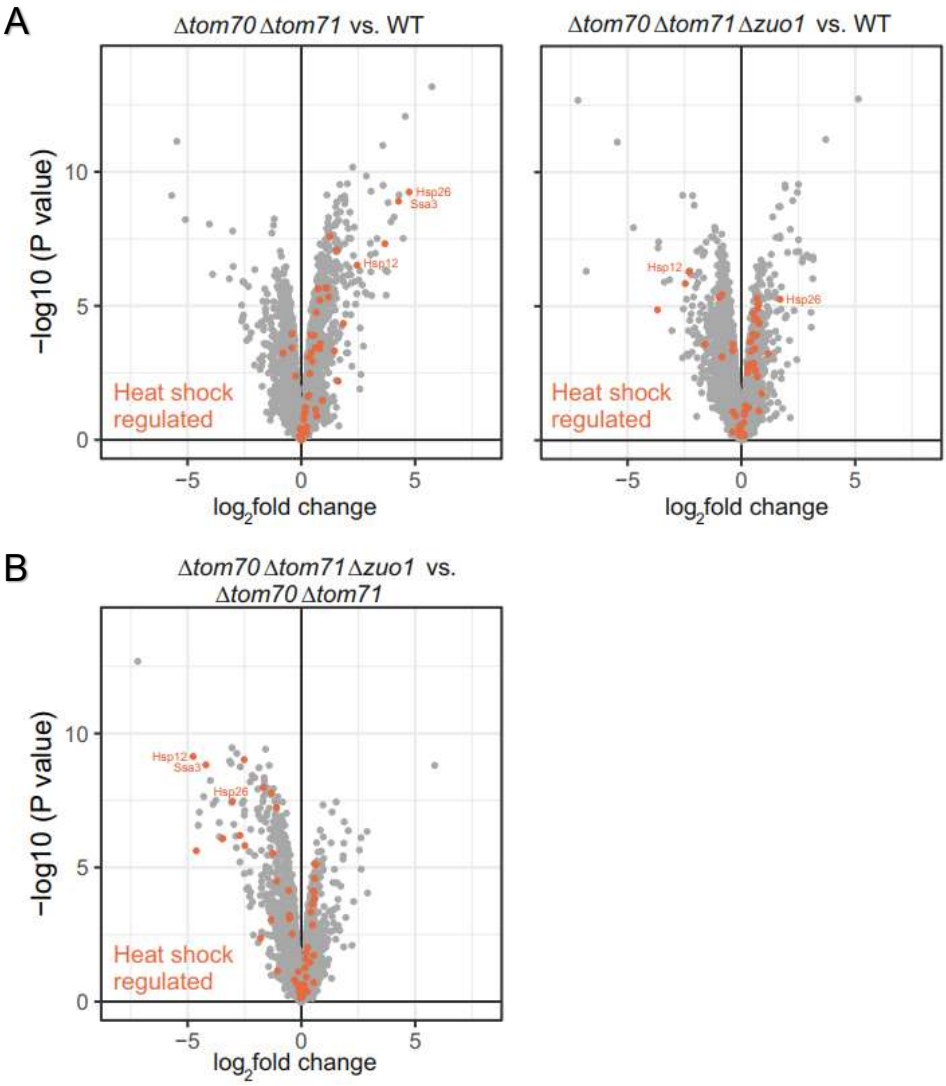

Figure 6.3.4 The proteostasis network is marked by the deletion of *TOM70/71* and *ZUO1*. (A and B) Volcano plots show that heat shock-regulated proteins are significantly upregulated upon deletion of *TOM70/71*, but *ZUO1* is not further deleted. WT, wildtype, ΔΔ, *tom70Δ/tom71Δ*, ΔΔΔ, *tom70Δ/tom71Δ/zuo1Δ*. This figure was created by the group of Professor Herrmann at Kaiserslautern University.

Not all cytosolic chaperones are showed this pattern, and the triple deletion strain had greater levels of the general chaperone Hsp82 than either the control or double deletion cells. Therefore, our results suggest that when *ZUO1* is deleted, the cytosolic stress response is remodelled.

6.4 Bringing back Zuo1 or overexpressing Zuo1 leads to change in phenotype and proteins' levels

In previous parts I found that the deletion of *ZUO1* in combination with the absence of Tom70 alone or the absence of both Tom70 and Tom71 causes dramatically changes in cell behaviour. To verify that these alterations are not the results of indirect effects, I aimed to test the outcome of re-expressing Zuo1 in the mutated cells.

The results of drop dilution assay suggest that, at 30°C, brought back Zuo1 improved the growth of *zuo1Δ* cells on both glucose- and galactose-containing media (Fig. 6.4.1). In previous experiments (Fig. 6.1.2), I found that the loss of Zuo1 only decreases a little on the growth. The additional obviously difference happens maybe because the synthetic medium causes some stress to the cell. Overexpression of Zuo1 slightly improved the growth of *tom70Δ* cells on these media (Fig. 6.4.1). Unexpectedly, bringing back Zuo1 to cells grown on galactose reduced the growth of *tom70Δ/zuo1Δ* and *tom70Δ/tom71Δ/zuo1Δ* strains (Fig. 6.4.1). Overexpression of Zuo1 slightly improved the growth of *tom70Δ/tom71Δ* in glucose media however, it did not change the growth in galactose media (Fig. 6.4.1).

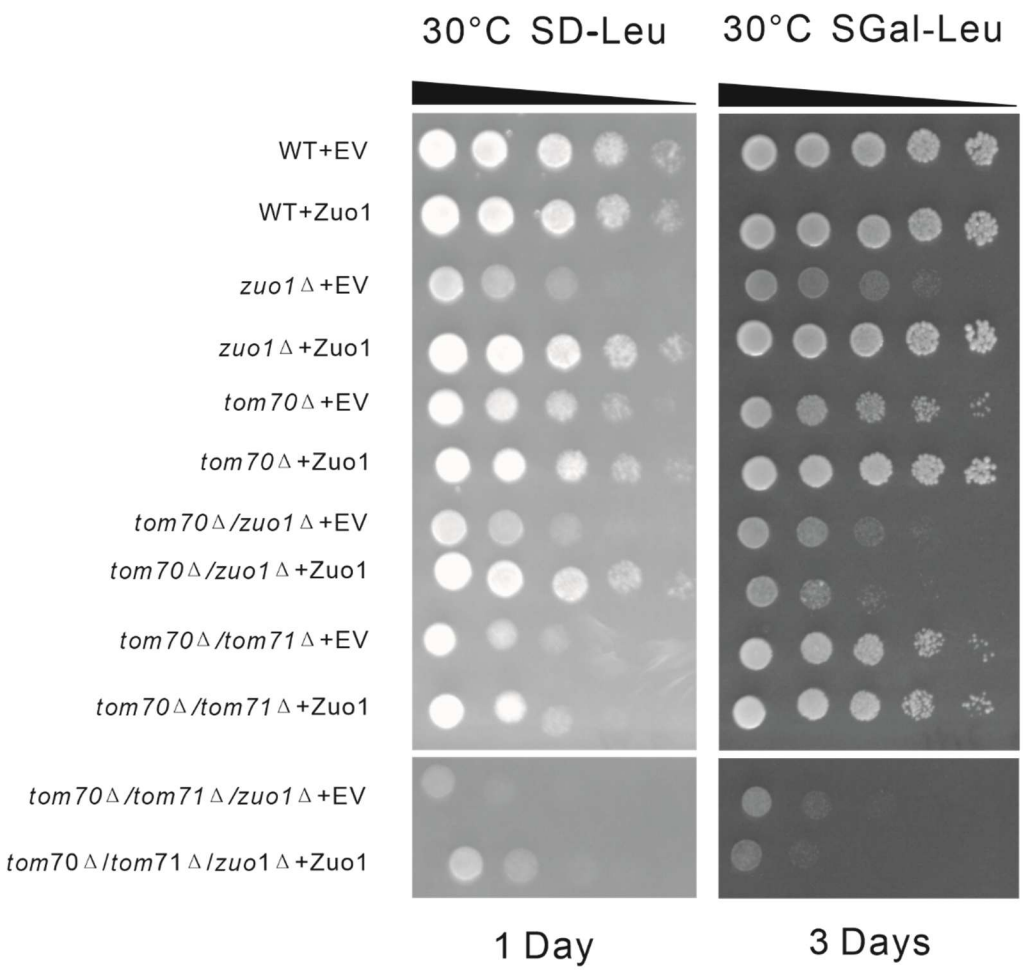

Figure 6.4.1 Reintroducing or overexpression of Zuo1 promotes growth of most of the investigated strains. The growth of the indicated strains was monitored at 30°C by drop dilution assay on solid synthetic medium containing either glucose (SD-Leu) or galactose (SGal-Leu).

At elevated temperature (37°C), re-introducing *ZUO1* in the strain deleted for Zuo1 (*zuo1Δ*) or overexpressing Zuo1 in *tom70Δ* strain did promote the rate of growth on both glucose and galactose media (Fig. 6.4.2). As expected, bringing back *ZUO1* reduced the growth of *tom70Δ/zuo1Δ* cells (Fig. 6.4.2). Interestingly, upon heat stress, re-expression of Zuo1 promoted the growth of the triple deletion cells *tom70Δ/tom71Δ/zuo1Δ* in glucose medium but, as expected, reduced the growth of these cells on galactose media (Fig. 6.4.2).

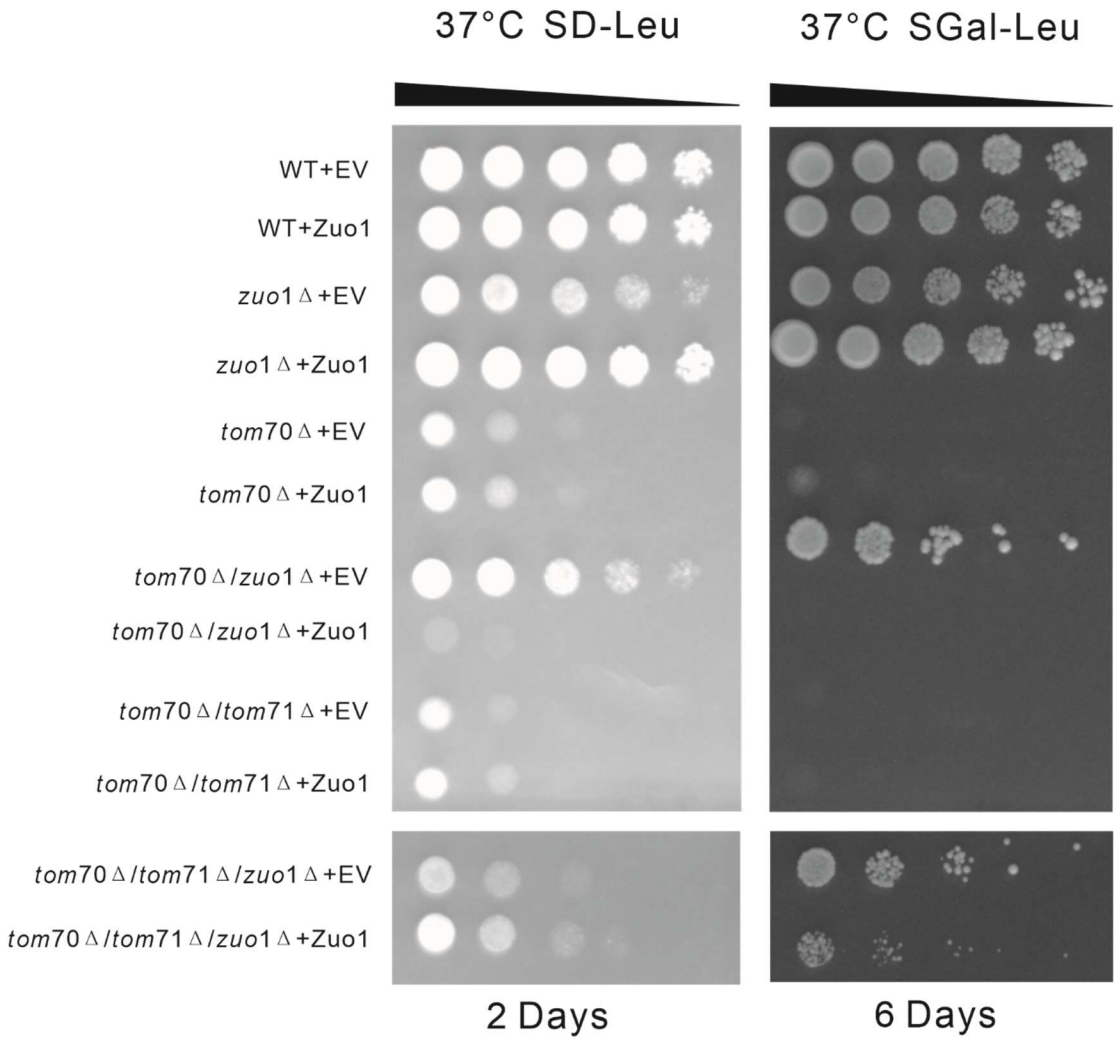

Figure 6.4.2 Reintroducing Zuo1 differentially affect the growth of mutated cells at elevated temperature. The growth of the indicated strains was monitored at 37°C by drop dilution assay on solid synthetic medium containing either glucose (SD-Leu) or galactose (SGal-Leu).

6.5 The amounts of Tom70 dictate changes in the levels of Hsp26 and Zuo1 upon heat stress

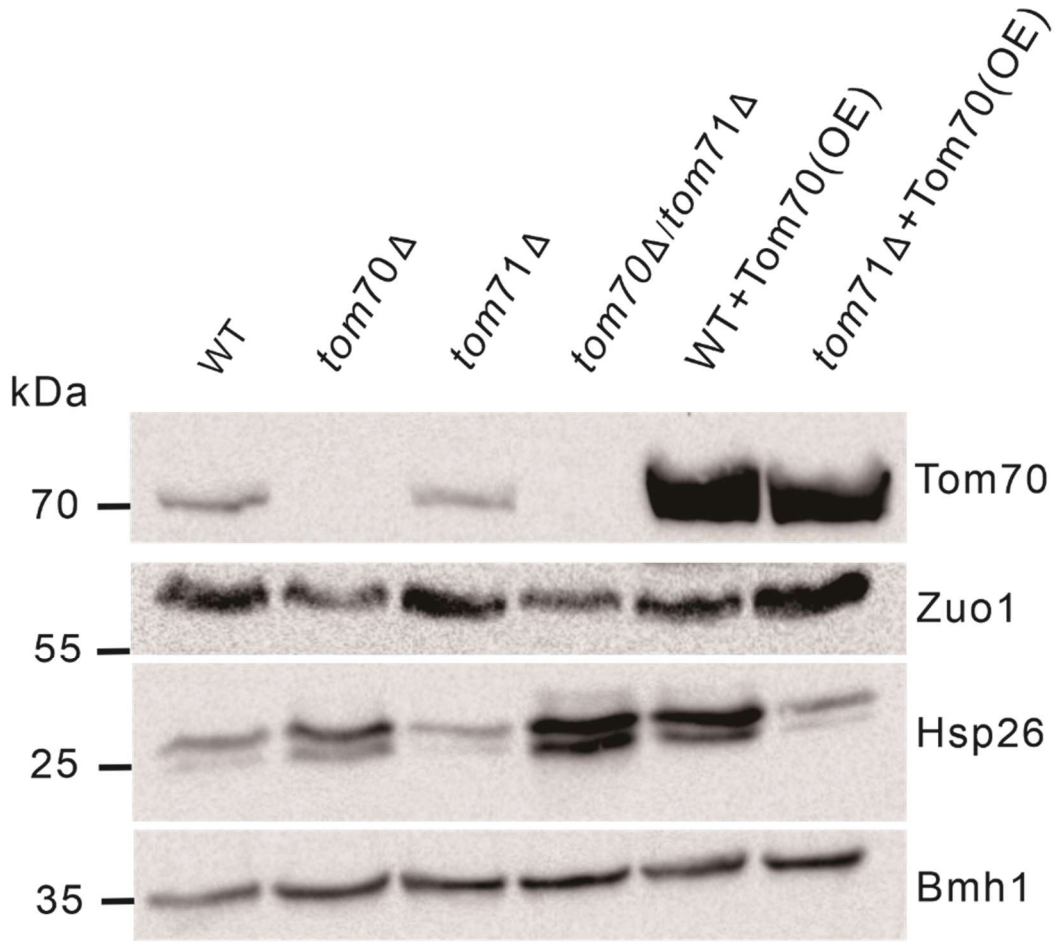

Figure 6.5.1 Changes in the levels of Hsp26 and Zuo1 in cells grown on YPD at 37°C upon overexpression or loss of Tom70. Proteins were extracted from the indicated strains and analyzed by SDS-PAGE and immunodecorated with the specified antibodies.

The absence of Tom70 seems result in lower levels of Zuo1 (Fig. 6.2.3). To verify this observation, we extracted proteins from the relevant strains and analyzed them by Western blotting. The results suggest that the absence of Tom71 results in increased amounts of Zuo1, although quantification revealed that the difference is not statistically significant. Elevated levels of Zuo1 are observed also in *tom71Δ* cells where Tom70 had been overexpressed (Figs. 6.5.1 & 6.5.2). In contrast, the protein levels of Zuo1 were slightly reduced in the absence of Tom70 as well as upon the overexpression of Tom70 in WT cells (Tom70-OE) (Figs. 6.5.1 & 6.5.2).

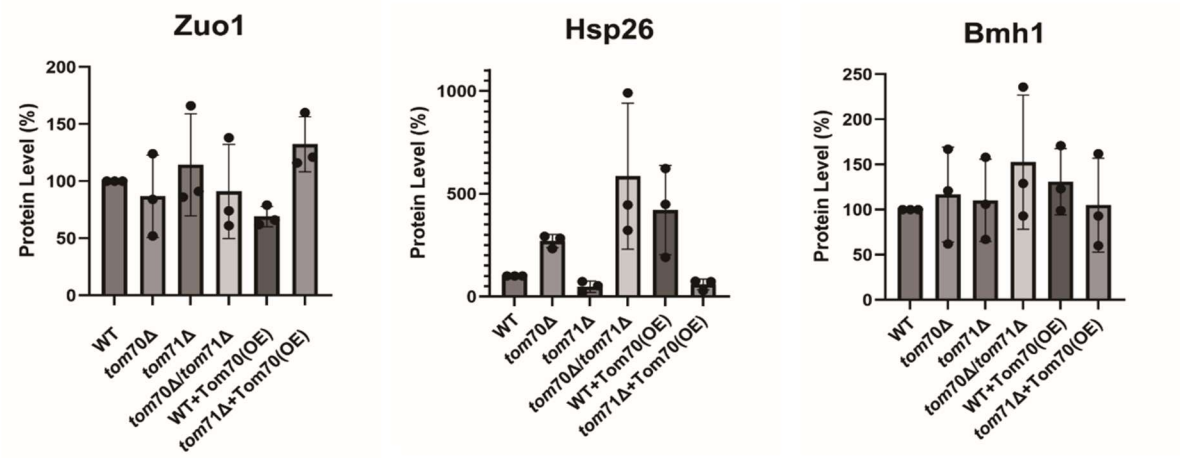

Figure 6.5.2 Quantification of the levels of Zuo1 and Hsp26. The bands corresponding to the indicated proteins from three independent experiments, as the one shown in Fig. 6.5.1were quantified and normalized to the intensities of the Ponceau S staining. The value of the WT cells was set as 100%. The bar diagram shows the average ± SD of three independent experiments. The levels of Bmh1 were analyzed as a control.

I next analyzed whether overexpressing Tom70 affects the levels of the small chaperone Hsp26. The absence of Tom71 caused moderate decrease in the amounts of Hsp26 which was not elevated upon overexpression of Tom70 (Figs. 6.5.1 & 6.5.2). In contrast, the protein levels of Hsp26 increased dramatically upon deletion of either Tom70 alone or both TOM70/71 and following the overexpression of Tom70 in WT cells (Figs. 6.5.1 & 6.5.2). Of note, the levels of the control protein, Bmh1 were hardly altered in the various strains.

6.6 A small amount of cochaperone Zuo1 pulled down specifically by Om14

To investigate whether Zuo1 interacts with mitochondrial precursor proteins, I performed pull-down assay with HA-tagged proteins expressed in yeast extract. The results with the lysate of W303 cells, but not those with lysate from BY4741 cells, suggested that Zuo1 could be pulled down by the precursor protein of Om14 but only to a very low extent (Fig. 6.6.1). As observed before (Jores et al. 2018), I could observe that Hsp104, Ssa1 and Sis1 could be pulled down by newly synthesized Om14 (Fig. 6.6.1). Newly synthesized Tom20 was used for comparison. Due to the low efficiency of the co-isolated Zuo1, this approach was not followed further.

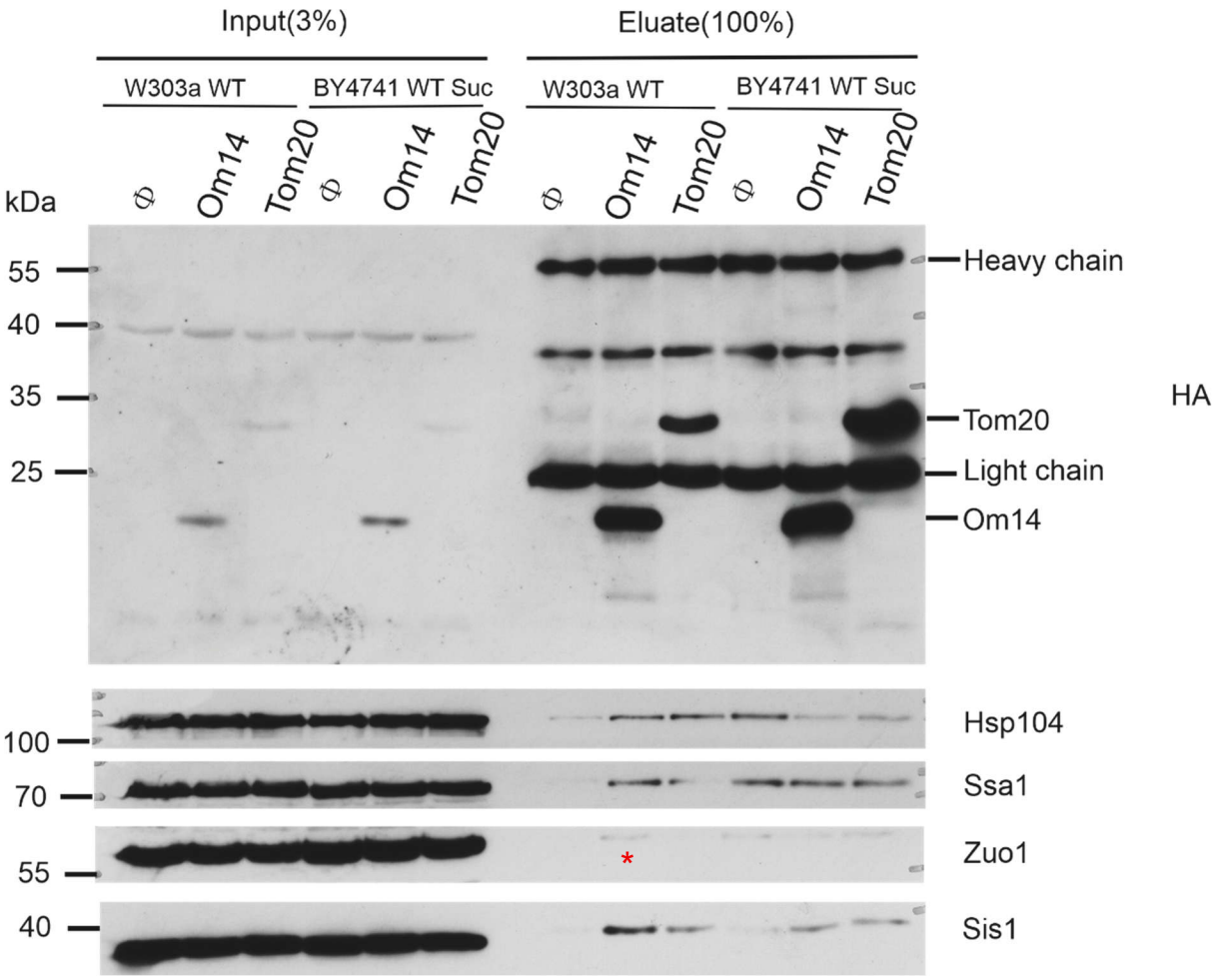

Figure 6.6.1 Pull-down analysis showed that Om14 pulled down a low level of Zuo1 from lysates of the WT W303a strain. Proteins were pulled down by anti-HA magnetic beads and analyzed by SDS-PAGE and immunodecorated with the indicated antibodies. The asterisk shows the small amount of Zuo1 which were pulled down by Om14.

6.7 The deletion of *TOM70* /*TOM71* and *ZUO1* reduces the Phospho-RPS6 level

The analysis of the global translation rate that was presented in my publication (Qian et al. 2025), led me to investigate the phosphorylation of the ribosomal protein S6 (RPS6). The phosphorylation of this protein occurs in response to a wide variety of stimuli and is a commonly-used readout for mTORC1 (Mechanistic Target of Rapamycin Complex 1) activity. I treated the relevant cells with Rapamycin, and checked with the help of a specific antibody the phosphorylation of the protein. As expected, the addition of Rapamycin, which inhibits mTOR

(mechanistic Target of Rapamycin) activity, resulted in a major reduction in the level of modified protein. Whereas the level of the phosphorylated protein in the *TOM70 /TOM71* double deletion strain was similar to its amounts in control cells, the additional deletion of *ZUO1* seems to cause a reduction in these levels (Fig 6.7.1). Hence, it seems that the increased translation activity in the triple deletion strain is not caused by elevated activity of the mTOR.

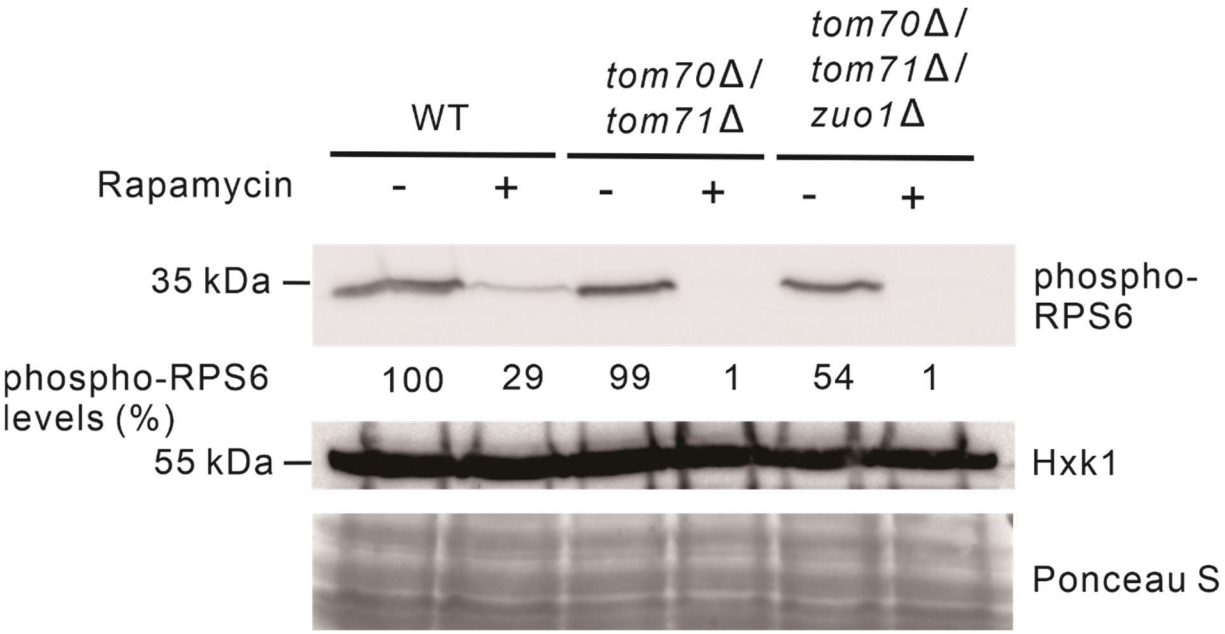

Figure 6.7.1 Western blot analysis revealed that rapamycin treatment significantly decreased the phosphorylation of ribosomal protein S6 (RPS6) in WT, *tom70Δ/tom71Δ*, and *tom70Δ/tom71Δ/zuo1Δ* strains. Wild type, *tom70Δ/tom71Δ*, *tom70Δ/tom71Δ/zuo1Δ* strains were inoculated in the YPD medium at 37°C for overnight. They were diluted and harvested in the logarithmic phase. Rapamycin (200 ng/ml) was added. Additionally, water in the same volume was added to another group of strains. The rapid protein extract assay was carried out following a 30-minute reaction.

6.8 The combined loss of Zuo1 and Tom71 causes elevated levels of Tom70

To investigate the influence of Tom71 and Zuo1 on the protein level of Tom70. I extracted proteins from WT, *zuo1Δ*, *tom71Δ*, or *tom71Δ/zuo1Δ* bells grown at 30°C in galactose media. The proteins were analyzed by western blotting and the results indicate that the single loss of either *ZUO1* or *TOM71* did not change the level of Tom70. However, the combined deletion of *ZUO1* and *TOM71* resulted in increased amounts of Tom70 (Figure 6.8.1). As a control, the levels of Bmh1 were unaffected in all strains. These results, might suggest a compensation

mechanism that results in elevated expression of Tom70 under these conditions.

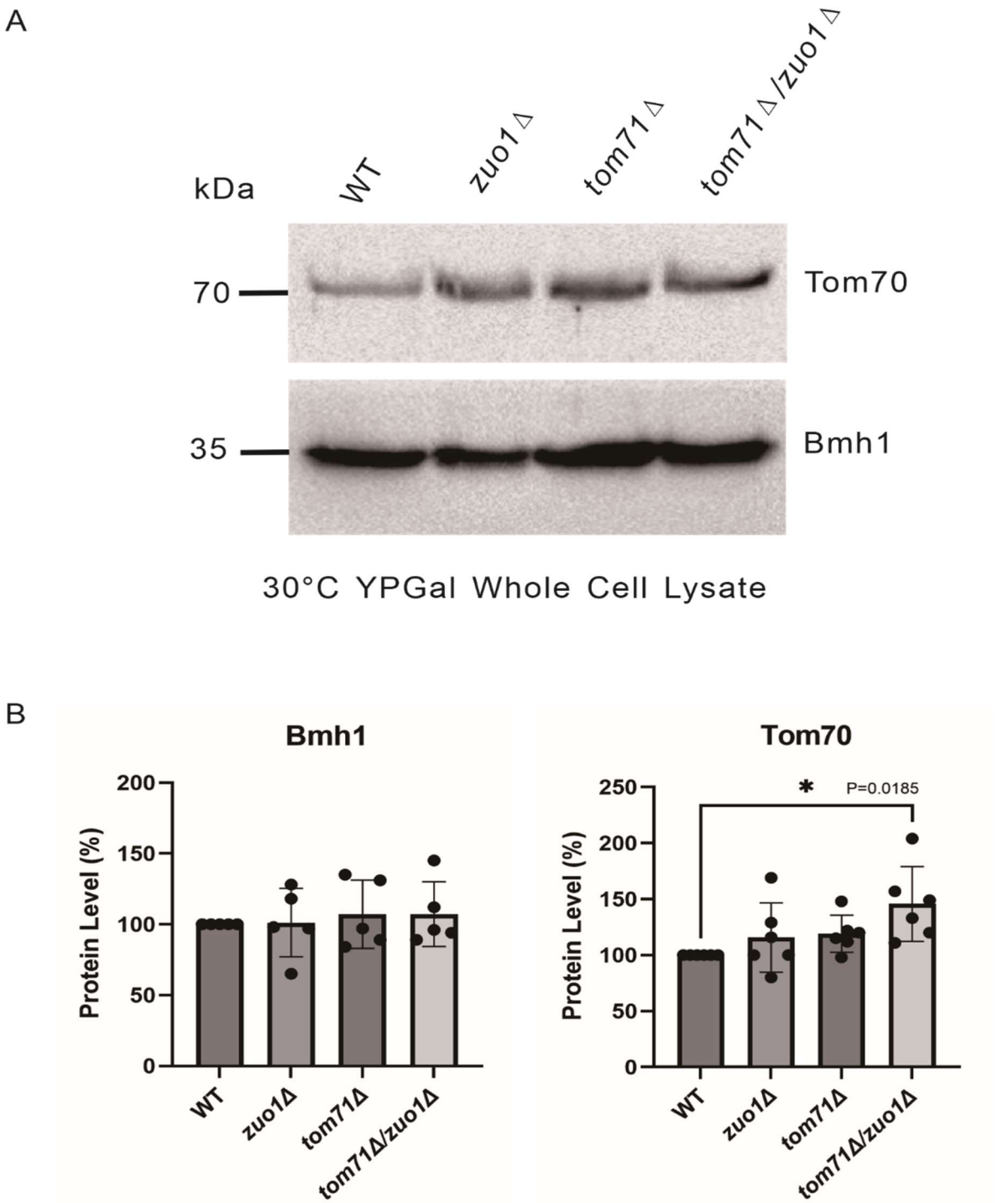

Figure 6.8.1 The double deletion of *TOM71* and *ZUO1* led to an increased level of Tom70. Wildtype, *zuo1Δ*,*tom71Δ*,*tom71Δ/zuo1Δ* were inoculated in the galactose medium at 30°C for overnight. Cells were grown to logarithmic phase and whole cell extract was performed. The samples were analyzed in the SDS-PAGE and Western Blots. (A) The western blot of Tom70 and Bmh1. (B) The quantification of protein level of Tom70 and Bmh1 with six biological repeats.

7 Discussion

7.1 Overview of the study and major findings

This study explored the physiological and molecular role of the co-chaperone Zuo1 in maintaining cellular proteostasis under both normal and heat stress conditions. There are six major findings of this study: (1) The absence of Zuo1 grows differently under normal and heat-stress conditions when Tom70 and Tom71 are lost. (2) the absence of Zuo1 changs the proteostasis of cells lacking Tom70/71. (3) Reintroduction or overexpression of Zuo1 modifies the growth phenotype. (4) The absence of Zuo1 in the *tom70Δ*/*tom71Δ* strain reduces cytosolic aggregation under heat stress and alteration of translation patterns. (5) Changes in Tom70 levels influence the steady-state amount of Hsp26 during heat stress. (6) The phosphorylation of the ribosomal protein S6 (RPS6) remains unchanged when Zuo1 is absent in the *tom70Δ/tom71Δ* cells. (7) Tom70 protein levels are raised when Zuo1 and Tom71 are lost together. Together, these results reveal that Zuo1 is not only a ribosome-associated chaperone but also a factor that links cytosolic protein quality control to mitochondrial import and stress responses.

7.2 The loss of Zuo1 reduces cellular growth under normal but increases growth under heat stress conditions in the absence of Tom70 and Tom70/Tom71

I observed that the absence of Zuo1 resulted in reduced growth of WT, *tom70Δ*, and *tom70Δ*/*tom71Δ* cells grown at normal temperature (Figs. 6.1.1 & 6.1.2). In contrast, upon heat stress (37°C), the loss of Zuo1 promoted the growth of *tom70Δ* and *tom70Δ/tom71Δ* cells (Figs. 6.1.3 & 6.1.4). Investigating the overall cellular translation at 37°C, our collaboration partners found that the loss of Zuo1 promoted the overall translation of the cell (Qian et al. 2025). In addition, upon heat stress, the loss of Zuo1 reduced the number of precursor proteins' aggregates per cell (Qian et al. 2025). These results can explain how the loss of Zuo1 can promote the growth of mutated cells.

Previous studies reported the following functions of Zuo1: (1) Zuo1 is responsible for glucose repression, possibly by increasing the mRNA levels of *SSB1/2* and *BMH1* during growth on glucose (Yamada et al. 2023).(2) Zuo1 supports nucleotide excision repair function and regulates the choice of the DNA repair pathway near G4 (guanines quadruplexes) structures (De Magis et al. 2020). (3) Zuo1 is required to reduce the rate of translation in TORC1-deficient conditions (Black et al. 2023). Considering this previous knowledge, our research is the first to indicate that Zuo1 regulates cytosolic translation upon mitoprotein-induced stress.

7.3 Tom70/71 guide mitochondrial precursor proteins and recruit chaperones, while Zuo1 aids co-translational protein folding

Tom70 and Tom71 are mitochondrial outer membrane proteins that have two functions. Primarily, they are suggested to act as receptors to help in guiding the precursor proteins from the cytosol into the mitochondria. Additionally, they recruit cytosolic chaperones to the mitochondrial surface. Zuo1 is a cochaperone of the Hsp70 chaperone Ssz1. Zuo1 functions to assist in the co-translational folding of newly synthesized proteins, preventing aggregation and misfolding.

My analysis of isolated mitochondrial of WT and *tom70⊿/tom71⊿* indicated that, at 37°C, the protein level of two IM protein, Pic2 and Aac2, had been strongly decreased (Figs. 6.2.6 & 6.2.7). In addition, the amount of matrix protein, Fum1, was also reduced (Figs. 6.2.6 & 6.2.7). It had been reported that due to the combined absence of Tom70 and Tom71, the biogenesis of many proteins (like Pet9, Oac1, and Atp1) had been hampered (Backes et al. 2021). This maybe because the Tom70 and Tom71 are the two mitochondrial receptors of precursor proteins. The absence of them influenced the specific precursor proteins binding to TOM complex and decreased the translocation of the proteins into the mitochondrial.

My analysis by blue native PAGE reveled that, at 37°C, the combined loss of Tom70 and Tom71 caused a reduction in the amount of the MOM protein Tob55 (Sam50) (Fig. 6.2.5). Sam50 is the key component of the SAM (Sorting and Assembly Machinery) complex. This complex is

crucial for the biogenesis of the outer mitochondrial membrane and for inserting β-barrel proteins into it (Chan and Lithgow 2008). Tom70 was found by Jores et al. 2016 to serve as a receptor for β -barrel proteins (Jores et al. 2016). So, it makes sense that the absence of Tom70 and Tom71 causes the protein levels of Tob55 and Porin, the β -barrel proteins, to be decreased.

The absence of Tom70/71 causes cytosolic precursor proteins aggregate under heat stress, which are reduced when Zuo1 is also absent. This is because Hsp12, Hsp26, Hsp42, and Hsp104 had been aggregated after Tom70 and Tom71 had been deleted. In previous studies, I only know the lack of Zuo1 was reported to cause cold-, NaCl- and paromomycin sensitivity of cells (Yan et al. 1998). In summary, Zuo1 can reduce the aggregates of precursor proteins upon heat stress (37°C).

Upon heat stress (37°C), the absence of Tom70/71 causes an increase in the protein levels of Mcr1, Om45, and Om14 (Figs. 6.2.1 & 6.2.2). However, the further loss of Zuo1 in the strain of *tom70Δ/tom71Δ* causes these proteins' levels to decrease (Figs. 6.2.1 & 6.2.2). Hence, Zuo1 may regulate the very beginning biogenesis processes of Om45, Om14, and Mcr1. The functions of Om45 and Om14 are still unknown. Two isoforms of the mitochondrial NADH-cytochrome b5 reductase are encoded by the yeast gene MCR1. One form is found in the intermembrane space (IMS), while the other is embedded in the outer membrane (Haucke et al. 1997). As Mcr1 involved in oxidative stress defense (Laleve et al. 2016). So, the combination loss of Tom70 and Tom71 may lead some stress that causes the amount of Mcr1 increased.

7.4 Zuo1 complementation and overexpression effects

To exclude potential secondary effects upon the deletion of *ZUO1*, I reintroduced plasmid-encoded Zuo1 into the mutated cells. Reintroduction of Zuo1 restores most of the *zuo1⊿* phenotypes except in the strain of *tom70⊿/tom71⊿/zuo1⊿* in YPGal medium under 30°C (Fig 6.4.1). Similarly, reintroduction of Zuo1 reduced the growth of the triple deletion strain (*tom70*

⊿/tom71⊿/zuo1⊿) except in YPD medium (Fig 6.4.1). Thus, despite these exceptional cases, these findings mostly confirm the specificity of the observed effects.

In the re-introduction experiments, Zuo1 was expressed from an overexpression vector. Thus, it might be that in those cases where re-expressing Zuo1 did not reverse the phenotype, the excessive Zuo1 amounts caused stress to the cell that reduced the growth rate of *tom70⊿ /tom71⊿/zuo1⊿* in YPGal medium under 30°C. Surprisingly, the overexpression of Zuo1 dramatically increased the growth of the triple deletion strain at 37°C (Fig 6.4.2). Unfortunately, the mechanism of these two phenomena is not clear. However, previous studies suggest that by increasing chaperones' levels, cells can enhance protein folding and production efficiency, leading to better yields of desired products (Vestergaard et al. 2025). To further understand these phenomena, it is essential to analyze the rate and efficiency of translation under these conditions.

7.5 Heat-Stress Regulation: Interplay of Tom70, Tom71 and Hsp26

The results indicated that the absence of Tom70 alone or both Tom70/Tom71 caused an increased amount of Hsp26, while the overexpression of Tom70 also had a similar effect (Figs. 6.5.1 & 6.5.2). However, upon the absence of Tom71, the overexpression of Tom70 did not change the amount of Hsp26 (Figs. 6.5.1 & 6.5.2). These observations might result from a situation where the absence of Tom70 or Tom70/Tom71 leads to the accumulation of precursor proteins in the cytosol, which is toxic to the cell (Backes et al. 2021). It is unknown that why the overexpression of Tom70 increased the protein level of Hsp26. Interestingly, the absence of Tom71 eliminated the increasing amount of Hsp26 caused by the overexpression of Tom70. It will be interesting to investigate in future studies the relationship between Hsp26 and Tom71.

7.6 Cytosolic aggregation and translation changes in Zuo1-deficient cells

The results of our collaborators indicated that under heat stress, the absence of Tom70/Tom71 resulted in aggregates of precursor proteins. However, upon the additional absence of Zuo1,

the number of aggregates in the cells got reduced (Qian et al. 2025). In addition, the absence of Zuo1 promoted the growth of the cell. Furthermore, when the overall rate of translation in the cell was studied using radiolabeled ^{35}S Methionine, the results showed that the absence of Zuo1 dramatically increased the overall translation of proteins at 37°C (Qian et al. 2025). It is well known that the cytosolic stress response involves a coordinated effort to reduce overall protein synthesis while simultaneously promoting the synthesis of proteins essential for cell survival under stress conditions. This phenomenon, which is part of the integrated stress response (ISR), helps cells to conserve energy and resources during stress (Costa-Mattioli and Walter 2020).

It is still unclear why the elevated translation increased the growth of cells under heat stress (37°C) but does not have this effect on cells grown at 30°C.

7.7 Interaction of Zuo1 with Om14 precursor protein

My results indicate that small amount of Zuo1 could be pulled down by newly synthesized Om14 precursor molecules in yeast extract (Fig 6.6.1). This might suggest that Zuo1 is involved in the early stages of the biogenesis of Om14. As a cochaperone of Ssz1, Zuo1 regulates proteins' translation (Black et al. 2023). Thus, one can speculate that the nascent Om14 can be immediately recognized and protected by Zuo1-associated complexes before its import. Further experiments are required to shed more light on this issue.

7.8 The absence of Zuo1 in *tom70Δ/tom71Δ* cells does not change the phosphorylation of the ribosomal protein S6 (RPS6)

Since the overall translation upon the absence of Zuo1 in the tom70Δ/tom71Δ cells was observed to be enhanced, I aimed to investigate the phosphorylation of the ribosomal protein S6 (RPS6), a marker for the activity of the mTOR system. Previous study reported that in the absence of Zuo1, translation does not decrease in response to the loss of TORC1 activity (Black et al. 2023). Our results show that the absence of Zuo1 in *tom70Δ/tom71Δ* cells does

not affect the activity of the mTOR complex (Fig. 6.7.1). Therefore, it appears that elevated mTOR activity is not the cause of the increased translation activity in the triple deletion strain.

7.9 The combined loss of Zuo1 and Tom71 leads to elevated levels of Tom70

I found that the double deletion strain of *ZUO1* and *TOM71* has elevated protein levels of Tom70 compared to those in other strains like WT, *zuo*1Δ, or *tom*71Δ (Fig. 6.8.1). But the absence of Zuo1 does not obviously change the protein level according to our results (Fig. 6.8.1). Of note, the absence of Tom71 does not change the amounts of Tom70. My results are the first to show that the combined deletion of *ZUO1* and *TOM71* causes the elevated amount of Tom70. This might be because Zuo1 and Tom71 play an important role in the transport of the precursor proteins. The loss of Zuo1 and Tom71 may cause the overexpression of Tom70, for the compensation of transportation of the precursor proteins.

7.10 A working model of how the cytosolic stress response is altered when *ZUO1* is deleted

Based on our results, we proposed a mechanism of how Zuo1 influences the biogenesis of precursor proteins (Fig. 7.10). In wild type strain, when Zuo1 and Tom70/Tom71 are present and functional, Tom70 and Tom71 primarily act as a receptor to facilitate the import of specific proteins into the mitochondria. However, with the combined absence of Tom70 and Tom71, high levels of non-imported precursor proteins are accumulated and aggregated in the cytosol. To counteract this effect, Zuo1 decreases the synthesis of new proteins. In contrast, the absence of Zuo1 in the strain *tom70⊿/tom71⊿* results in the removal of the Zuo1-mediated inhibition of nascent peptide synthesis. Hence, the overall translation is increased. Under heat stress (37°C), this improves the growth of the cell. We put forth a novel paradigm in which RAC functions as a regulatory component of the cytosolic translation machinery under stress.

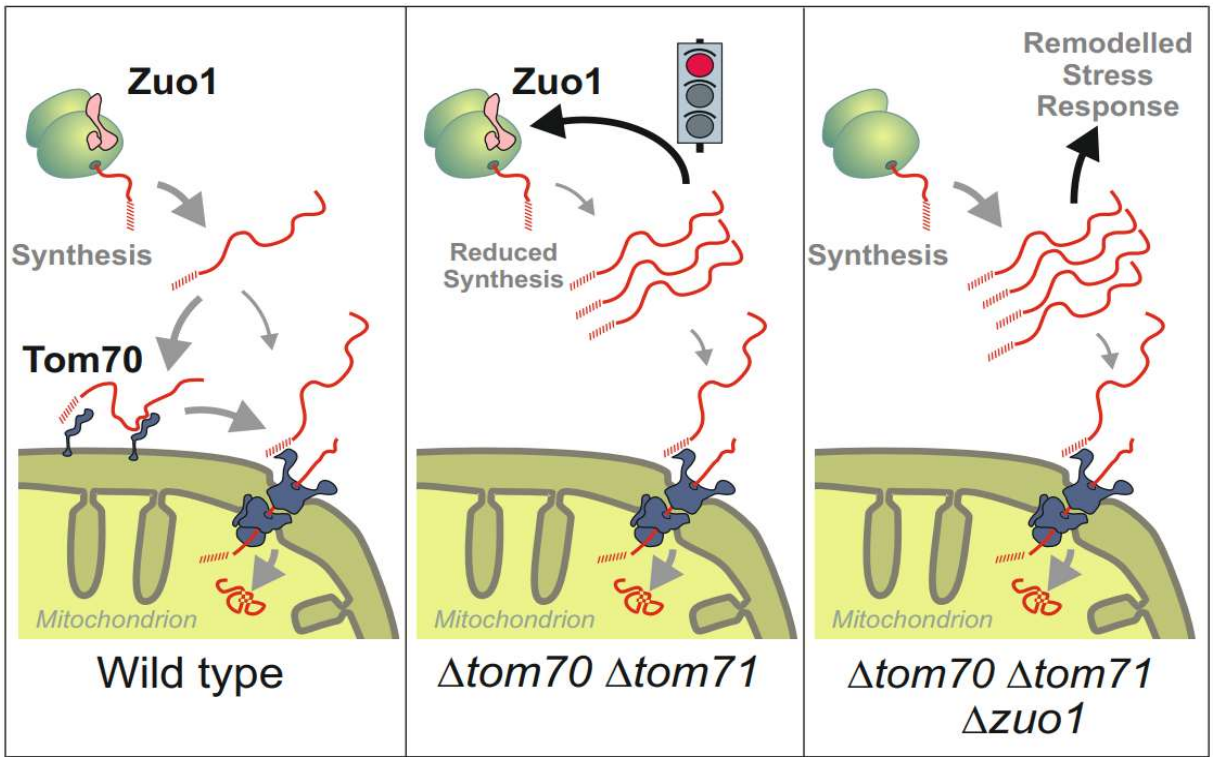

Figure 7.10 An illustration of how the cytosolic stress response is altered when *ZUO1* is deleted. Protein import into mitochondria is facilitated by the non-essential mitochondrial outer membrane proteins Tom70/71. Thus, reduced protein import levels in mutants lacking Tom70 and its paralog Tom71 cause non-imported precursor proteins to accumulate. These non-imported precursor proteins cause a stress response and protein synthesis is slowed down. Interestingly, the RAC subunit Zuo1 is required for the mitoprotein-induced reduction of translation, indicating that Zuo1 is an essential part of the signaling pathway that inhibits protein synthesis in response to mitochondrial dysfunction. This figure is taken from (Qian et al. 2025).

7.11 Potential role of Ssb1/2 and Ssz1

In our experiments, we only investigated the effect of Zuo1. However, as Ssz1 is the partner of Zuo1 in the RAC complex, it is also worth studying whether the loss of Ssz1 would also have similar effects. In addition, Ssb1/2 also have a close relationship with Zuo1. Accordingly, it was reported that the absence of Zuo1 and Ssb1/2 have similar sensitivity to a variety of cations (Kim and Craig 2005) . Hence, it will be of interest to investigate how the absence of Ssb1/2 will affect the phenotypes of the double deletion strain *tom70Δ/tom71Δ*.

7.12 Broader implications and future perspectives

Further potential research could be divided into several parts. (1) Investigating whether Zuo1

influences the mRNA levels of *OM45*, *OM14*, *MCR1*, *HSP104*, *HSP42*, and *HSP26* upon the deletion of *TOM70/TOM71* under the heat stress (37°C). (2) Studying how Zuo1 influences the early stages of biogenesis of the precursors of Om45, Om14, and Mcr1 in the very beginning after translation (3) The absence of Tom70 and Tom71 caused, upon heat stress (37°C), elevated levels of proteins (like Om45, Om14, and Mcr1) in mitochondria. However, the amount of those three proteins decreased in the triple deletion strain *tom70Δ/tom71Δ/zuo1Δ*. It will be of interest to investigate the transport routine of these proteins by using a proximity labeling assay.

8 References

Abe, Y., T. Shodai, T. Muto, K. Mihara, H. Torii, S. Nishikawa, T. Endo, and D. Kohda. 2000. 'Structural basis of presequence recognition by the mitochondrial protein import receptor Tom20', *Cell*, 100: 551-60.

Albanèse, V., S. Reissmann, and J. Frydman. 2010. 'A ribosome-anchored chaperone network that facilitates eukaryotic ribosome biogenesis', *Journal of Cell Biology*, 189: 69-U105.

Araiso, Y., K. Imai, and T. Endo. 2022. 'Role of the TOM Complex in Protein Import into Mitochondria: Structural Views', *Annu Rev Biochem*, 91: 679-703.

Atlante, A., and D. Valenti. 2023. 'Mitochondria Have Made a Long Evolutionary Path from Ancient Bacteria Immigrants within Eukaryotic Cells to Essential Cellular Hosts and Key Players in Human Health and Disease', *Current Issues in Molecular Biology*, 45: 4451-79.

Backes, S., Y. S. Bykov, T. Flohr, M. Raschle, J. Zhou, S. Lenhard, L. Kramer, T. Muhlhaus, C. Bibi, C. Jann, J. D. Smith, L. M. Steinmetz, D. Rapaport, Z. Storchova, M. Schuldiner, F. Boos, and J. M. Herrmann. 2021. 'The chaperone-binding activity of the mitochondrial surface receptor Tom70 protects the cytosol against mitoprotein-induced stress', *Cell Rep*, 35: 108936.

Barilari, M., G. Bonfils, C. Treins, V. Koka, D. De Villeneuve, S. Fabrega, and M. Pende. 2017. 'ZRF1 is a novel S6 kinase substrate that drives the senescence programme', *EMBO J*, 36: 736-50.

Bhagawati, M., T. Arroum, N. Webeling, A. G. Montoro, H. D. Mootz, and K. B. Busch. 2021. 'The receptor subunit Tom20 is dynamically associated with the TOM complex in mitochondria of human cells', *Molecular Biology of the Cell*, 32.

Black, A., T. D. Williams, F. Soubigou, I. M. Joshua, H. Zhou, F. Lamoliatte, and A. Rousseau. 2023. 'The ribosome-associated chaperone Zuo1 controls translation upon TORC1

inhibition', *EMBO J*, 42: e113240.

Bose, H. S., M. Bose, and R. M. Whittal. 2023. 'Tom40 in cholesterol transport', *iScience*, 26.

Bradford, M. M. 1976. 'A rapid and sensitive method for the quantitation of microgram quantities of protein utilizing the principle of protein-dye binding', *Anal Biochem*, 72: 248-54.

Caruso Bavisotto, C., G. Alberti, A. M. Vitale, L. Paladino, C. Campanella, F. Rappa, M. Gorska, E. Conway de Macario, F. Cappello, A. J. L. Macario, and A. Marino Gammazza. 2020. 'Hsp60 Post-translational Modifications: Functional and Pathological Consequences', *Front Mol Biosci*, 7: 95.

Chan, N. C., and T. Lithgow. 2008. 'The peripheral membrane subunits of the SAM complex function codependently in mitochondrial outer membrane biogenesis', *Molecular Biology of the Cell*, 19: 126-36.

Cheetham, M. E., and A. J. Caplan. 1998. 'Structure, function and evolution of DnaJ: conservation and adaptation of chaperone function', *Cell Stress Chaperones*, 3: 28-36.

Chiosis, G., C. S. Digwal, J. B. Trepel, and L. Neckers. 2023. 'Structural and functional complexity of HSP90 in cellular homeostasis and disease', *Nature Reviews Molecular Cell Biology*, 24: 797-815.

Costa-Mattioli, M., and P. Walter. 2020. 'The integrated stress response: From mechanism to disease', *Science*, 368: 384-+.

De Magis, A., S. Gotz, M. Hajikazemi, E. Fekete-Szucs, M. Caterino, S. Juranek, and K. Paeschke. 2020. 'Zuo1 supports G4 structure formation and directs repair toward nucleotide excision repair', *Nat Commun*, 11: 3907.

den Brave, Fabian, Jeannine Engelke, and Thomas Becker. 2021. 'Quality control of protein import into mitochondria', *Biochemical Journal*, 478: 3125-43.

Deuerling, E., M. Gamerdinger, and S. G. Kreft. 2019. 'Chaperone Interactions at the Ribosome', *Cold Spring Harbor Perspectives in Biology*, 11.

Drwesh, L., B. Heim, M. Graf, L. Kehr, L. Hansen-Palmus, M. Franz-Wachtel, B. Macek, H. Kalbacher, J. Buchner, and D. Rapaport. 2022. 'A network of cytosolic (co)chaperones promotes the biogenesis of mitochondrial signal-anchored outer membrane proteins', *Elife*, 11.

Duarte, F. V., D. Ciampi, and C. B. Duarte. 2023. 'Mitochondria as central hubs in synaptic modulation', *Cellular and Molecular Life Sciences*, 80.

Eliyahu, E., L. Pnueli, D. Melamed, T. Scherrer, A. P. Gerber, O. Pines, D. Rapaport, and Y. Arava. 2010. 'Tom20 Mediates Localization of mRNAs to Mitochondria in a Translation-Dependent Manner', *Molecular and Cellular Biology*, 30: 284-94.

Endo, T., and D. Kohda. 2002. 'Functions of outer membrane receptors in mitochondrial protein import', *Biochimica Et Biophysica Acta-Molecular Cell Research*, 1592: 3-14.

Fenech, E. J., M. Kupervaser, A. Boshnakovska, S. Ravid, I. G. Castro, Y. Asraf, S. Callegari, C. Lenz, H. Urlaub, P. Rehling, and M. Schuldiner. 2025. 'Profiling the LAM Family of Contact Site Tethers Provides Insights into Their Regulation and Function', *Contact (Thousand Oaks)*, 8: 25152564251321770.

Ferreira, T., and S. Rodriguez. 2024. 'Mitochondrial DNA: Inherent Complexities Relevant to Genetic Analyses', *Genes*, 15.

Frezza, C. 2014. 'The role of mitochondria in the oncogenic signal transduction', *International Journal of Biochemistry & Cell Biology*, 48: 11-17.

Gabriel, K., B. Egan, and T. Lithgow. 2003. 'Tom40, the import channel of the mitochondrial outer membrane, plays an active role in sorting imported proteins', *EMBO J*, 22: 2380-86.

Geissler, A., T. Krimmer, U. Bömer, B. Guiard, J. Rassow, and N. Pfanner. 2000. 'Membrane

potential-driven protein import into mitochondria. The sorting sequence of cytochrome b(2) modulates the deltapsi-dependence of translocation of the matrix-targeting sequence', *Mol Biol Cell*, 11: 3977-91.

Goffin, L., and C. Georgopoulos. 1998. 'Genetic and biochemical characterization of mutations affecting the carboxy-terminal domain of the molecular chaperone DnaJ', *Molecular Microbiology*, 30: 329-40.

Gorenberg, E. L., and S. S. Chandra. 2017. 'The Role of Co-chaperones in Synaptic Proteostasis and Neurodegenerative Disease', *Front Neurosci*, 11: 248.

Greene, M. K., K. Maskos, and S. J. Landry. 1998. 'Role of the J-domain in the cooperation of Hsp40 with Hsp70', *Proc Natl Acad Sci U S A*, 95: 6108-13.

Haucke, V., and T. Lithgow. 1997. 'The first steps of protein import into mitochondria', *Journal of Bioenergetics and Biomembranes*, 29: 11-7.

Haucke, V., C. S. Ocana, A. Honlinger, K. Tokatlidis, N. Pfanner, and G. Schatz. 1997. 'Analysis of the sorting signals directing NADH-cytochrome b5 reductase to two locations within yeast mitochondria', *Mol Cell Biol*, 17: 4024-32.

Helary, L., J. Castille, B. Passet, A. Vaiman, C. Beauvallet, F. Jaffrezic, M. Charles, M. Tamzini, F. Baraige, M. Letheule, J. Laubier, K. Moazami-Goudarzi, J. L. Vilotte, V. Blanquet, and A. Duchesne. 2019. 'DNAJC2 is required for mouse early embryonic development', *Biochemical and Biophysical Research Communications*, 516: 258-63.

Hennessy, F., M. E. Cheetham, H. W. Dirr, and G. L. Blatch. 2000. 'Analysis of the levels of conservation of the J domain among the various types of DnaJ-like proteins', *Cell Stress & Chaperones*, 5: 347-58.

Hu, M. L., F. L. He, E. W. Thompson, K. Ostrikov, and X. F. Dai. 2022. 'Lysine Acetylation, Cancer Hallmarks and Emerging Onco-Therapeutic Opportunities', *Cancers*, 14.

Huang, P., M. Gautschi, W. Walter, S. Rospert, and E. A. Craig. 2005. 'The Hsp70 Ssz1

modulates the function of the ribosome-associated J-protein Zuo1', *Nat Struct Mol Biol*, 12: 497-504.

Hulett, J. M., F. Lueder, N. C. Chan, A. J. Perry, P. Wolynec, V. A. Likíc, P. R. Gooley, and T. Lithgow. 2008. 'The transmembrane segment of Tom20 is recognized by Mim1 for docking to the mitochondrial TOM complex', *Journal of Molecular Biology*, 376: 694-704.

Hundley, H. A., W. Walter, S. Bairstow, and E. A. Craig. 2005. 'Human Mpp11 J protein: Ribosome-tethered molecular chaperones are ubiquitous', *Science*, 308: 1032-34.

Jores, T., A. Klinger, L. E. Gross, S. Kawano, N. Flinner, E. Duchardt-Ferner, J. Wohnert, H. Kalbacher, T. Endo, E. Schleiff, and D. Rapaport. 2016. 'Characterization of the targeting signal in mitochondrial beta-barrel proteins', *Nat Commun*, 7: 12036.

Jores, T., J. Lawatscheck, V. Beke, M. Franz-Wachtel, K. Yunoki, J. C. Fitzgerald, B. Macek, T. Endo, H. Kalbacher, J. Buchner, and D. Rapaport. 2018. 'Cytosolic Hsp70 and Hsp40 chaperones enable the biogenesis of mitochondrial beta-barrel proteins', *J Cell Biol*, 217: 3091-108.

Kampinga, H. H., and E. A. Craig. 2010. 'The HSP70 chaperone machinery: J proteins as drivers of functional specificity (vol 11, pg 579, 2010)', *Nature Reviews Molecular Cell Biology*, 11.

Kato, H., and K. Mihara. 2008. 'Identification of Tom5 and Tom6 in the preprotein translocase complex of human mitochondrial outer membrane', *Biochemical and Biophysical Research Communications*, 369: 958-63.

Kaymak, A., and H. Richly. 2016. 'Zrf1 controls mesoderm lineage genes and cardiomyocyte differentiation', *Cell Cycle*, 15: 3306-17.

Kelley, W. L. 1998. 'The J-domain family and the recruitment of chaperone power', *Trends Biochem Sci*, 23: 222-7.

Kim, S. Y., and E. A. Craig. 2005. 'Broad sensitivity of Saccharomyces cerevisiae lacking ribosome-associated chaperone ssb or zuo1 to cations, including aminoglycosides', *Eukaryot Cell*, 4: 82-9.

Kisonaite, M., K. Wild, K. Lapouge, G. V. Gese, N. Kellner, E. Hurt, and I. Sinning. 2023. 'Structural inventory of cotranslational protein folding by the eukaryotic RAC complex', *Nat Struct Mol Biol*, 30: 670-77.

Kota, P., D. W. Summers, H. Y. Ren, D. M. Cyr, and N. V. Dokholyan. 2009. 'Identification of a consensus motif in substrates bound by a Type I Hsp40', *Proc Natl Acad Sci U S A*, 106: 11073-8.

Kyhse-Andersen, J. 1984. 'Electroblotting of multiple gels: a simple apparatus without buffer tank for rapid transfer of proteins from polyacrylamide to nitrocellulose', *J Biochem Biophys Methods*, 10: 203-9.

Laleve, A., C. Vallieres, M. P. Golinelli-Cohen, C. Bouton, Z. Song, G. Pawlik, S. M. Tindall, S. V. Avery, J. Clain, and B. Meunier. 2016. 'The antimalarial drug primaquine targets Fe-S cluster proteins and yeast respiratory growth', *Redox Biol*, 7: 21-29.

Li, J. X., X. G. Qian, J. B. Hu, and B. D. Sha. 2009. 'Molecular Chaperone Hsp70/Hsp90 Prepares the Mitochondrial Outer Membrane Translocon Receptor Tom71 for Preprotein Loading', *Journal of Biological Chemistry*, 284: 23852-59.

Li, J. Z., X. G. Oian, and B. Sha. 2003. 'The crystal structure of the yeast Hsp40 Ydj1 complexed with its peptide substrate', *Structure*, 11: 1475-83.

Li, Xiaoyu, Ou Jiang, Mo Chen, and Songlin Wang. 2024. 'Mitochondrial homeostasis: shaping health and disease', *Current Medicine*, 3: 5.

Li, Y., L. Liu, Y. Zhu, and Q. Chen. 2019. 'Mitochondria organize the cellular proteostatic response and promote cellular senescence', *Cell Stress*, 3: 110-14.

Liao, P. C., T. Y. Lin, C. A. Tsang, C. J. Huang, K. Filpo, I. Boldogh, and L. A. Pon. 2025. 'Tom40

functions as a channel for protein retrotranslocation in the mitochondria-associated degradation (MAD) pathway', *Communications Biology*, 8.

Linke, K., T. Wolfram, J. Bussemer, and U. Jakob. 2003. 'The roles of the two zinc binding sites in DnaJ', *J Biol Chem*, 278: 44457-66.

Liu, Q., C. E. Chang, A. C. Wooldredge, B. Fong, B. K. Kennedy, and C. Zhou. 2022. 'Tom70-based transcriptional regulation of mitochondrial biogenesis and aging', *Elife*, 11.

Lu, Z., and D. M. Cyr. 1998. 'The conserved carboxyl terminus and zinc finger-like domain of the co-chaperone Ydj1 assist Hsp70 in protein folding', *J Biol Chem*, 273: 5970-8.

Makhnevych, T., and W. A. Houry. 2012. 'The role of Hsp90 in protein complex assembly', *Biochimica Et Biophysica Acta-Molecular Cell Research*, 1823: 674-82.

Miller, A. P., and S. L. Reichow. 2025. 'Mechanism of small heat shock protein client sequestration and induced polydispersity', *Nat Commun*, 16: 3635.

Mills, E. L., B. Kelly, and L. A. J. O'Neill. 2017. 'Mitochondria are the powerhouses of immunity', *Nat Immunol*, 18: 488-98.

Neupert, W., and J. M. Herrmann. 2007. 'Translocation of proteins into mitochondria', *Annu Rev Biochem*, 76: 723-49.

Nguyen, Thanh T., Shibo Wei, Thu Ha Nguyen, Yunju Jo, Yan Zhang, Wonyoung Park, Karim Gariani, Chang-Myung Oh, Hyeon Ho Kim, Ki-Tae Ha, Kyu Sang Park, Raekil Park, In-Kyu Lee, Minho Shong, Riekelt H. Houtkooper, and Dongryeol Ryu. 2023. 'Mitochondria-associated programmed cell death as a therapeutic target for age-related disease', *Experimental & Molecular Medicine*, 55: 1595-619.

Ohtsuka, K., and M. Hata. 2000. 'Mammalian HSP40/DNAJ homologs: cloning of novel cDNAs and a proposal for their classification and nomenclature', *Cell Stress & Chaperones*, 5: 98-112.

Ornelas, P., T. Bausewein, J. Martin, N. Morgner, S. Nussberger, and W. Kuehlbrandt. 2023. 'Two conformations of the Tom20 preprotein receptor in the TOM holo complex', *Proceedings of the National Academy of Sciences of the United States of America*, 120.

Palma, F. R., B. N. Gantner, M. J. Sakiyama, C. Kayzuka, S. Shukla, R. Lacchini, B. Cunniff, and M. G. Bonini. 2024. 'ROS production by mitochondria: function or dysfunction?', *Oncogene*, 43: 295-303.

Paschen, S. A., and W. Neupert. 2001. 'Protein import into mitochondria', *Iubmb Life*, 52: 101-12.

Pfanner, N., B. Warscheid, and N. Wiedemann. 2019. 'Mitochondrial proteins: from biogenesis to functional networks', *Nat Rev Mol Cell Biol*, 20: 267-84.

Qian, J., A. Nutz, K. Hansen, L. Bertgen, M. Franz-Wachtel, B. Macek, J. M. Herrmann, and D. Rapaport. 2025. 'The ribosome-associated complex regulates cytosolic translation upon mitoprotein-induced stress', *FEBS J*.

Rapaport, D., W. Neupert, and R. Lill. 1997. 'Mitochondrial protein import - Tom40 plays a major role in targeting and translocation of preproteins by forming a specific binding site for the presequence', *Journal of Biological Chemistry*, 272: 18725-31.

Rossmann, M. P., S. M. Dubois, S. Agarwal, and L. I. Zon. 2021. 'Mitochondrial function in development and disease', *Dis Model Mech*, 14.

Ruger-Herreros, C., L. Svoboda, A. Mogk, and B. Bukau. 2024. 'Role of J-domain proteins in yeast physiology and protein quality control', *J Mol Biol*: 168484.

Ryu, S. W., R. Stewart, D. C. Pectol, N. A. Ender, O. Wimalarathne, J. H. Lee, C. P. Zanini, A. Harvey, J. M. Huibregtse, P. Mueller, and T. T. Paull. 2020. 'Proteome-wide identification of HSP70/HSC70 chaperone clients in human cells', *PLOS Biol*, 18: e3000606.

Saitoh, T., M. Igura, T. Obita, T. Ose, R. Kojima, K. Maenaka, T. Endo, and D. Kohda. 2007. 'Tom20 recognizes mitochondrial presequences through dynamic equilibrium among

multiple bound states', *EMBO J*, 26: 4777-87.

Sayyed, U. M. H., and R. Mahalakshmi. 2022. 'Mitochondrial protein translocation machinery: From TOM structural biogenesis to functional regulation', *Journal of Biological Chemistry*, 298.

Schmidt, O., N. Pfanner, and C. Meisinger. 2010. 'Mitochondrial protein import: from proteomics to functional mechanisms', *Nature Reviews Molecular Cell Biology*, 11: 655-67.

Sherman, E. L., R. D. Taylor, N. E. Go, and F. E. Nargang. 2006. 'Effect of mutations in Tom40 on stability of the translocase of the outer mitochondrial membrane (TOM) complex, assembly of Tom40, and import of mitochondrial preproteins', *Journal of Biological Chemistry*, 281: 22554-65.

Shokolenko, I. N., G. L. Wilson, and M. F. Alexeyev. 2016. 'The "fast" and the "slow" modes of mitochondrial DNA degradation', *Mitochondrial DNA Part A*, 27: 490-98.

Soubannier, V., and H. M. McBride. 2009. 'Positioning mitochondrial plasticity within cellular signaling cascades', *Biochim Biophys Acta*, 1793: 154-70.

Stewart, M., and J. C. Schisler. 2024. 'Targeting chaperone modifications: Innovative approaches to cancer treatment', *J Biol Chem*, 300: 107907.

Sun, Y. M., X. Y. Wang, X. R. Zhou, C. Zhang, K. J. Liu, F. Y. Zhang, and B. Xiang. 2022. 'Salidroside Ameliorates Radiation Damage by Reducing Mitochondrial Oxidative Stress in the Submandibular Gland', *Antioxidants*, 11.

Tebbenkamp, A. T., and D. R. Borchelt. 2010. 'Analysis of chaperone mRNA expression in the adult mouse brain by meta analysis of the Allen Brain Atlas', *PLOS One*, 5: e13675.

Thirunavukarasu, D., and H. Shi. 2016. 'Aptamer-Enabled Manipulation of the Hsp70 Chaperone System Suggests a Novel Strategy for Targeted Ubiquitination', *Nucleic Acid Ther*, 26: 20-8.

Tomiczek, B., W. Delewski, L. Nierzwicki, M. Stolarska, I. Grochowina, B. Schilke, R. Dutkiewicz, M. A. Uzarska, S. J. Ciesielski, J. Czub, E. A. Craig, and J. Marszalek. 2020. 'Two-step mechanism of J-domain action in driving Hsp70 function', *PLOS Comput Biol*, 16: e1007913.

Towbin, H., T. Staehelin, and J. Gordon. 1979. 'Electrophoretic transfer of proteins from polyacrylamide gels to nitrocellulose sheets: procedure and some applications', *Proc Natl Acad Sci U S A*, 76: 4350-4.

Vestergaard, A. M., W. Nurani, P. Cachera, and U. H. Mortensen. 2025. 'Chaperone overexpression boosts heterologous small molecule production in', *Microbial Cell Factories*, 24.

Wessel, D., and U. I. Flugge. 1984. 'A method for the quantitative recovery of protein in dilute solution in the presence of detergents and lipids', *Anal Biochem*, 138: 141-3.

Wu, I. H., J. S. Yoon, Q. Yang, Y. Liu, W. Skach, and P. Thomas. 2021. 'A role for the ribosome-associated complex in activation of the IRE1 branch of UPR', *Cell Rep*, 35: 109217.

Wu, Y., J. Li, Z. Jin, Z. Fu, and B. Sha. 2005. 'The crystal structure of the C-terminal fragment of yeast Hsp40 Ydj1 reveals novel dimerization motif for Hsp40', *J Mol Biol*, 346: 1005-11.

Yamada, Y., A. Shiroma, S. Hirai, and J. Iwasaki. 2023. 'Zuo1, a ribosome-associated J protein, is involved in glucose repression in Saccharomyces cerevisiae', *FEMS Yeast Res*, 23.

Yamamoto, A., Y. Mizukami, and H. Sakurai. 2005. 'Identification of a novel class of target genes and a novel type of binding sequence of heat shock transcription factor in', *Journal of Biological Chemistry*, 280: 11911-19.

Yamamoto, H., N. Itoh, S. Kawano, Y. Yatsukawa, T. Momose, T. Makio, M. Matsunaga, M. Yokota, M. Esaki, T. Shodai, D. Kohda, A. E. Hobbs, R. E. Jensen, and T. Endo. 2011. 'Dual role of the receptor Tom20 in specificity and efficiency of protein import into

mitochondria', *Proc Natl Acad Sci U S A*, 108: 91-6.

Yamano, K., Y. I. Yatsukawa, M. Esaki, A. E. A. Hobbs, R. E. Jensen, and T. Endo. 2008. 'Tom20 and Tom22 share the common signal recognition pathway in mitochondrial protein import', *Journal of Biological Chemistry*, 283: 3799-807.

Yan, W., B. Schilke, C. Pfund, W. Walter, S. Kim, and E. A. Craig. 1998. 'Zuotin, a ribosome-associated DnaJ molecular chaperone', *EMBO J*, 17: 4809-17.

Zhang, B., C. Pan, C. Feng, C. Yan, Y. Yu, Z. Chen, C. Guo, and X. Wang. 2022. 'Role of mitochondrial reactive oxygen species in homeostasis regulation', *Redox Rep*, 27: 45-52.

Zhang, R., D. Malinverni, D. M. Cyr, P. L. Rios, and N. B. Nillegoda. 2023. 'J-domain protein chaperone circuits in proteostasis and disease', *Trends Cell Biol*, 33: 30-47.

Zhang, S., C. Lockshin, A. Herbert, E. Winter, and A. Rich. 1992. 'Zuotin, a putative Z-DNA binding protein in Saccharomyces cerevisiae', *EMBO J*, 11: 3787-96.

Zhang, Y., I. Sinning, and S. Rospert. 2017. 'Two chaperones locked in an embrace: structure and function of the ribosome-associated complex RAC', *Nat Struct Mol Biol*, 24: 611-19.

Zhang, Y., G. Valentin Gese, C. Conz, K. Lapouge, J. Kopp, T. Wolfle, S. Rospert, and I. Sinning. 2020. 'The ribosome-associated complex RAC serves in a relay that directs nascent chains to Ssb', *Nat Commun*, 11: 1504.

9 Acknowledgements

First and foremost, I would like to express my deepest gratitude to my supervisor, Prof. Dr. Doron Rapaport, for his exceptional efficiency, expertise, and unwavering support. I have learned tremendously from his patient guidance and his continual encouragement, which greatly motivated my research throughout the years.

My sincere thanks also go to Prof. Dr. Ralf Jansen, Prof. Dr. Gabriele Dodt, and Prof. Dr. Dirk Schwarzer for kindly serving as examiners on my defense committee. I truly appreciate their time, insightful comments, and valuable feedback.

I am also grateful to all my colleagues for creating such a supportive and inspiring working environment. Special thanks to Elena, our technician, whose warm help and constant readiness to assist made my daily work much easier. My heartfelt thanks to Kai for generously sharing his experience during my research, for his careful review of my thesis, and for translating the summary into German.

To Layla and Nitya, my very first “teachers”, thank you for introducing me to experimental techniques at the very beginning of my journey. Anasuya, I am grateful for the countless presentation skills you taught me. My thanks also go to Vitasta, for kindly transferring your apartment to me during my first days here. And to Pari and Lucie, thank you for your bright smiles that lit up each day.

Finally, I owe my deepest gratitude to my parents, whose constant support, love, and encouragement carried me through every step of this PhD journey.

10 Declaration of Contribution

This work was entirely written by the author. The large language model–based artificial intelligence tools, ChatGPT and Deepseek, were used for occasional grammatical assistance and language improvement in the thesis.

11 Published manuscripts

Qian, J., Nutz, A., Hansen, K., Bertgen, L., Franz-Wachtel, M., Macek, B., Herrmann, J.M. and Rapaport, D. (2025), The ribosome-associated complex regulates cytosolic translation upon mitoprotein-induced stress. FEBS J. https://doi.org/10.1111/febs.70356

The FEBS Journal

FEBS PRESS science publishing by scientists

The ribosome-associated complex regulates cytosolic translation upon mitoprotein-induced stress

Jiaxin Qian[1], Annika Nutz[2], Katja Hansen[2], Lea Bertgen[2], Mirita Franz-Wachtel[3], Boris Macek[3], Johannes M. Herrmann[2] and Doron Rapaport[1]

1 Interfaculty Institute of Biochemistry, University of Tübingen, Germany
2 Cell Biology, University of Kaiserslautern, Germany
3 Proteome Center Tübingen, University of Tübingen, Germany

Keywords
mitochondria; protein import; proteostasis; ribosome-associated complex; Tom70

Correspondence
D. Rapaport, Interfaculty Institute of Biochemistry, University of Tübingen, Auf der Morgenstelle 34, 72076 Tübingen, Germany
Tel: +49 7071 2974184
E-mail: doron.rapaport@uni-tuebingen.de

(Received 21 August 2025, revised 27 October 2025, accepted 25 November 2025)

doi:10.1111/febs.70356

The biogenesis of mitochondria relies on the import of newly synthesized precursor proteins from the cytosol. Tom70 is a mitochondrial surface receptor which recognizes precursors and serves as an interface between mitochondrial protein import and the cytosolic proteostasis network. Mitochondrial import defects trigger a complex stress response, in which compromised protein synthesis rates are a characteristic element. The molecular interplay that connects mitochondrial (dys)function to cytosolic translation rates in yeast cells is however poorly understood. Here, we show that the deletion of the two Tom70 paralogs of yeast (*TOM70* and *TOM71*) leads to defects in mitochondrial biogenesis and slow cell growth. Surprisingly, upon heat stress, the deletion of *ZUO1*, a chaperone of the ribosome-associated complex (RAC), largely prevented the slow growth and the reduced translation rates in the *tom70Δ/tom71Δ* double deletion mutant. In contrast, the mitochondrial defects were not cured but even enhanced by *ZUO1* deletion. Our study shows that Zuo1 is a critical component in the signaling pathway that mutes protein synthesis upon mitochondrial dysfunction. We propose a novel paradigm according to which RAC serves as a stress-controlled regulatory element of the cytosolic translation machinery.

Introduction

Mitochondrial proteins are mostly synthesized in the cytosol and then must be imported into the organelle via a set of complex processes involving multiple factors and pathways [1]. Cytosolic chaperones and their co-chaperones, particularly those from the Hsp40, Hsp70 and Hsp90 families, contribute to these pathways by maintaining mitochondrial precursor proteins in an import-competent conformation [2–5]. These (co) chaperones not only prevent aggregation and misfolding of newly synthesized proteins in the cytosol but also ensure they are properly delivered to and inserted into the mitochondria [6]. Such interactions with (co) chaperones keep the precursor proteins in a loosely folded, unfolded, or partially folded conformation that is compatible with the import machinery [7]. The initial interactions with surface import receptors are essential for the specific recognition of the mitochondrial precursor proteins and for their subsequently efficient translocation across the mitochondrial membranes.

Abbreviations
DTT, Dithiothreitol; GFP, green fluorescent protein; GO, gene ontology; HPLC, high-performance liquid chromatography; Hsp, heat shock protein; iMTS, internal mitochondrial targeting signal; ISR, integrated stress response; LFQ, label-free quantification; MS, mass spectrometry; OD, optical density; PAGE, polyacrylamide gel electrophoresis; PMSF, phenylmethylsulfonyl fluoride; RAC, ribosome-associated complex; RT, room temperature; SD, standard deviation; TCA, trichloroacetic acid; WT, wild-type.

We and others observed that the mitochondrial surface receptors Tom70 and its paralogue Tom71 contribute to the recognition of newly synthesized mitochondrial proteins and in addition serve as a docking site for cytosolic (co)chaperones on the surface of the organelle [2–4,8,9]. Furthermore, Tom70 was recently reported to be involved in the localized condensation of protein aggregates on the mitochondrial surface [10]. Both Tom70 and Tom71 are anchored to the mitochondrial outer membrane via a single transmembrane segment at their N-terminal region and contain multiple tetratricopeptide repeat (TPR) domains [11,12]. Tom70 plays a crucial role particularly in recognizing and importing precursor proteins with internal targeting sequences like multispan membrane proteins residing in both mitochondrial membranes and matrix-destined proteins with internal mitochondrial targeting signal (iMTS) [13–15]. Tom71, a less abundant paralogue of Tom70, shares sequence similarity with Tom70, but its precise molecular function is still being investigated [16–18].

In line with their central role in the import of mitochondrial proteins, the combined absence of both Tom70 and Tom71 causes proteostasis stress in the cytosol [2]. Such stress manifests as an accumulation of misfolded or unfolded mitochondrial precursor proteins in the cytosol, triggering cytosolic responses and potentially leading to cell damage if not resolved [19,20]. To reduce such cytosolic proteostasis stress, cells developed a combined approach targeting protein synthesis, folding, and degradation [21–24]. Such an adaptation involves optimizing the ubiquitin-proteasome system (UPS), promoting proper protein folding, and regulating protein synthesis. The latter element is currently understudied, and it is unclear how changes in cytosolic proteostasis and mitoprotein-induced stress in yeast cells can influence the quantity and quality of protein synthesis.

A potential player in translation regulation is Zuo1, also known as Zuotin, a ribosome-associated J-protein with multiple functions [25,26]. It primarily acts as a co-chaperone for Hsp70 (Ssb1) forming together with another Hsp70 (Ssz1) the ribosome-associated complex (RAC) [27], assisting in the co-translational folding of nascent polypeptides [28]. Additionally, Zuo1 plays a role in ribosome biogenesis, DNA repair, rRNA processing, and the regulation of translation [29–31].

In the current study, we investigated the interplay between the mitochondrial surface receptors Tom70/71 and the co-chaperone Zuo1. Surprisingly, we observed that, at elevated temperatures, the absence of Zuo1 improves the growth of cells deleted for Tom70/71 and accelerates translation in this double deletion strain. The absence of Zuo1 also resulted in a reduction in the levels of cytosolic stress chaperones like Hsp42 and Hsp26. Thus, we discovered a Zuo1-mediated crosstalk between the accumulation of mitochondrial precursor proteins and the regulation of cytosolic translation.

Results

The deletion of *ZUO1* has temperature-dependent effect on growth of yeast cells

To better understand the crosstalk between Zuo1 and the proteostasis of mitochondrial precursor proteins, we aimed to test the effect of the deletion of *ZUO1* on the growth of yeast cells under various conditions. To achieve that aim, we monitored growth on different carbon sources, at various temperatures, and in combination with mitoprotein-induced stress. We observed that the deletion of *ZUO1* resulted in slower growth on fermentable carbon sources like glucose or galactose as well as on the nonfermentable carbon source glycerol (Fig. 1A–C). These results are in line with previous studies reporting a growth retardation of *zuo1Δ* cells at 30 °C on glucose-containing media [25,26]. To create cytosolic accumulation of nonimported mitochondrial proteins, we deleted the import receptor Tom70 and its less studied paralogue, Tom71. This double deletion resulted in minorly retarded growth at 30 °C on the tested carbon sources (Fig. 1A–C). Importantly, a triple deletion strain (*tom70Δ*/*tom71Δ*/*zuo1Δ*) showed a genetic negative interaction and grew much slower than the tested single or double deletion strains (Fig. 1A–C). These findings suggest that under normal temperature a functional Zuo1 is beneficial when the mitochondrial proteins Tom70/71 are absent.

Next, we asked whether increasing stress by growing the cells at an elevated temperature (37 °C) will change the behavior of the mutated strains. As expected [2], cells lacking both import receptors hardly grew under these conditions, while the single deletion of *ZUO1* had only a mild growth defect (Fig. 2A–C). Surprisingly, the deletion of the J-protein in the strain lacking both receptors (*tom70Δ*/*tom71Δ*) resulted in cells that grew much better than the original double deletion strain (Fig. 2A–C). Importantly, this improvement in growth was observed on solid medium containing glucose, galactose, or glycerol as well as in liquid medium harboring either glucose or galactose. The growth enhancement upon deletion of *ZUO1* was detected also in combination with the single deletion of *TOM70* (Fig. 2A–C). In summary, at elevated temperature the absence of Zuo1 promotes the viability of cells that suffer from mitoprotein-induced stress.

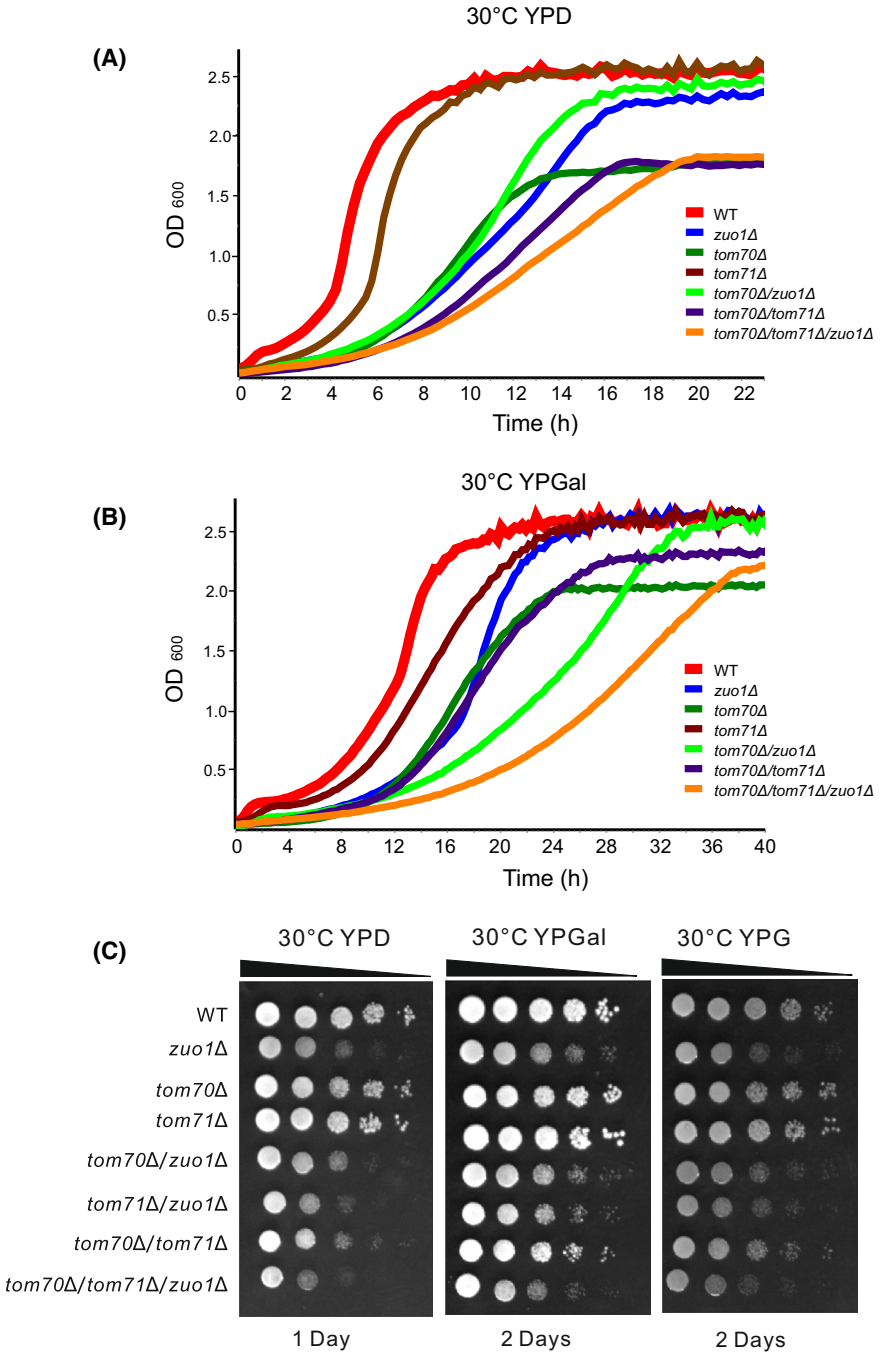

Fig. 1. Cells deleted for *ZUO1* display retarded growth at 30 °C. (A, B) The growth of the indicated strains at 30°C in rich liquid medium containing either glucose (A, YPD) or galactose (B, YPGal) was monitored using OD_{600} measurements for 24 or 40 h, respectively. At the beginning of the measurements (Time 0), the strains were diluted to an OD_{600} of 0.1. (C) The growth of the indicated strains was monitored at 30°C by drop dilution assay on solid rich medium containing glucose (YPD), galactose (YPGal), or glycerol (YPG). Plates were incubated for 1 or 2 days before pictures were taken. All the results displayed in this figure are representative of three identical experiments ($n = 3$).

Cells lacking Zuo1 have altered proteome

To understand the cellular events that resulted in this unexpected benefit of cells deleted for *ZUO1*, we compared by an unbiased approach the proteome of the mutated cells to those of control cells. To this goal, we isolated proteins from control [wild-type (WT)],

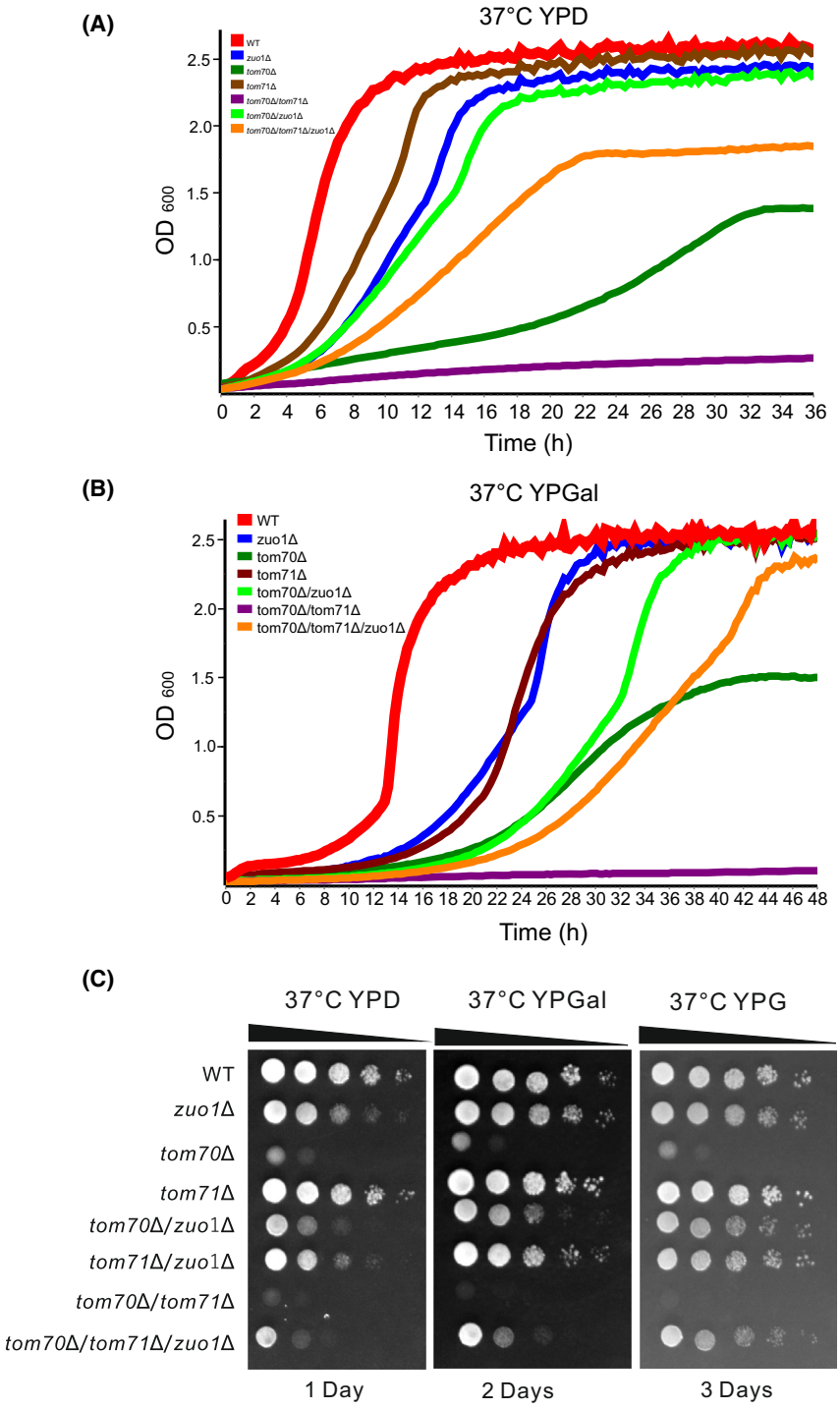

Fig. 2. Absence of Zuo1 at elevated temperature restores the compromised growth of *tom70Δ/tom71Δ* cells. (A, B) The growth of the indicated strains at 37 °C was monitored as described in Fig. 1A,B. (C) The growth of the indicated strains was monitored at 37 °C by drop dilution assay as described in Fig. 1C. All the results displayed in this figure are representative of three identical experiments (n = 3).

double deletion (*tom70Δ/tom71Δ*), and triple deletion cells (*tom70Δ/tom71Δ/zuo1Δ*) grown at 37 °C on glucose-containing medium and analyzed them by mass spectrometry (Fig. 3A). This analysis indicated a unique protein composition of the different cell types and a similar coverage of the yeast proteome among

the investigated cells (Fig. 3B,C). Initially, we compared the proteome of the control cells to that of the double deletion ones. As observed before for *tom70Δ/tom71Δ* cells [2], they harbor reduced amounts of many mitochondrial proteins, among the most affected ones are Coq2 and Mdm36 (Fig. 3D–F and Table S1). Similarly, the triple deletion cells also contained, as compared to control cells, fewer mitochondrial proteins where the levels of subunits of the respiratory chain complexes and mitochondrial ribosomes as well as mitochondrial inner membrane proteins were specially reduced (Fig. 3F and Table S1).

A specific group of yeast genes is expressed under the control of a dedicated heat response program (Fig. 4A and Table S2) [32]. The protein products of these genes are often involved in counteracting cytosolic protein aggregation and misfolding. Thus, we were particularly interested in the expression of such proteins in the different examined strains. In agreement with the enhanced protein aggregation upon the absence of Tom70/71, we detected elevated levels of the small chaperones Hsp12 and Hsp26 in these cells (Fig. 4B–D). Of note, comparison of the triple deletion strain with the control cells revealed that these increased expression levels were mainly diminished for Hsp26 and the levels of Hsp12 were even lower than those of the control cells (Fig. 4B–D). This trend was not observed for all cytosolic chaperones and the amounts of the rather generic chaperone Hsp82 were higher in the triple deletion strain compared with the control or the double deletion cells (Table S1). Hence, our findings hint at a remodeling of the cytosolic stress response upon deletion of *ZUO1*.

Next, we aimed to confirm our mass spectrometry findings by an unrelated method. To this end, we analyzed the protein extracts of the investigated cells, grown on glucose at 37 °C, by SDS/PAGE followed by immunostaining. Indeed, we could verify that the double deletion of *TOM70/71* caused a significant increase in the amounts of cytosolic chaperones with anti-stress activity like Hsp12, Hsp26, and Hsp104. Notably, these elevated levels were reduced back to normal levels upon the additional deletion of *ZUO1* on top of the absence of Tom70/71 (Fig. 5A,B). Interestingly, the amounts of general chaperones like Hsp70 (Ssa1) or Hsp90 (Hsp82) did not change much among the various strains. Similarly unchanged were the amounts of the unrelated cytosolic proteins Bmh1 and hexokinase (Hxk) 1 (Fig. 5A,B).

Since most of the mitochondrial outer membrane (MOM) proteins were reported to be substrates of Tom70/71, we also monitored their amounts in the various strains. While some proteins (like Tom20, Tom40, Msp1, and Fis1) were only mildly affected or not at all, the levels of others were dramatically altered. For example, the absence of Tom70 alone or in combination with Tom71 resulted in a major reduction in the levels of the β-barrel protein Porin (VDAC1). This reduction was partially compensated by the additional deletion of *Zuo1* (Fig. 6A,B). However, the absence of Zuo1 did not have the same effect on all proteins. A somewhat different pattern was observed for another β-barrel protein, Tob55/Sam50 where the absence of Zuo1 did not enhance the compromised levels upon the removal of Tom70 or Tom70/71 (Fig. 6A,B).

A completely distinctive picture emerged for three proteins (Om45, Om14, and Mcr1) that were suggested to participate in mitochondrial metabolic processes. Against our expectations, the double deletion of Tom70 and Tom71 resulted in enhanced amounts of these proteins. However, the additional deletion of *ZUO1* caused a dramatic decrease in the amounts of these proteins to a level much below that in control cells (Fig. 6A,B). Taking together, the western analysis demonstrated individual effects for the absence of Zuo1 on the levels of various MOM proteins.

The absence of Zuo1 enhances translation and changes the pattern of cytosolic aggregates

The aforementioned observations encouraged us to investigate the contribution of Zuo1 to additional cellular processes like the formation of cytosolic aggregates or translation. To monitor the number of aggregates per cell, we used a previously established method namely, the staining of such aggregates with a disaggregase Hsp104 fused to GFP [33]. Using this approach, we noticed that the single absence of Zuo1 resulted in a slight increase in the number of cells with several aggregates. The double deletion of Tom70/71 resulted in even more cells with many aggregates; however, the additional deletion of *ZUO1* from *tom70Δ/tom71Δ* cells reduced the number of aggregates per cell without affecting much the overall number of cells with any number of aggregates (Fig. 7A,B).

Considering this observation, we wished to determine the effect of Zuo1 on translation. To achieve this aim, we employed radioactive *in vivo* labeling followed by extracting proteins from the cells and analyzing the newly synthesized proteins by either SDS/PAGE or dot blot. Proteins were detected in both cases by autoradiography. Both assays revealed that the absence of Zuo1 increases overall translation at 30 °C and the dot blot assay expanded this finding also to cells grown at 37 °C (Fig. 7C–E). Collectively, these results

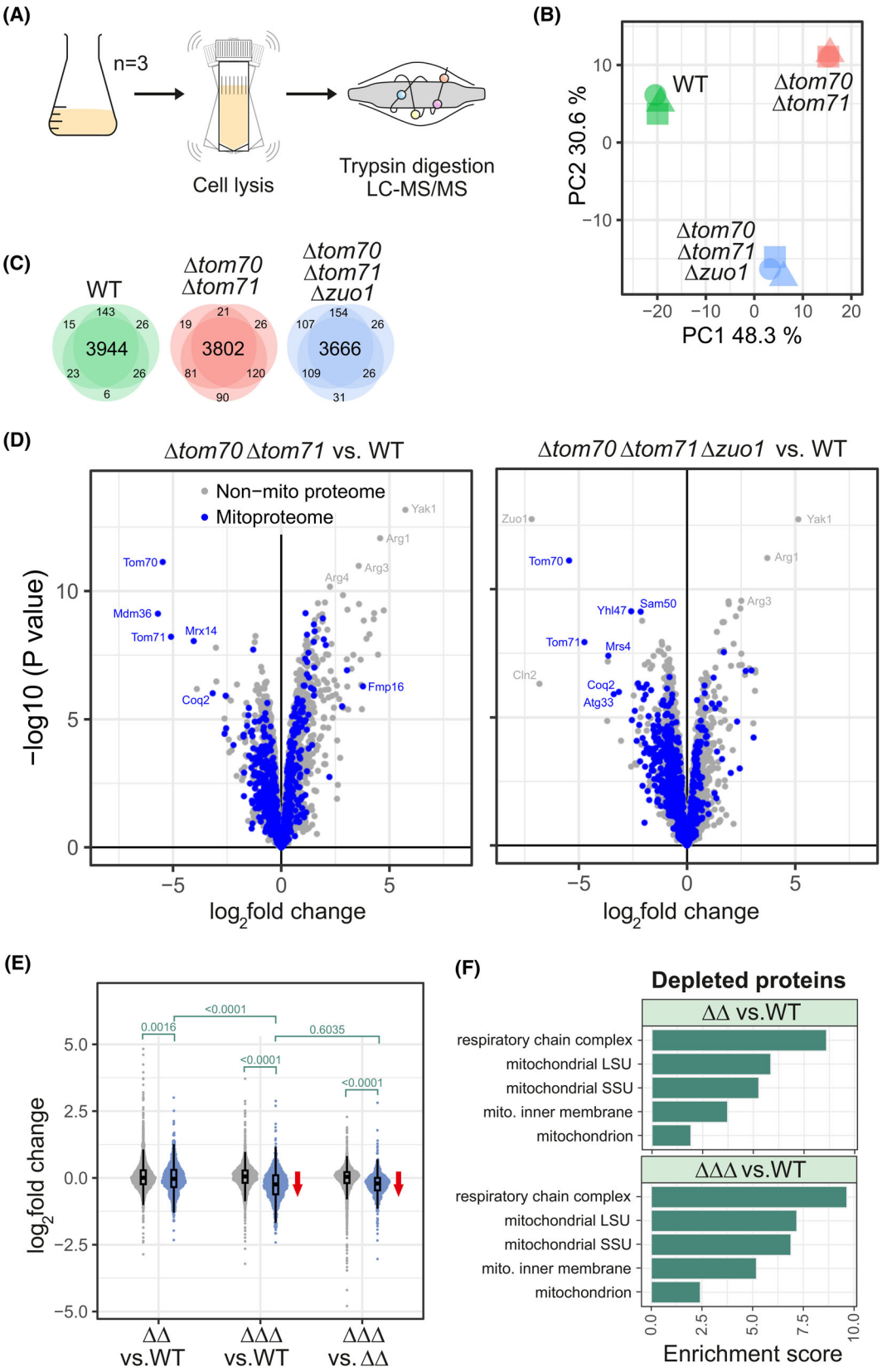

Fig. 3. Absence of Zuo1 does not restore the depletion of mitochondrial proteins in *tom70Δ/tom71Δ* cells. (A) Scheme of the mass spectrometry measurement of cellular proteins. (B) Principal component analysis. (C) Venn diagrams showing the number of proteins that were identified in the different replicates. (D) Volcano plots comparing the proteomes of the indicated strains. Mitochondrial proteins are shown in blue. (E) Violin plots to compare the abundance of nonmitochondrial and mitochondrial (in blue) proteins in the different strains. A two-sided Wilcoxon rank-sum test with continuity correction was used to calculate *P*-values for indicated comparisons. (F) Enrichment of gene ontology terms was performed for the most extremely depleted proteins ($\log_2$ fold change > −0.8 in the limma analysis) using the GOrilla website (http://cbl-gorilla.cs.technion.ac.il); see Table S3 for details. WT, wild-type, ΔΔ, *tom70Δ/tom71Δ*, ΔΔΔ, *tom70Δ/tom71Δ/zuo1Δ*.

indicate that the removal of Zuo1 from cells lacking Tom70/71 improves the growth of the latter cells probably by reducing the number of aggregates per cell in combination with enhancing global protein synthesis.

Discussion

Defects in the import of mitochondrial proteins have a well-documented impact on proteostasis in the cytosol and are associated with protein aggregation diseases [23,24,34]. Thus, understanding the mechanisms that contribute to proteostasis during inhibition in mitochondrial protein import can shed new light on cellular stress responses. It is well established that the absence of the mitochondrial surface proteins Tom70 and its paralogue Tom71 causes defects in mitochondrial biogenesis combined with mitoprotein-induced stress in the cytosol [2]. This complex outcome is related to the double function of these proteins; they play a role in the recognition of newly synthesized mitochondrial proteins and serve as a docking site for cytosolic (co) chaperones loaded with mitochondrial precursor proteins [3,4,35–37]. To better understand the cellular importance of these proteins in the context of cellular stress, we combined their absence with the alteration of protein translation via the deletion of the RAC subunit, Zuotin (Zuo1).

Surprisingly, at elevated temperature, these triple deleted cells (*tom70Δ/tom71Δ/zuo1Δ*) grew better than cells lacking only the two receptor proteins. This improved growth was accompanied by fewer aggregates per cell and enhanced translation. The latter effect is especially of interest because it is well known that the cytosolic stress response involves a coordinated effort to reduce overall protein synthesis while simultaneously promoting the synthesis of proteins essential for cell survival under stress conditions. This phenomenon, which is part of the integrated stress response (ISR), helps cells to conserve energy and resources during stress [38]. Indeed, we observed such differential alterations upon the deletion of *ZUO1*. Despite the general trend of enhanced translation, we observed that the levels of the small chaperones Hsp12 and Hsp26, which increased dramatically upon the deletion of *TOM70/71*, went down upon the removal of Zuo1.

In human cells, the link between cytosolic proteostasis stress and regulation of protein synthesis often involves the translation initiation factor 2 subunit-α (eIF2α). It is well established that an increased level of phosphorylation of eIF2α is a hallmark of the ISR. Stress-activated kinases phosphorylate eIF2α, leading to a global reduction in protein synthesis initiation [38,39]. Mitochondrial stress is relayed to this system in mammalian cells via the protein Deleted in Liver Cancer 1 (DELE1) [40]. When mitochondria experience stress, DELE1, which is normally imported into the mitochondrial matrix, is cleaved by the OMA1 protease and translocates to the cytoplasm, where it interacts with heme-regulated inhibitor (HRI) kinase that subsequently phosphorylates eIF2α [40,41]. However, despite this wealth of knowledge about the mammalian system, it was unclear how mitochondrial-induced stress is causing translation slowdown in yeast cells. Our findings shed light on this issue by suggesting that Zuo1 is part of this missing link. It seems that under stress conditions, Zuo1 contributes to the reduction of translation efficiency, and therefore, its absence under such circumstances results in an elevated protein synthesis rate (Fig. 8).

Previous studies are not conclusive regarding the effect of Zuo1 on protein translation rate. One work reported that the deletion of Zuo1 by itself or in combination with Arsen-induced stress causes a reduction in global translation [42]. On the contrary, another report indicated that while *zuo1Δ* cells have lower polysome levels in basal conditions [43], this does not seem to affect the *in vivo* global translation rate [29]. Hence, it appears that Zuo1 might be involved in fine-tuning translation in response to different signaling inputs and in accordance with the proteostasis situation at the cytosol. Supporting this assumption is a previous high-throughput study reporting that the overexpression of *ZUO1* suppresses mitochondria-induced cell death [24]. Hence, it seems that alterations of the expression levels of Zuo1 in both directions can

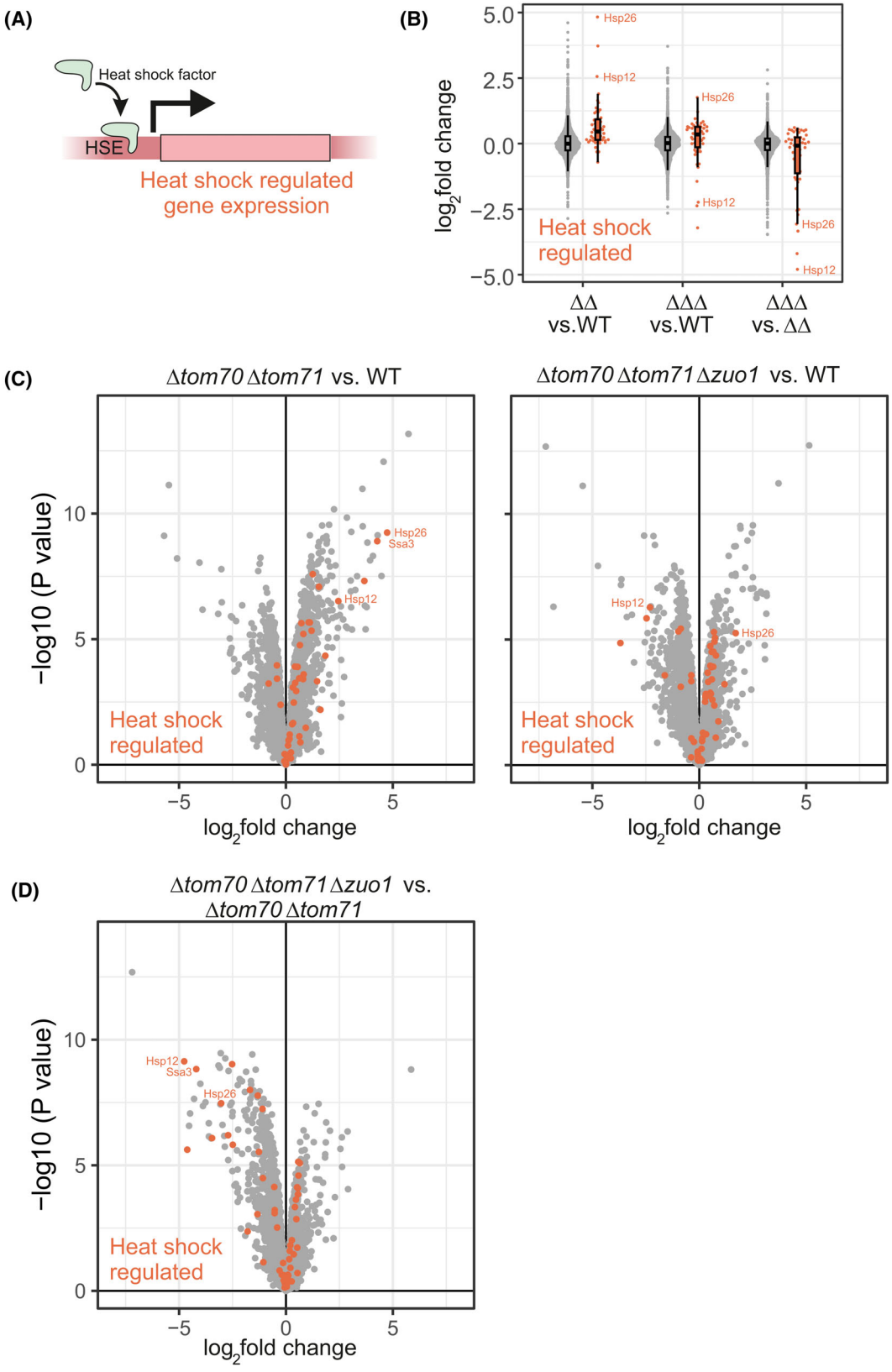

Fig. 4. Deletion of *TOM70/71* and *ZUO1* leaves a characteristic footprint on the proteostasis network. (A) Scheme of the heat response program. (B) Violin plots comparing the abundance of proteins that are heat shock regulated (in orange, see [32] and Table S2) to nonheat shock regulated proteins in the different strains. (C, D) Volcano plots demonstrating that deletion of *TOM70/71* leads to a marked upregulation of heat shock regulated proteins but not the additional deletion of *ZUO1*. WT, wild-type, ΔΔ, *tom70Δ/tom71Δ*, ΔΔΔ, *tom70Δ/tom71Δ/zuo1Δ*.

be beneficial for yeast cells under various stress conditions.

Zuo1 forms together with Ssz1 the RAC, which is known to facilitate the interaction of the ribosome-associated Hsp70 Ssb with a variety of nascent chains [25]. In this context, it is interesting to note that the aforementioned screens identified in addition to *ZUO1* also *SSB1*/2, but not *SSZ1*, as multicopy suppressors of the mitochondria-induced growth retardation [24]. To better understand the link between translation regulation and mitoprotein-induced stress, it will be interesting to investigate in future studies the role of Ssb1/2 and Ssz1 under these conditions.

We observed that the absence of Tom70/71 causes an increased number of cells with a large number of aggregates and elevated levels of the small stress proteins Hsp12 and Hsp26 [44,45], supporting their role as docking sites for substrate-associated chaperones [2]. However, the absence of Zuo1 resulted, despite the enhanced global translation, in a reduced number of cells with many aggregates and highly reduced levels of Hsp12 and Hsp26. These observations further support the notion that Zuo1 can differentially affect the synthesis of various proteins.

Our proteomic approach clearly demonstrated that the deletion of Tom70/71 resulted, as reported before, in compromised levels of many mitochondrial proteins. However, although the further deletion of *ZUO1* on this background did not restore the levels of the mitochondrial proteins, it did improve considerably the growth ability of the cells. An interesting exception for this general trend is formed by the three outer membrane proteins Om14, Om45, and Mcr1. In cells grown at elevated temperature, the levels of these proteins are actually enhanced in cells lacking TOM70/71 as compared to control cells. Importantly, the expression levels are reduced when, in addition, Zuo1 is deleted as well. Although all three proteins are highly expressed when cells grow on a nonfermentable carbon source, suggesting their necessity for optimal mitochondrial function, their precise molecular function is not clear. Thus, one can only speculate that their increased expression under these conditions is part of a stress response and/or metabolic rewiring which is not required when additionally, Zuo1 is absent as well.

In summary, our findings demonstrate that the main problem in cells lacking Tom70/71 is likely not the compromised mitochondrial biogenesis but rather the cytosolic proteostasis stress. Deciphering the mechanism by which the absence of Zuo1 counteracts this latter problem is an important question that awaits future studies.

Methods

Growth curves

Yeast cells were precultured in glucose medium until the exponential phase was reached. Cells equivalent to an OD_{600} of 1.0 were harvested for 5 min at 3000× ***g*** and resuspended in water. Cells were diluted to an OD_{600} of 0.1 into media containing either glucose or galactose as a carbon source. Cells were rotating for 20–50 h at either 30 °C or 37 °C in a SPECTROstar^{Nano} plate reader (BMG LABTECH, Ortenberg, Germany) with the settings shaking between reads at 500 rpm and double orbital. Three technical replicates were used per strain and condition. The data were visualized in R.

Monitoring yeast growth on solid medium

Yeast cells were initially cultured overnight in 5 mL of glucose-containing medium. The cultures were then diluted to an OD_{600} of 0.2–0.3 and incubated for a further 2–4 h until reaching an OD_{600} of 0.8–1.5. Next, cells equivalent to 2.0 units of OD_{600} were collected and resuspended in 1 mL of sterile water. A series of 1 : 10 serial dilutions were prepared, and 4 µL of each dilution was spotted onto agar plates with the indicated carbon source. The plates were incubated at different temperatures for further analysis.

Whole cell lysates

Cells were cultured at either 30 °C or 37 °C until they reached exponential phase (OD_{600} of 0.5–1.5), and then, 2–10 OD_{600} units were harvested for lysis. Cells were lysed by one of the following options: (i) Cells were washed twice with water and resuspended in 30 µL loading dye supplemented with 50 mM DTT. Cells were lysed for 5 min at 4 °C with the help of four to five glass beads (diameter of 1 mm). Afterward, samples were boiled for 5 min at 96 °C

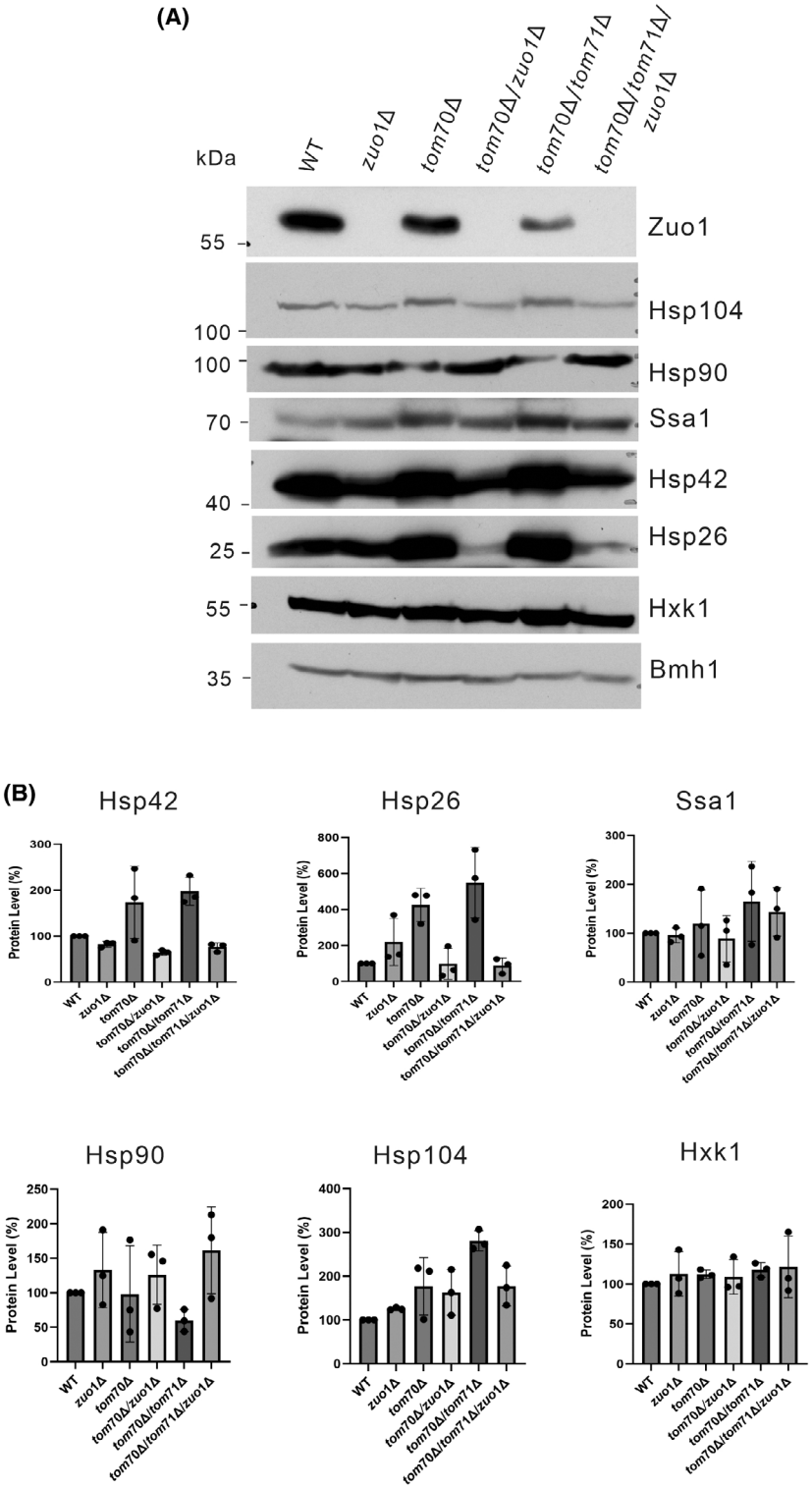

Fig. 5. Additional deletion of *ZUO1* differentially affects the levels of cytosolic chaperones. (A) Proteins were extracted from the indicated strains and analyzed by SDS/PAGE and immunodecorated with the indicated antibodies. (B) The bands corresponding to the indicated proteins from three independent experiments as the one shown in (A) were quantified and normalized to the intensities of the Ponceau S staining. The value of the WT cells was set at 100%. The bar diagram shows the average ± SD of three independent experiments.

and additional 50 µL of loading dye with DTT was added. (ii) Alternatively, the cells pellet was resuspended in 800 µL of 0.1 M NaOH and incubated for 5 min at room temperature (RT). After centrifugation (13 000× ***g***, 1 min, RT), cells were resuspended in 50 µL of 2 × loading dye containing 5% β-mercaptoethanol. The samples were then incubated at 95 °C for 3 min, centrifuged again (13 000× ***g***, 1 min, RT), and the supernatant was collected for further analysis. In both cases, samples were analyzed by SDS/PAGE and immunostaining. Signals were detected using the chemiluminescence mode and either the Chemi-Doc MP Imaging System (Bio-Rad, Hercules, CA, USA) or appropriate films.

Trichloroacetic acid (TCA) precipitation of proteins

Proteins were precipitated by adding 72% TCA to the solution to achieve a final concentration of 12% TCA. The samples were incubated overnight at −20 °C to ensure complete precipitation. Proteins were sedimented by centrifugation (25 000× ***g***, 30 min, 4 °C) washed with ice-cold acetone (−20 °C) and pelleted again under the same conditions. The resulting protein pellets were dried at RT and resuspended in sample buffer.

Radioactive *in vivo* labeling of translation products

Cells were cultured in glucose- or galactose-containing medium at 30 °C or 37 °C until reaching the exponential growth phase and were then harvested for further analysis. For radioactive *in vivo* labeling of translation products, cells of 1 OD_{600} unit were washed with synthetic glucose- or galactose-containing medium lacking methionine. Radiolabeling was initiated by adding ^{35}S-methionine (0.75 µL of an 11 µCi solution) to the suspension for incubation at the indicated temperature for 2, 5, 10, or 15 min. The reactions were quenched by adding 8 mM cold methionine in the case of the dot blot experiment or cells were directly lysed after 5 or 15 min of incubation. Cells were lysed using 0.3 M NaOH, 1% β-mercaptoethanol, and 2 mM phenylmethylsulfonyl fluoride (PMSF), and proteins were precipitated with 12% TCA. The samples were analyzed using SDS/PAGE or dot blotting.

For dot blot analysis, 5 µL of a 1 : 30 diluted sample was loaded onto a nitrocellulose membrane using the SCR 96 Minifold I apparatus under vacuum. Radiolabeled proteins were detected by autoradiography by exposing the dried membrane to an imaging plate (Fujifilm, Tokyo, Japan) and visualizing it with Typhoon FLA 7000 phospho-imager (GE Healthcare, Chicago, IL, USA) or on Super RX Medical X-Ray Films (Fuji) using the Optimax Type developer (MS Laborgeräte, Wiesloch, Germany). Images were scanned in an 8-bit or 16-bit grayscale format, and signal intensities were quantified using Image Lab software (Bio-Rad). Normalization was performed based on the immunostaining with antibodies against Rpl6B (antibody in a 1 : 2000 dilution) that served as a loading control, and the WT sample labeled for 15 min was set as 100%.

Fluorescence microscopy

Cells were transformed with a pYX142 Hsp104-GFP yeast expression plasmid [33]. Cells equivalent to one unit of OD_{600} were harvested via centrifugation, and cell pellets were resuspended in 30 µL of water. A small aliquot (3 µL) was pipetted onto a glass slide and covered with a cover slip. Manual microscopy was performed using a Leica Dmi8 Thunder Imager, with an external LED8 light source and a Leica DFC9000GTC camera. Images were acquired using an HC PL APO 100×/1.44 Oil UV objective with Immersion Oil Type A 518 F, a DFT51010 filter cube for GFP excitation at 475 nm at 540 MHz as quality mode at 16-bit and saved in the Leica Image Format. The resolution was 2048 × 2048 pixels and a physical size of 132.03 µm. Image analysis was performed with LAS X software, and further processing was conducted in Fiji/IMAGEJ. The number of Hsp104-GFP foci per cell was counted manually and categorized into three groups: cells with no foci, 1–4 foci, or ≥ 5 foci per cell. The percentage of cells in each category was calculated and the data were visualized using R.

LC MS/MS

Proteins were precipitated overnight at −20°C with an ice-cold acetone-methanol mixture. After centrifugation (2000× ***g***, 20 min, 4 °C), protein pellets were washed with 80% ice-cold acetone. The pellet was dried, and proteins were resolved in denaturation buffer (6 M urea, 2 M thiourea, 10 mM Tris, pH 8.0). Protein concentration was determined with the Bradford assay, and 10 micrograms of protein were subjected to in-solution digestion with trypsin as described previously [46]. Desalted peptides [47] were analyzed on a Vanquish Neo nano-UHPLC coupled to an Orbitrap Exploris 480 mass spectrometer through a nano-electrospray ion source (all Thermo Scientific, Waltham, MA, USA): 0.25 µg peptides were loaded onto a 20 cm HPLC column with 75 µm inner diameter (ICT36007508F-50; CoAnn Technologies, Richland, VA, USA) in-house packed with 1.9 µm ReproSil-Pur C18-AQ silica beads (r119.aq.; Dr. Maisch HPLC GmbH: Ammerbuch-Entringen, Germany) under pressure control (1000 bar). Elution was performed with a 45 min segmented gradient of 5–55% of HPLC solvent B (80% acetonitrile in 0.1% formic acid) at a flow rate of 300 nL·min^{-1} and a constant temperature of 40 °C. The mass spectrometer was operated

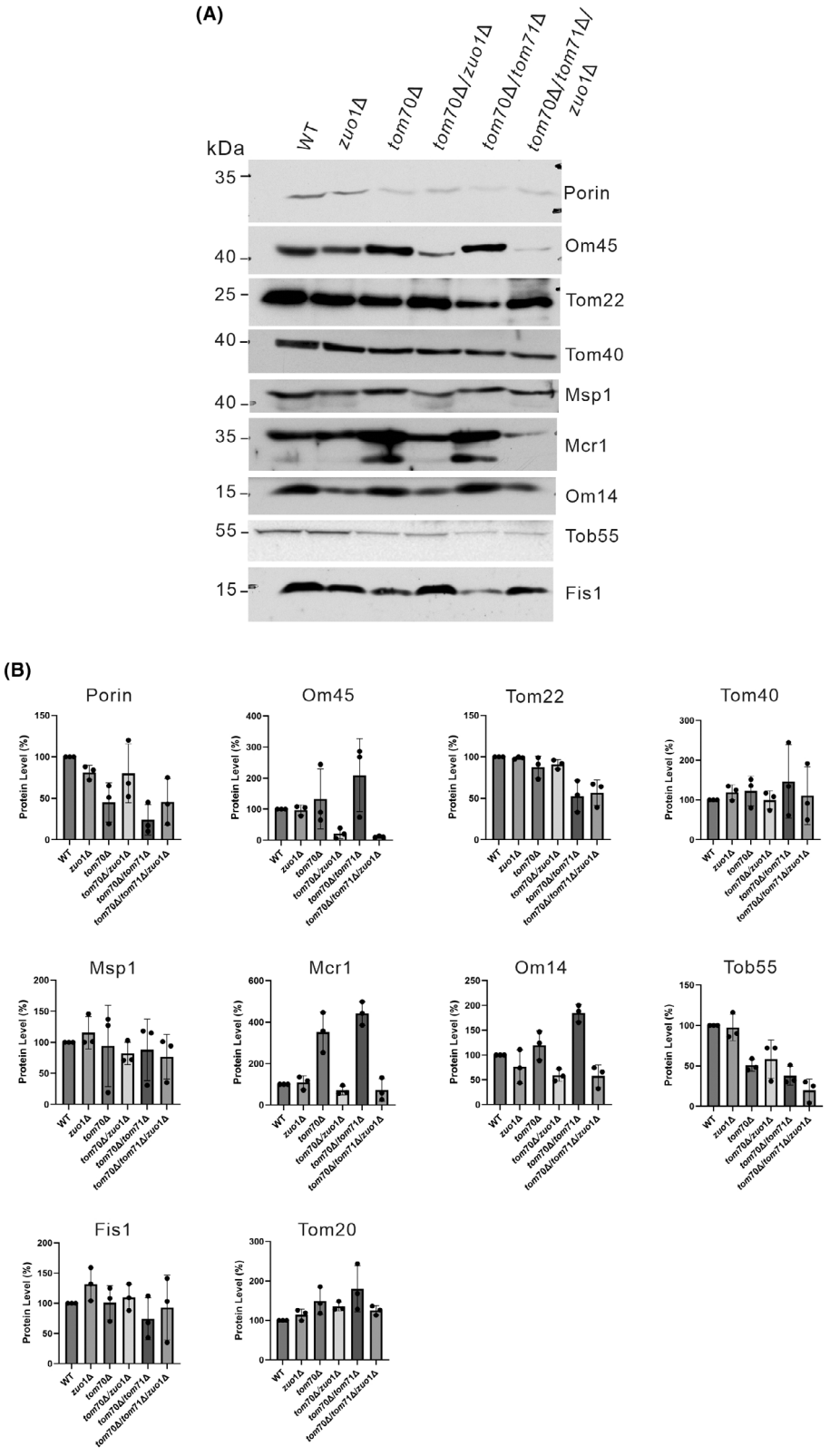

Fig. 6. Removal of Zuo1 affects a different extent of the levels of mitochondrial outer membrane proteins. (A) Proteins were extracted from the indicated strains and analyzed by SDS/PAGE and immunodecorated with the indicated antibodies. (B) The bands corresponding to the indicated proteins from three independent experiments as the one shown in (A) were quantified and normalized to the intensities of the Ponceau S staining. The value of the WT cells was set at 100%. The bar diagram shows the average ± SD of three independent experiments.

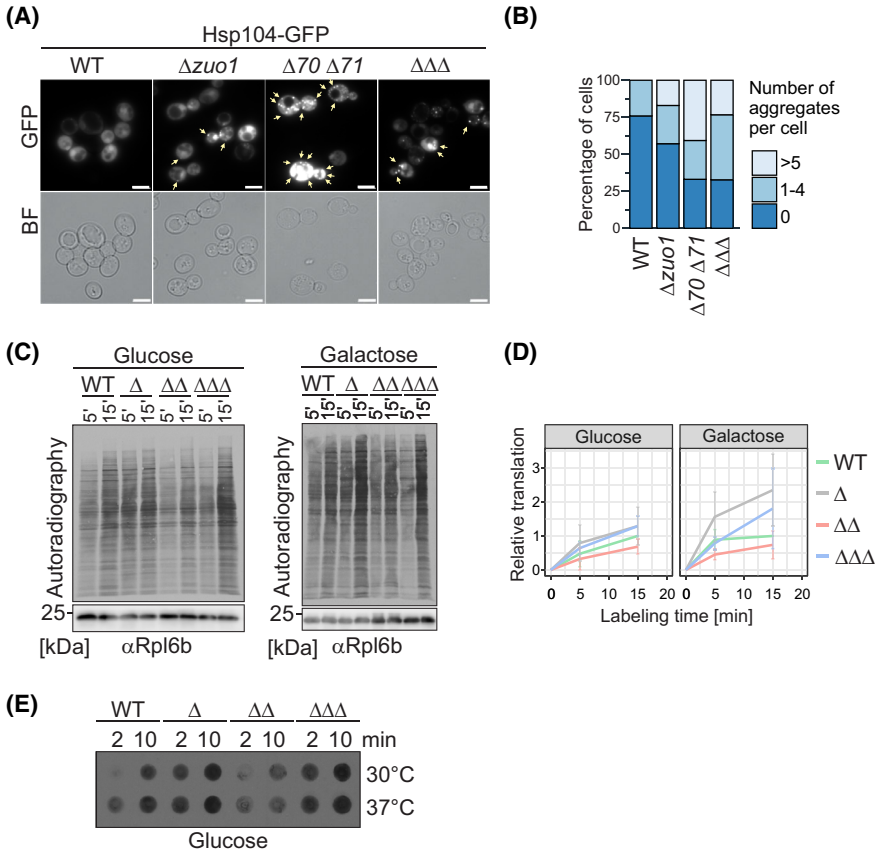

Fig. 7. Deletion of *TOM70/71* leads to the formation of cytosolic aggregates and slows down protein synthesis. (A) Strains expressing Hsp104-GFP were analyzed by fluorescence microscopy. Hsp104-bound aggregates are indicated with yellow arrows. Scale bars, 5 μm. (B) Quantification of cells containing aggregates. Cell populations were categorized into cells with no aggregates (dark blue), with 1–4 aggregates (medium blue), or with ≥ 5 aggregates (light blue). The portion of cells in each category is shown as the percentage of all cells counted with $n = 137$ for WT, $n = 182$ for *zuo1Δ*, $n = 145$ for *tom70Δ/tom71Δ*, and $n = 297$ for the triple mutant. (C) *In vivo* labeling of newly synthesized proteins at 30 °C in media containing either glucose or galactose for either 5 or 15 min. Proteins were analyzed by SDS/PAGE, and the radiolabeled translation products of the different strains were detected by autoradiography. Immunostaining against Rpl6b is shown as a loading control. (D) The signal of all detected proteins for a certain lane as in (C) was quantified and normalized to the loading control Rpl6b. The indicated data points at 5 and 15 min represent the relevant intensity of the radiolabeled translation products of three biological replicates. The intensity of the translation products in WT cells after 15 min was set to 1. Error bars represent ± S.D. (E) Cells were grown at the indicated temperature on glucose as a carbon source. Radiolabeled translation products after a labeling period of either 2 or 10 min were analyzed by dot blot and autoradiography. The results displayed in this panel are representative of two identical experiments ($n = 2$).

in a positive ion and data-independent acquisition (DIA) mode. MS1 spectra were acquired at a resolution of 120 k in the range of m/z 400–1000 with automatic gain control (AGC) set to 300%, and maximum ion injection time (MaxIT) set to auto. MS2 spectra were acquired in the range of m/z 145–1450 with a normalized collision energy of 27% at a resolution of 30 k, whereby AGC was set to 800%, and MaxIT was set to auto. DIA isolation windows of 10 m/z (60 scan events) were defined as the window placement optimization. The mass spectrometry proteomics

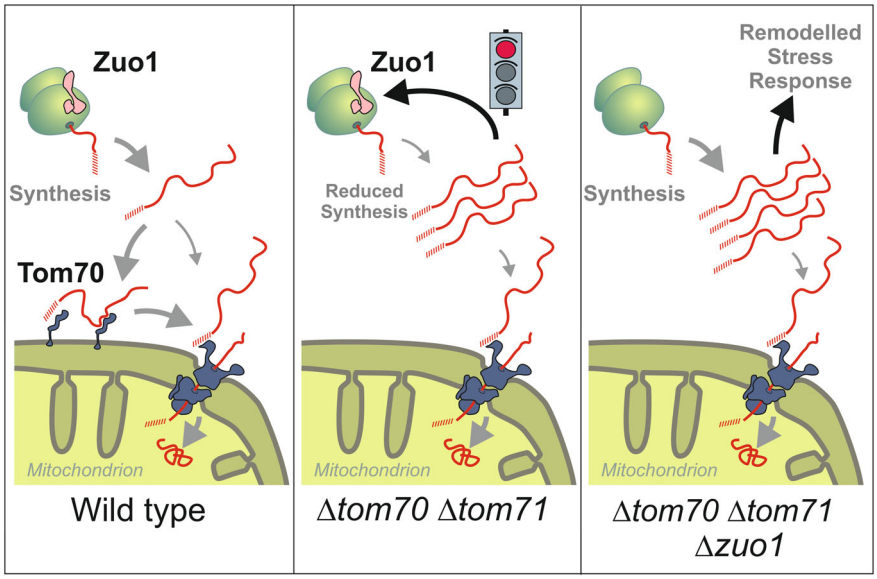

Fig. 8. Schematic model for how ZUO1 deletion leads to remodeling of the cytosolic stress response. Tom70 is a nonessential mitochondrial outer membrane protein that supports the import of proteins into mitochondria. Mutants lacking Tom70 and its paralog Tom71 show reduced protein import levels, leading to the accumulation of nonimported precursor proteins. These nonimported precursor proteins slow down protein synthesis. Interestingly, the mitoprotein-induced reduction of translation depends on the RAC subunit Zuo1, suggesting that Zuo1 is a critical component in the signaling pathway that mutes protein synthesis upon mitochondrial dysfunction. We propose a novel paradigm according to which RAC serves as a stress-controlled regulatory element of the cytosolic translation machinery.

data have been deposited to the ProteomeXchange Consortium via the PRIDE partner repository with the dataset identifier PXD067604.

MS data processing

DIA-based MS data were processed in directDIA+ mode using the Spectronaut software version 19.5 (Biognosys) using default search parameters with more stringent identification settings [48]. Spectra were predicted using a *Saccharomyces cerevisiae* database obtained from Uniprot (downloaded 30 January 2024; 6091 entries). Results were exported using the Pivot Report showing all identified and quantified protein groups.

These were further processed using the R programming language (R version 4.5.1, https://www.R-project.org). The following procedure was based on methods that have been described previously [7,49]. For each condition, proteins that were identified in less than two replicates were removed ($N = 3$). This resulted in 4254 total identified protein groups whose quantities were $\log_2$-transformed, normalized using variance stable normalization [50], and batch-cleaned using limma [51]. Lastly, missing values were imputed by sampling $N = 3$ values from a normal distribution (seed = 127 851) and using them whenever there were no valid values in a triplicate of a condition. The mean of this normal distribution corresponds to the 1% percentile of label-free quantification (LFQ) intensities. Its standard deviation is determined as the median of LFQ intensity sample standard deviations calculated within and then averaged over each triplicate. Proteins were tested for differential expression using limma for the indicated pairwise comparison of samples and a Benjamini–Hochberg procedure was used to account for multiple testing. All relevant test results are listed in Table S1. Principal component analysis was carried out on the processed intensities by singular value decomposition. For Gene Ontology (GO) enrichment analysis of depleted proteins, proteins with smaller than -0.8 $\log_2$ fold change were used as a target set and analyzed using the GOrilla tool (http://cbl-gorilla.cs.technion.ac.il/) [52] with all quantified proteins as a background set (Table S3).

Author contributions

JQ, KH, and LB planned and performed the experiments and analyzed data. AN analyzed the data. MF-W performed the mass spectrometry analysis. BM supervised the analysis. JMH and DR planned the experiments, analyzed the data, and wrote the manuscript.

Acknowledgements

We thank E. Kracker for excellent technical assistance, K.S. Dimmer for helpful discussions, and S. Rospert

and J. Buchner for antibodies. This work was supported by the Deutsche Forschungsgemeinschaft (RA 1028/11-1 to D.R. and HE 2803/11-1 to J.M.H), the European Research Council (MitoCyto 101052639 to J.M.H.), and the doctoral fellowship of the Chinese Scholarship Council (CSC) to J.Q. Open Access funding enabled and organized by Projekt DEAL.

Conflict of interest

The authors declare no conflict of interest.

Peer review

The peer review history for this article is available at https://www.webofscience.com/api/gateway/wos/peer-review/10.1111/febs.70356.

Data availability statement

The mass spectrometry proteomics data have been deposited in the ProteomeXchange Consortium via the PRIDE partner repository with the dataset identifier PXD067604. All other datasets used in this study are available from the corresponding author on request.

References

1 Endo T & Wiedemann N (2025) Molecular machineries and pathways of mitochondrial protein transport. *Nat Rev Mol Cell Biol* **26**, 848–867.
2 Backes S, Bykov YS, Flohr T, Raschle M, Zhou J, Lenhard S, Kramer L, Muhlhaus T, Bibi C, Jann C *et al.* (2021) The chaperone-binding activity of the mitochondrial surface receptor Tom70 protects the cytosol against mitoprotein-induced stress. *Cell Rep* **35**, 108936.
3 Drwesh L, Heim B, Graf M, Kehr L, Hansen-Palmus L, Franz-Wachtel M, Macek B, Kalbacher H, Buchner J & Rapaport D (2022) A network of cytosolic (co) chaperones promotes the biogenesis of mitochondrial signal-anchored outer membrane proteins. *elife* **11**, e77706.
4 Jores T, Lawatscheck J, Beke V, Franz-Wachtel M, Yunoki K, Fitzgerald JC, Macek B, Endo T, Kalbacher H, Buchner J *et al.* (2018) Cytosolic Hsp70 and Hsp40 chaperones enable the biogenesis of mitochondrial beta-barrel proteins. *J Cell Biol* **217**, 3091–3108.
5 Hoseini H, Pandey S, Jores T, Schmitt A, Franz-Wachtel M, Macek B, Buchner J, Dimmer KS & Rapaport D (2016) The cytosolic cochaperone Sti1 is relevant for mitochondrial biogenesis and morphology. *FEBS J* **283**, 3338–3352.
6 Bykov YS, Rapaport D, Herrmann JM & Schuldiner M (2020) Cytosolic events in the biogenesis of mitochondrial proteins. *Trends Biochem Sci* **45**, 650–667.
7 Roedl S, Hoffman Y, Jung F, Egeler A, Nutz A, Simoncik O, Jung M, Raschle M, Muller P, Storchova Z *et al.* (2025) A protein-specific priority code in presequences determines the efficiency of mitochondrial protein import. *PLoS Biol* **23**, e3003298.
8 Brix J, Ziegler GA, Dietmeier K, Schneider-Mergener J, Schulz GE & Pfanner N (2000) The mitochondrial import receptor Tom70: identification of a 25 kDa core domain with a specific binding site for preproteins. *J Mol Biol* **303**, 479–488.
9 Papic D, Elbaz-Alon Y, Koerdt SN, Leopold K, Worm D, Jung M, Schuldiner M & Rapaport D (2013) The role of Djp1 in import of the mitochondrial protein Mim1 demonstrates specificity between a cochaperone and its substrate protein. *Mol Cell Biol* **33**, 4083–4094.
10 Liu Q, Fong B, Yoo S, Unruh JR, Guo F, Yu Z, Chen J, Si K, Li R & Zhou C (2023) Nascent mitochondrial proteins initiate the localized condensation of cytosolic protein aggregates on the mitochondrial surface. *Proc Natl Acad Sci USA* **120**, e2300475120.
11 Li J, Qian X, Hu J & Sha B (2009) Molecular chaperone Hsp70/Hsp90 prepares the mitochondrial outer membrane translocon receptor Tom71 for preprotein loading. *J Biol Chem* **284**, 23852–23859.
12 Wu Y & Sha B (2006) Crystal structure of yeast mitochondrial outer membrane translocon member Tom70p. *Nat Struct Mol Biol* **13**, 589–593.
13 Backes S, Hess S, Boos F, Woellhaf MW, Godel S, Jung M, Muhlhaus T & Herrmann JM (2018) Tom70 enhances mitochondrial preprotein import efficiency by binding to internal targeting sequences. *J Cell Biol* **217**, 1369–1382.
14 Jores T, Klinger A, Gross LE, Kawano S, Flinner N, Duchardt-Ferner E, Wohnert J, Kalbacher H, Endo T, Schleiff E *et al.* (2016) Characterization of the targeting signal in mitochondrial beta-barrel proteins. *Nat Commun* **7**, 12036.
15 Brix J, Rudiger S, Bukau B, Schneider-Mergener J & Pfanner N (1999) Distribution of binding sequences for the mitochondrial import receptors Tom20, Tom22, and Tom70 in a presequence-carrying preprotein and a non-cleavable preprotein. *J Biol Chem* **274**, 16522–16530.
16 Aravindan N, Vitali DG, Breuer J, Oberst J, Zalckvar E, Schuldiner M & Rapaport D (2025) Mpf1 affects the dual distribution of tail-anchored proteins between mitochondria and peroxisomes. *EMBO Rep* **26**, 2622–2653.
17 Kondo-Okamoto N, Shaw JM & Okamoto K (2008) Tetratricopeptide repeat proteins Tom70 and Tom71

mediate yeast mitochondrial morphogenesis. *EMBO Rep* **9**, 63–69.
18 Schlossmann J, Lill R, Neupert W & Court DA (1996) Tom71, a novel homologue of the mitochondrial preprotein receptor Tom70. *J Biol Chem* **271**, 17890–17895.
19 Nowicka U, Chroscicki P, Stroobants K, Sladowska M, Turek M, Uszczynska-Ratajczak B, Kundra R, Goral T, Perni M, Dobson CM *et al*. (2021) Cytosolic aggregation of mitochondrial proteins disrupts cellular homeostasis by stimulating the aggregation of other proteins. *elife* **10**, e65484
20 Kaushik P, Herrmann JM & Hansen KG (2025) MitoStores: stress-induced aggregation of mitochondrial proteins. *Biol Chem* **406**, 237–249.
21 Boos F, Labbadia J & Herrmann JM (2020) How the Mitoprotein-induced stress response safeguards the cytosol: a unified view. *Trends Cell Biol* **30**, 241–254.
22 Topf U, Uszczynska-Ratajczak B & Chacinska A (2019) Mitochondrial stress-dependent regulation of cellular protein synthesis. *J Cell Sci* **132**, jcs226258.
23 Wrobel L, Topf U, Bragoszewski P, Wiese S, Sztolsztener ME, Oeljeklaus S, Varabyova A, Lirski M, Chroscicki P, Mroczek S *et al*. (2015) Mistargeted mitochondrial proteins activate a proteostatic response in the cytosol. *Nature* **524**, 485–488.
24 Wang X & Chen XJ (2015) A cytosolic network suppressing mitochondria-mediated proteostatic stress and cell death. *Nature* **524**, 481–484.
25 Gautschi M, Lilie H, Funfschilling U, Mun A, Ross S, Lithgow T, Rucknagel P & Rospert S (2001) RAC, a stable ribosome-associated complex in yeast formed by the DnaK-DnaJ homologs Ssz1p and zuotin. *Proc Natl Acad Sci USA* **98**, 3762–3767.
26 Yan W, Schilke B, Pfund C, Walter W, Kim S & Craig EA (1998) Zuotin, a ribosome-associated DnaJ molecular chaperone. *EMBO J* **17**, 4809–4817.
27 Huang P, Gautschi M, Walter W, Rospert S & Craig EA (2005) The Hsp70 Ssz1 modulates the function of the ribosome-associated J-protein Zuo1. *Nat Struct Mol Biol* **12**, 497–504.
28 Lee K, Ziegelhoffer T, Delewski W, Berger SE, Sabat G & Craig EA (2021) Pathway of Hsp70 interactions at the ribosome. *Nat Commun* **12**, 5666.
29 Black A, Williams TD, Soubigou F, Joshua IM, Zhou H, Lamoliatte F & Rousseau A (2023) The ribosome-associated chaperone Zuo1 controls translation upon TORC1 inhibition. *EMBO J* **42**, e113240.
30 Kisonaite M, Wild K, Lapouge K, Gese GV, Kellner N, Hurt E & Sinning I (2023) Structural inventory of cotranslational protein folding by the eukaryotic RAC complex. *Nat Struct Mol Biol* **30**, 670–677.
31 De Magis A, Gotz S, Hajikazemi M, Fekete-Szucs E, Caterino M, Juranek S & Paeschke K (2020) Zuo1 supports G4 structure formation and directs repair toward nucleotide excision repair. *Nat Commun* **11**, 3907.
32 Yamamoto A, Mizukami Y & Sakurai H (2005) Identification of a novel class of target genes and a novel type of binding sequence of heat shock transcription factor in *Saccharomyces cerevisiae*. *J Biol Chem* **280**, 11911–11919.
33 Kramer L, Dalheimer N, Raschle M, Storchova Z, Pielage J, Boos F & Herrmann JM (2023) MitoStores: chaperone-controlled protein granules store mitochondrial precursors in the cytosol. *EMBO J* **42**, e112309.
34 Boos F, Kramer L, Groh C, Jung F, Haberkant P, Stein F, Wollweber F, Gackstatter A, Zoller E, van der Laan M *et al*. (2019) Mitochondrial protein-induced stress triggers a global adaptive transcriptional programme. *Nat Cell Biol* **21**, 442–451.
35 Young JC, Hoogenraad NJ & Hartl FU (2003) Molecular chaperones Hsp90 and Hsp70 deliver preproteins to the mitochondrial import receptor Tom70. *Cell* **112**, 41–50.
36 Schlossmann J, Dietmeier K, Pfanner N & Neupert W (1994) Specific recognition of mitochondrial preproteins by the cytosolic domain of the import receptor MOM72. *J Biol Chem* **269**, 11893–11901.
37 Brix J, Dietmeier K & Pfanner N (1997) Differential recognition of preproteins by the purified cytosolic domains of the mitochondrial import receptors Tom20, Tom22, and Tom70. *J Biol Chem* **272**, 20730–20735.
38 Costa-Mattioli M & Walter P (2020) The integrated stress response: from mechanism to disease. *Science* **368**, eaat5314.
39 Pakos-Zebrucka K, Koryga I, Mnich K, Ljujic M, Samali A & Gorman AM (2016) The integrated stress response. *EMBO Rep* **17**, 1374–1395.
40 Guo X, Aviles G, Liu Y, Tian R, Unger BA, Lin YT, Wiita AP, Xu K, Correia MA & Kampmann M (2020) Mitochondrial stress is relayed to the cytosol by an OMA1-DELE1-HRI pathway. *Nature* **579**, 427–432.
41 Romanelli S & Trempe JF (2025) Stressful situations: molecular insights on mitochondrial quality control pathways. *J Biol Chem* **301**, 110483.
42 Rodrigues JI, Lorentzon E, Hua S, Boucher A & Tamas MJ (2023) Yeast chaperones and ubiquitin ligases contribute to proteostasis during arsenite stress by preventing or clearing protein aggregates. *FEBS Lett* **597**, 1733–1747.
43 Albanese V, Reissmann S & Frydman J (2010) A ribosome-anchored chaperone network that facilitates eukaryotic ribosome biogenesis. *J Cell Biol* **189**, 69–81.
44 Cashikar AG, Duennwald M & Lindquist SL (2005) A chaperone pathway in protein disaggregation. Hsp26 alters the nature of protein aggregates to facilitate reactivation by Hsp104. *J Biol Chem* **280**, 23869–23875.

45 Welker S, Rudolph B, Frenzel E, Hagn F, Liebisch G, Schmitz G, Scheuring J, Kerth A, Blume A, Weinkauf S *et al*. (2010) Hsp12 is an intrinsically unstructured stress protein that folds upon membrane association and modulates membrane function. *Mol Cell* **39**, 507–520.
46 Borchert N, Dieterich C, Krug K, Schutz W, Jung S, Nordheim A, Sommer RJ & Macek B (2010) Proteogenomics of *Pristionchus pacificus* reveals distinct proteome structure of nematode models. *Genome Res* **20**, 837–846.
47 Rappsilber J, Mann M & Ishihama Y (2007) Protocol for micro-purification, enrichment, pre-fractionation and storage of peptides for proteomics using StageTips. *Nat Protoc* **2**, 1896–1906.
48 Baker CP, Bruderer R, Abbott J, Arthur JSC & Brenes AJ (2024) Optimizing spectronaut search parameters to improve data quality with minimal proteome coverage reductions in DIA analyses of heterogeneous samples. *J Proteome Res* **23**, 1926–1936.
49 Flohr T, Raschle M & Herrmann JM (2025) Dysfunctional mitochondria trap proteins in the intermembrane space. *EMBO J* **44**, 4352–4377.
50 Huber W, von Heydebreck A, Sultmann H, Poustka A & Vingron M (2002) Variance stabilization applied to microarray data calibration and to the quantification of differential expression. *Bioinformatics* **18**, S96–S104.
51 Ritchie ME, Phipson B, Wu D, Hu Y, Law CW, Shi W & Smyth GK (2015) Limma powers differential expression analyses for RNA-sequencing and microarray studies. *Nucleic Acids Res* **43**, e47.
52 Eden E, Navon R, Steinfeld I, Lipson D & Yakhini Z (2009) GOrilla: a tool for discovery and visualization of enriched GO terms in ranked gene lists. *BMC Bioinformatics* **10**, 48.

Supporting information

Additional supporting information may be found online in the Supporting Information section at the end of the article.
Table S1. Mass spectrometry data.
Table S2. HSF dependent genes.
Table S3. Analysis of GO terms.